A STUDY OF GLUTAMATE RECEPTOR FUNCTION IN THE RAT BARREL CORTEX

By Molupe Lehohla

Submitted in fulfilment of the requirements for the degree of Master of Science (MSc.) (Med) in the Faculty of Health Sciences at the University of Cape Town

November 2001

Supervisors: Associate Professor V.A. Russell

Dr L.A. Kellaway

Declaration

I, Molupe Lehohla declare that the work in this dissertation is original (except where acknowledgements indicate otherwise) and that neither the whole work nor any part of it has been, or is being, or is to be submitted for another degree in this or another University

I give permission to the University to reproduce for purposes of research either the whole or any part of the contents of this dissertation.

Signed:.....

Date:.....30-11-2001.....

Publications and Congress Presentations

Parts of this dissertation have been published as follows:

1. Lehohla, M., Russell, V.A., Kellaway, L., Govender, A. (2000) Development of a method to evaluate glutamate receptor function in rat barrel cortex. Metab Brain Dis 15: 305 – 314

2. Lehohla, M., Russell, V.A., Kellaway, L. (2001) NMDA-Stimulated Ca^{2+} Uptake Into Barrel Cortex Slices of Spontaneously Hypertensive Rats. Metab Brain Dis 16: 135 - 143

Congress Presentations

1. Lehohla, M., Russell, V.A., Kellaway, L., Govender, A., Developing a technique to measure glutamate function in the rat barrel cortex. Joint meeting of the South African Pharmacology Society and the Neuroscience Society. Durban, South Africa, 20 – 23 September 2000

2. Lehohla, M., Russell, V.A., Kellaway, L., Govender, A., A study of glutamate receptor function in rat barrel cortex slices. 5th Society of Neuroscientists of Africa International Conference Nairobi, Kenya, 23 – 27 April 2001

Acknowledgements:

I would like to extend my sincere thanks and appreciation to the following people:

The head of the department of Human Biology for giving me the opportunity and providing the facilities to carry out my studies.

My supervisors, **Associate Professor V Russell** and **Dr L. Kellaway**, for their assistance and guidance during the study and most importantly the insight and valuable criticisms during the final preparation of this thesis.

Mr P. Rossouw, for assisting with keeping the glassware clean, decontaminated and always ready to be used, **Mr B. Sedres**, for breeding the animals and furnishing me with accurate data on the rats which was crucial to my experiments, **Mr H. Hall** for making the experimental set up and **Mrs B Young** for teaching me the technique.

To my wife who agreed to be temporarily widowed while I was busy with this work. Thank you for your patience and loyalty. It wasn't easy but it was worth it.

My family, friends and all people with a unique bearing in my life; for all the support you gave me: I say thank you!

List of abbreviations

ADHD	attention-deficit hyperactivity disorder
APV	D-2-amino-5-phosphonopentanoate
D-APS	D-2-amino-5-phosphopentanoic acid
AMPA,	α-amino-3-hydroxy-5-methyl-4-isoxazole propionic acid
BSA	bovine serum albumin
Ca^{2+}	calcium
cAMP	cyclic adenosine monophosphate
$[Ca^{2+}]_I$	intracellular calcium concentration
$^{45}Ca^{2+}$	radioactively labelled calcium
Ci	curie
CNQX	6-cyano-7-nitroquinoxaline-2,3-dione
CNS	central nervous system
CP	caudate-putamen
CPM	counts per minute
CPP	3-(2-carboxy-piperazin-4-yl)propyl-1-phosphonate
DAG	diacycl glycerol
DOM	domoic acid
DPM	disintegrations per minute
G	Gasserian ganglion
GABA	gamma-aminobutyric acid
GAD	glutamic acid decarboxylase
GLU	glutamate

IP_3	inositol triphosphate
KA	kainate
K^+	potassium
$[K^+]_E$	extracellular potassium concentration
LE	Long Evans rat
LTD	long term depression
LTP	long term potentiation
mg	milligram
mGluR	metabotropic glutamate receptor
MK-801	(+-)-5-methyl-10,11-dihydro-5H-dibenzo(a,d)cycloheptan-5,10-imine maleate
ml	millilitre
mM	millimolar
mm	millimeter
nM	nanomolar
NMDA	N-methyl-D-aspartate
P	pons
PCP	phencyclidine
PFC	prefrontal cortex
PIPs	phosphatidyl inositol
PLC	phospholipase C
PO	posterior nucleus of the thalamus
PR	perirhinal cortex
QA	quisqualate

RT	reticular nucleus of the thalamus
SC	superior colliculus
SD	standard deviation
SEM	standard error of the mean
SII	secondary somatosensory area
SHR	spontaneously hypertensive rat
VB	ventrobasal nucleus of the thalamus
VGCCs	voltage-gated calcium channels
WKY	Wistar Kyoto rat
μg	microgram
μl	microlitre
μm	micrometer
μM	micromolar

List of figures

List of tables

Abstract

The rat is a nocturnal animal and uses its vibrissae extensively to navigate its environment. The vibrissae are linked to a highly organised part of the sensory cortex, called the barrel cortex which contains spiny neurons that receive whisker specific thalamic input and distribute their output mainly within the cortical column. The aim of the present study was to develop a method to measure NMDA receptor function, to establish whether NMDA receptor function is altered in barrel cortex slices of 4-to 6- week old SHR compared to WKY and to test whether ageing and exposure to an enriched environment affects the two strains differently.

Firstly a technique was developed using 4-to 6- week-old Long Evans rats. The rats were killed by cervical dislocation and decapitated. The brain was rapidly removed, cooled in a continuously oxygenated ice-cold HEPES buffer (pH 7.4) and sliced using a vibratome to produce 0.35mm slices. The barrel cortex was dissected from slices corresponding to 8.6 to 4.8mm anterior to the interaural line and divided into rostral, middle and caudal regions. The prefrontal cortex was dissected from slices corresponding to 14.2 to 12.2mm anterior to the interaural line and divided into rostral, middle and caudal regions.

Depolarisation-induced uptake of $^{45}Ca^{2+}$ was achieved by incubating test slices in a high concentration K^+ (62.5mM) buffer for 2 minutes at 35°C. Potassium-stimulated uptake of $^{45}Ca^{2+}$ into the rostral region was significantly lower than uptake into middle and caudal regions of the barrel cortex. Optimising conditions by lowering external concentration of both calcium and potassium to physiological levels reduced

the total and basal uptake of $^{45}Ca^{2+}$ but without any increase in the amount of $^{45}Ca^{2+}$ taken up by the slices in response to K^+ stimulation. The final optimised conditions of 1.2 mM Ca^{2+} and 3.36 mM K^+ were used for subsequent studies despite the fact that they did not increase the amount of $^{45}Ca^{2+}$ taken up. NMDA (100 μM) significantly increased uptake of $^{45}Ca^{2+}$ into all regions of the barrel cortex. Lower concentrations of NMDA did not cause significant uptake in the presence of elevated external K^+ concentration. Glycine did not enhance NMDA stimulated $^{45}Ca^{2+}$ uptake into barrel cortex slices. Calcium uptake was completely blocked by the NMDA receptor antagonist MK-801 showing that uptake was via the NMDA receptors.

The first study was used to investigate possible differences in NMDA receptor function between spontaneously hypertensive rats (SHR) that are used as a model for attention deficit disorder and their normotensive Wistar Kyoto (WKY) control rats. The average total $^{45}Ca^{2+}$ uptake into the barrel cortex of SHR as well as total uptake into the rostral, middle and caudal regions of SHR was significantly lower than WKY. Average basal $^{45}Ca^{2+}$ uptake into SHR barrel cortex as well as $^{45}Ca^{2+}$ uptake into rostral and caudal regions of SHR was significantly lower compared to WKY but basal uptake into the middle region was the same for both strains. There was no difference in the average NMDA-stimulated $^{45}Ca^{2+}$ uptake between SHR and WKY into the barrel cortex and into the rostral and caudal regions, however, NMDA-stimulated uptake was significantly lower in the middle region of SHR barrel cortex than WKY. These findings suggest that calcium metabolism maybe disturbed in somatosensory cortex of SHR but that NMDA receptor function is not significantly altered.

In a second study the effects of exposure to an enriched environment, age and strain on NMDA receptor function were investigated. Exposure of both SHR and WKY to a novel environment did not have a significant effect on $^{45}Ca^{2+}$ uptake through NMDA receptors. Average total $^{45}Ca^{2+}$ uptake into adult (12 to 18 weeks old) rats was significantly lower than average total $^{45}Ca^{2+}$ uptake into young (4 to 6 weeks old) rats. In adult rats total $^{45}Ca^{2+}$uptake into the rostral, middle and caudal regions of the barrel cortex was significantly lower than total $^{45}Ca^{2+}$uptake into the rostral, middle and caudal regions of young rats. Average basal $^{45}Ca^{2+}$ uptake was significantly higher in adult rats than average basal $^{45}Ca^{2+}$ uptake into barrel cortex of young rats. Basal uptake into the rostral region of adult rats was significantly higher than basal uptake into young rats while there was no difference in basal $^{45}Ca^{2+}$ uptake into the middle and caudal regions between the young and adult rats. The average NMDA-stimulated $^{45}Ca^{2+}$uptake was significantly lower in adult rats compared to young rats. NMDA-stimulated uptake into rostral, middle and caudal regions was significantly lower in adult rats compared to young rats, showing that NMDA receptor function decreases with increasing age for both SHR and WKY. This could be due to either a decrease in sensitivity of NMDA receptors with age or a decrease in the number of NMDA receptors with increasing age. The average total $^{45}Ca^{2+}$ uptake into SHR barrel cortex was significantly lower than uptake into WKY. Total uptake into the rostral and middle regions of the SHR barrel cortex was significantly lower than total $^{45}Ca^{2+}$ uptake into WKY barrel cortex. There was no strain effect on basal $^{45}Ca^{2+}$ uptake and on NMDA-stimulated $^{45}Ca^{2+}$ uptake into the different regions of the barrel cortex.

In the third study NMDA-stimulated $^{45}Ca^{2+}$ uptake into prefrontal cortex slices of SHR and WKY and the effect of enriched environment on $^{45}Ca^{2+}$ uptake was studied. The results showed that the enriched environment did not have an effect on $^{45}Ca^{2+}$ uptake into the prefrontal cortex. The average total $^{45}Ca^{2+}$ uptake into prefrontal cortex of SHR was significantly lower than the average total $^{45}Ca^{2+}$ uptake into WKY prefrontal cortex. Total $^{45}Ca^{2+}$ uptake into the rostral and middle regions of the SHR prefrontal cortex was significantly lower than in WKY while total $^{45}Ca^{2+}$ uptake into the caudal region was not different between the two strains. There was no difference in the average basal $^{45}Ca^{2+}$ uptake into prefrontal cortex or uptake into the rostral, middle and caudal regions of the prefrontal cortex between SHR and WKY. NMDA-stimulated $^{45}Ca^{2+}$uptake into rostral, middle and caudal regions of the prefrontal cortex was not different in the two strains. However, there was a lower average NMDA-stimulated $^{45}Ca^{2+}$ uptake into the prefrontal cortex of SHR compared to WKY. The results from the prefrontal cortex compare with results from the barrel cortex, suggesting that there maybe a disturbance in Ca^{2+} metabolism in the brains of SHR and not necessarily a malfunction in the NMDA receptor. Exposure to an enriched environment did not have an effect on NMDA receptor function in both the barrel and prefrontal cortex.

Chapter 1 Introduction

The rat is a nocturnal animal and uses its olfactory sense and vibrissae to navigate its environment. Tactile information acquired through the vibrissae is therefore of great behavioural significance to rodents. The mystacial vibrissae significantly influenced the performance of rats in a maze (Woosley and Van der Loos, 1970). Without the vibrissae the animals appeared to be lost in their environment and ran through the mazes more slowly (Woosley and Van der Loos, 1970). They held their bodies close to the floor, apparently depending for information on increased contact of their mouths and ventral surfaces with the maze (Woosley and Van der Loos, 1970). If the vibrissae were removed from one side of the snout the rats could run the maze as fast as with all vibrissae intact (Woosley and Van der Loos, 1970). However they preferred to run with their intact side close to the maze edges or walls (Woosley and Van der Loos, 1970). The rat vibrissae system is exquisitely sensitive (Peterson *et al.*, 1998). Using their whiskers, trained rats can reliably discriminate a smooth surface from one with 30 μm grooves separated by 90 μm intervals (Peterson *et al.*, 1998). The vibrissae are linked to the somatosensory cortex of the rat brain by a network of neurons that pass through the thalamic 'relay nuclei' on the way to the cortex (Woolsey and Van der Loos, 1970, Feldmeyer *et al.*, 1999).

The rat somatosensory cortex is organised into a typical lamina form with 6 layers where layer I is distinguished by its relatively low cell density (Keller 1995). Layers II and III are difficult to distinguish because of the packing density of small to medium-sized cells (Keller 1995). Layers II and III are referred to as the

supragranular layers (Staiger *et al.*, 2000b). Layer IV, the granular layer (Staiger *et al.*, 2000b) can be subdivided into two sublaminae IVa and IVb on the basis of the types and packing density of their constituent neurons (Keller 1995). Layer IVa contains a larger number of cells and a higher proportion of spiny cells compared to layer IVb (Keller 1995). Layer V can be subdivided into two sublaminae, one a pale cell-sparse superficial sublamina (layer Va) and another the deeper sublamina (layer Vb) containing the largest somata in the barrel cortex (Keller 1995). Layer VI contains both regular and modified pyramidal cells, and can be subdivided into a superficial sublayer containing small cells and a thinner, deep sublamina of slightly larger cells (Keller 1995). Layers V and VI are referred to as infragranular layers (Staiger *et al.*, 2000b).

The barrel cortex is also composed of functional columns like all cortical areas (Keller, 1995). Barrels are only present in layer IV and each barrel is just a component of a columnar module termed a barrel column extending throughout the thickness of the barrel cortex (Keller, 1995). Cells throughout depths of a barrel column respond preferentially to stimulation of the same, single whisker that is topographically related to the barrel on which that column is centred (Keller, 1995).

Layer IV of the barrel cortex has a unique architecture compared to the other layers and thus it appears to be more specialised (Woosley and Van der Loos, 1970). The cells in the barrel cortex are organised into aggregates and these aggregates of cells are arranged so as to represent the pattern of individual whiskers on the animal's snout and this is referred to as somatotopic mapping (Woosley and Van der Loos, 1970). Woosley and Van der Loos, (1970) called these aggregates of cell bodies,

barrels. The name originates from the shapes of the aggregates observed under Nissl staining (Woosley and Van der Loos, 1970). Each barrel consists of several thousand neurons densely packed in a circular or ellipsoid arrangement (Peterson *et al.,* 1998) surrounding a "hollow", cell sparse area which forms the inside of the barrel (Woosley and Van Der Loos, 1970). The individual barrels are separated by the septum, which is devoid of cells compared to the cell sparse hollow (Woosley and Van Der Loos, 1970). The extent of layer IV containing clusters of barrels is termed the barrel field and the cortical region containing the barrel field is termed the barrel cortex (Keller, 1995). The barrel field in each hemisphere contains 165 to 225 barrels in the rat and 170 to 210 barrels in the mouse (Keller, 1995). Barrels in the anterior portion of the barrel field are of diverse sizes with roughly circular shape (Keller, 1995). They do not show characteristic arrangement of barrels in the posterior portion of the barrel field, which consists of roughly ellipsoid barrels that are constant in number and organisation (Chmielowska *et al.,* 1988, Keller, 1995). The barrels in the posterior portion of the barrel field range between 70 to 300 μm in size while the hollow areas range from 60 to 290 μm. The septum ranges from 2.5 to 20 μm in size (Woosley and Van der Loos, 1970).

Neurons of the barrel cortex

Excitatory neurons in the barrel cortex are mainly spiny stellate or pyramidal neurons, and differ from inhibitory GABAergic neurons by their spherical to ovoid somata (Lubke *et al.,* 2000). In addition the somata of excitatory neurons tend to be larger than that of GABAergic aspiny interneurons but smaller than that of GABAergic interneurons with fusiform somata (Lubke *et al.,* 2000). The spiny cells make up 80% while the remaining 20% is made up by the pyramidal cells (Lubke *et al.,* 2000,

Feldmeyer *et al.*, 1999). Within a single barrel the somata of neurons tend to be organised in clusters of 5 – 15 neurons with a predominant location at the edges of individual barrels (Lubke *et al.*, 2000). Dendritic and axonal arbors of layer IV spiny neurons extend mainly into the barrel hollow (Figure 1.1, Egger *et al.*, 2000) and are confined to the home barrel, the barrel where the soma are located (Peterson and Sakmann, 2000). This happens irrespective of the position of the neuron in the barrel. To account for the spatial arrangement, neurons close to the border of a barrel have polarised axonal and dendritic arbors that are directed towards the centre of the barrel whereas neurons located in the middle of a barrel are less polarised (Peterson and Sakmann, 2000). The function of spiny layer IV neurons within the cortical circuitry differs from that of layer V pyramidal neurons: spiny layer IV neurons receive whisker specific input and distribute their output within the cortical column whereas the layer V pyramidal neurons seem to integrate cortical activity across different columns (Egger *et al.*, 2000).

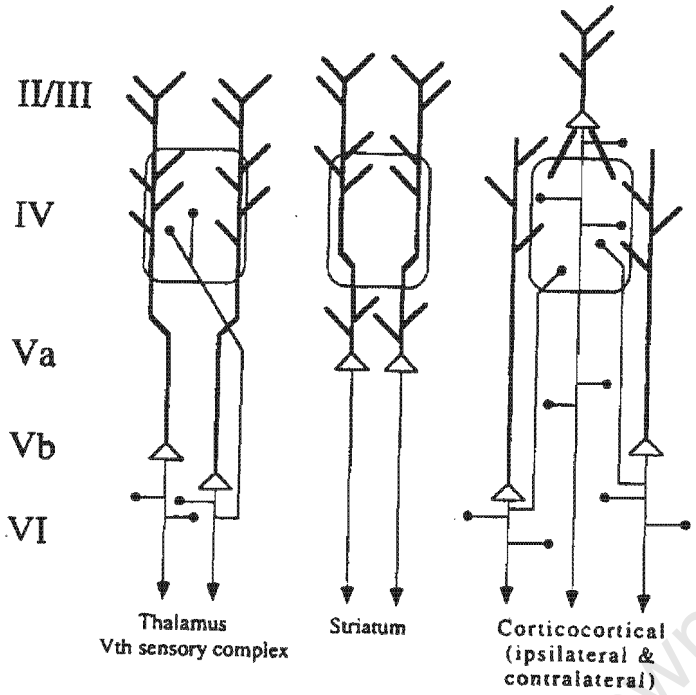

Figure 1.1

Schematic diagram showing the lamina distribution of somata (triangles) belonging to several classes of corticofugal neurons in the barrel cortex. Also depicted are the relationships between the apical and basal dendrites (thick lines) and the axon collaterals (thin lines) and the barrels in layer IV (Keller, 1995).

Pyramidal neurons

Pyramidal neurons are located throughout the layers of the cortex but preferentially in layers II/III and V/VI (Figure 1.1, Keller, 1995). Pyramidal neurons have a prominent apical dendrite extending to middle layer II/III without forming a dendritic tuft (Feldmeyer *et al.*, 1999). The axonal arbor of pyramidal cells can be several millimetres long with both vertical and horizontal collaterals (Feldmeyer and Sakmann, 2000). Vertical axon collaterals form connections between neurons of different layers while horizontal axons form synpatic contacts between neurons in the vicinity of the cell bodies and also with neurons in different cortical columns

(Feldmeyer and Sakmann, 2000). The axons of star pyramidal cells project into all cortical layers and their collaterals are largely confined to a single cortical column (Lubke *et al.*, 2000). The main axon emerges either directly from the soma or from one of the primary basal dendrites and descends towards the white matter (Lubke *et al.*, 2000). The most dense axonal projection is found in layers IV and II/III, but the density of collaterals and the degree of branching of the axon collaterals are less than the axonal arborization of spiny stellate cells (Lubke *et al.*, 2000). Synaptic contacts are located on primary to sexternary branches of the dendrites at distances of 12 μm to 122 μm from the soma (Feldmeyer *et al.*, 1999). Synaptic contacts are only formed by proximal axon collaterals (Feldmeyer *et al.*, 1999).

Two major classes of pyramidal cells are described in layer V and referred to as, the intrisically burst spiking cells (IB) and the regular spiking cells (RS) because of their different properties (Schubert *et al.*, 2001). The intrisically burst spiking cells have large soma and a thick apical dendrite, which gives off oblique collateral branches in layer V and bifurcates in layer IV, giving rise to a rich terminal tuft (Schubert *et al.*, 2001). In addition the intrisically burst spiking cells are capable of discharging high-frequency bursts of action potentials in response to injection of a suprathreshold depolarising current (Schubert *et al.*, 2001). The regular spiking cells have smaller soma and a thinner apical dendrite and the apical dendritic tree as well as the basal dendrites are ramified less extensively compared to the intrisically burst spiking cells (Schubert *et al.*, 2001). The regular spiking cells respond to suprathreshold current injection with a series of single action potentials (Schubert *et al.*, 2001).

Three to seven basal dendrites emerge from the spherical to ovoid soma that give rise to secondary, tertiary and higher-order basal dendrites of various lengths and most of the dendrites are restricted to a single barrel (Lubke *et al.*, 2000). The thick apical dendrite emerges from the upper pole of the soma and ascends through layer IV, giving rise to several oblique apical dendrites (Lubke *et al.*, 2000).

Spiny stellate neurons

The spiny neurons receive sensory input from afferent fibres originating from thalamic relay nuclei and from the axon collaterals of other layer IV spiny stellate neurones located in the same barrel (Feldmeyer and Sakmann, 2000). The first step of intracortical signal processing takes place between synaptically coupled spiny neurons in layer IV before information is relayed to supragranular laminae (Feldmeyer *et al.*, 1999). Spiny layer IV neurons are connected by glutamatergic synapses (Egger *et al.*, 1999). Connected spiny neurons are confined to a single barrel and synaptic contacts are established exclusively within the barrel (Egger *et al.*, 1999; Feldmeyer and Sakmann, 2000). These properties allow synaptically connected spiny stellate neurons within layer IV to function as a cortical amplifier of incoming thalamic signals within the cortical column (Egger *et al.*, 1999; Feldmeyer and Sakmann, 2000). These neurons may boost the stream of excitatory synaptic activity from the thalamus causing widespread activation within a single barrel (Feldmeyer *et al.*, 1999).

The axonal arbor of spiny stellate neurons in the barrel cortex is oriented almost exclusively vertically (Feldmeyer and Sakmann, 2000). It spans all cortical layers up to layer I and down to layer VI and into the white matter (Feldmeyer and Sakmann,

2000) and remains largely confined to a single cortical column (Lubke *et al.*, 2000). The main axon emerges from the soma and descends towards the white matter, giving rise to numerous collaterals (Lubke *et al.*, 2000). The most dense axonal projection of spiny stellate neurons is found in layers IV and II/III where the axons show a high degree of collateralization (Lubke *et al.*, 2000). In these layers most of the axon collaterals are confined to a single cortical column (Lubke *et al.*, 2000).

Spiny stellate cell dendrites in the barrel cortex have a characteristic asymmetric orientation in contrast to spiny stellate cells in layer IV of the visual cortex that display a multipolar, almost radially symmetric dendritic field (Lubke *et al.*, 2000). Three to six thick primary dendrites emerge from the spherical to ovoid somata that give rise to several secondary, tertiary and higher-order dendrites (Lubke *et al.*, 2000). These dendrites form an asymmetric dendritic field of variable size that is confined to a single barrel and is always oriented towards its centre (Lubke *et al.*, 2000).

Inhibitory neurons

Not all neurons in the barrel cortex are excitatory as some were shown to contain the inhibitory γ-aminobutyric acid (GABA) or its synthesizing enzyme glutamic acid decarboxylase (GAD) (Keller, 1995). GABA is the major inhibitory neurotransmitter in the central nervous system (Chmieloska *et al.*, 1988) and is synthesized from glutamate (Figure 1.3, Ganong, 1999). Inhibitory GABAergic neurons are distributed in all layers of the barrel cortex but are more concentrated in the upper portion of layers II/III and in layers IV and VI (Keller, 1995). They are distributed preferentially within barrel sides and include type II multipolar and a subpopulation of bipolar cells (Keller, 1995). GABAergic neurons are very heterogeneous with respect to their

dendritic arborisation and axonal projections (Feldmeyer *et al.,* 1999). GABAergic neurons have different shapes, circular, ellipsiod and fusiform but characteristically in layer IV most GABA cells are circular in appearance (Chmieloska *et al.,* 1988). Chmieloska *et al.,* (1988) suggested several roles for GABAergic neurons according to their location. In the barrel hollow they play a role in preservation of specific information from a single vibrissa, in the barrel centre they are suggested to maintain specific features of a peripheral stimulus such as the direction, velocity and amplitude of vibrissal deflection (Chmieloska *et al.,* 1988). In the barrel side and septa they could participate in the functional interactions that occur between adjacent barrels (Chmieloska *et al.,* 1988).

Incoming signals

Thalamocortical projections

Sensory input to the barrel cortex originates from the subcortical and cortical areas involved in processing sensory information from the vibrissae and in motor control of whisking behaviour (Keller, 1995). Sensory afferent pathways from the whiskers project first to the trigeminal nuclei (Figure 1.2, Wright *et al.,* 2000, Keller, 1995) from which they form two parallel pathways, the lemniscal and paralemniscal pathways (Figure 1.2, Ahissar *et al.,* 2000). The lemniscal pathway ascends through the ventral posterior medial nucleus of the thalamus to layer IV of the cortex and to layers Vb and VI (Ahissar *et al.,* 2000). The paralemniscal pathway ascends through the medial division of the posterior nucleus of the thalamus to layers I and Va and to the septa between the barrels in layer IV (Ahissar *et al.,* 2000). Of the two pathways the lemniscal pathway is the predominant one (Keller, 1995). Sensory afferents

terminate primarily on the cells of layer IV where their extent is matched by the outline of the barrels (Wright *et al.*, 2000). Individual thalamic afferents usually form, within layer IV, a single cluster of axon terminals that occupies the entire vertical height of a single barrel (Keller, 1995). In addition some afferents from the ventral posterior medial nucleus of the thalamus branch and form terminal clusters in layers Vb and VIa, below a barrel hollow, and a few afferents project to and terminate in layer I – III (Keller, 1995). Thalamic afferents only form about 19% of the total synapse population in the barrel hollows (Keller, 1995) while the remaining excitatory connections are with other cortical neurons including other spiny stellate cells (Fleidervish *et al.*, 1998).

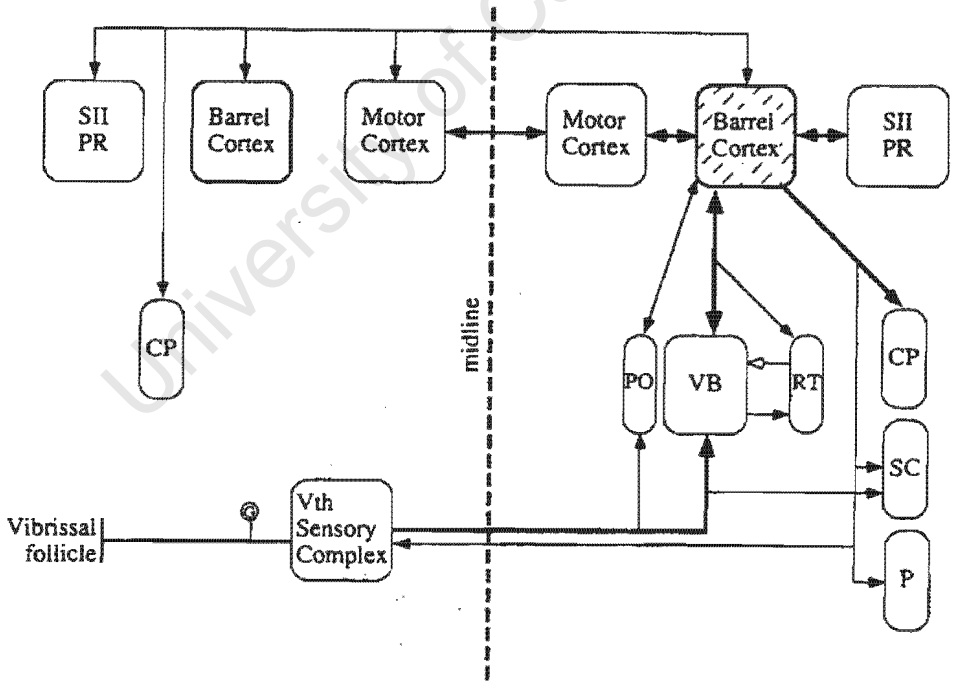

Figure 1.2: A schematic diagram summarising the major afferent and efferent pathways involving the barrel cortex. The relative magnitude of a pathway is represented by the thickness of the arrows, filled arrowheads indicate excitatory

interactions, open arrowheads represent inhibitory inputs. Abbreviations CP, caudate-putamen; G, Gasserian ganglion; P, pons: PO, posterior nucleus of the thalamus; PR, perirhinal cortex; RT, reticular nucleus of the thalamus; SC, superior colliculus; SII, secondary somatosensory area; VB, ventrobasal nucleus of the thalamus (Keller, 1995).

Corticocortical projections

Intracortical connections of the barrels are predominantly to the regions surrounding the barrels themselves (the septa) (Wright *et al.*, 2000). Intracortical synaptic interactions and enhanced propagation of thalamic input in the barrel cortex are dependent on activation of NMDA receptors (Laaris *et al.*, 2000) since the NMDA receptor antagonist AP5 suppressed the enhanced propagation of thalamic input (Laaris *et al.*, 2000). The barrel cortex is reciprocally connected with a number of ipsilateral and contralateral cortical regions (Keller, 1995).

Ipsilateral corticocortical projections

The ipsilateral connections with other cortical areas arise from cells in the infragranular and supragranular layers of the barrel cortex and project to the face area of the secondary somatosensory cortex (SII), the primary motor cortex and the perirhinal cortex (Figure 1.2, Keller, 1995). Projections from the barrel cortex to the secondary somatosensory cortex and to the motor cortex appear to be topographical in that the afferents from the posterior portion of the barrel field cortex terminate in a single dense cluster in these areas (Keller, 1995). Reciprocal connections from the secondary somatosensory cortex and primary motor cortex are also topographically mapped terminating in a restricted columnar zone within the barrel field (Keller, 1995).

Contralateral corticocortical projections

The barrel cortex is connected to the contralateral barrel field, SII and the perirhinal cortex via the callosal pathways (Keller, 1995). The corpus callosum connects the primary cortices of both hemispheres (Hayama and Ogawa, 1997). Inputs from the callosal projections terminate within the dysgranular or intercalated zones surrounding the barrels and in the barrel septa while few callosal axons terminate within barrel hollows (Keller, 1995).

Outgoing signals

Projections to Subcortical areas

Output from the barrel cortex is sent to the subcortical areas that include the ipsilateral and contralateral striatum (caudate-putamen), superior colliculus, the pons, the contralateral trigeminal complex (Figure 1.2, Keller, 1995) and the ventral posterior medial nucleus of the thalamus and the ipsilateral posterior nucleus of the thalamus (White and DeAmics, 1977). Efferent projections from individual barrel columns maintain a topological relationship with some of their target sites (Keller, 1995). Efferents to the trigeminal sensory complex terminate within the termination zone of primary trigeminal afferents of individual vibrissa follicles and may be involved in facilitation of trigeminothalamic afferents (Keller, 1995). Efferents to the ventral posterior medial nucleus of the thalamus project to a series of barreloids representing an arc of whiskers (Keller, 1995). Barreloids are cell aggregates found in the medial portion of the ventrobasal nucleus of the thalamus, arranged in the pattern of rows and arcs that resemble the distribution of vibrissae on the face (Land *et al.*, 1995). Projections from a single barrel column to the superior colliculus terminate within the

representation of a single arc of whiskers (Keller, 1995). Corticothalamic projections may be involved in modulation of transmission of somatosensory inputs to the barrel cortex (Keller, 1995). The dorsolateral neostriatum also receives excitatory projections from the barrel cortex, referred to as corticostriatal projections (Alloway *et al.,* 1999). Corticostriatal projections from barrels representing either posterior or anterior whiskers merge into each other and occupy overlapping parts of the neostriatal neuropil (Alloway *et al.,* 1999).

Synapses within the barrel cortex

Synapses in the barrel cortex include both types of chemical synapses namely asymmetric and symmetric synapses (Keller, 1995). Asymmetric synapses represent zones of excitatory synaptic transmission whereas symmetric synapses are inhibitory and contain either GABA or its synthetic enzyme glutamic acid decarboxylase (Keller, 1995). A large proportion of synapses in the barrel cortex is asymmetrical indicating that neural elements in the barrel cortex are subjected to excitatory synaptic inputs (Keller, 1995). Thalamocortical synapses are specific and the specificity of cortical circuitry involving thalamic afferents is related to the number and location of synapses a thalamic axon forms with particular postsynaptic targets (Keller, 1995).

Synaptic contacts made by cortical projection neurons onto target neurons are exclusively found on dendrites within layer IV and they are distributed over the entire dendritic arbor but are preferentially established on tertiary dendritic branches (30%) (Feldmeyer *et al.,* 1999). Most contacts are relatively close to the soma; however, a few were located at more distal portions of the dendrite (Feldmeyer *et al.,* 1999). The majority (70%) of putative synaptic contacts are established on the dendritic spines

and the remainder are found on dendritic shafts (Feldmeyer *et al.,* 1999). The highest number approximately 70%, of synaptic boutons, estimated by counting the number of boutons in each layer, is found in layers IV and II/III with the highest density in layers II/III for both spiny stellate and star pyramidal neurons (Lubke *et al.,* 2000). The remaining 30% of synaptic boutons is found in layers V and VI (Lubke *et al.,* 2000). In both the spiny stellate and star pyramidal neurons the number of synaptic boutons per 100 μm axonal segment is significantly higher in layers II/III compared to other layers (Lubke *et al.,* 2000). The fact that the number of axonal collaterals as well as the density of synaptic boutons was highest in layers IV and II/III suggests that the main stream of excitation via spiny layer IV neurons is directed to layers IV and II/III (Lubke *et al.,* 2000).

Glutamate

Glutamate is the major neurotransmitter in the CNS for rapid neuronal excitation (Nakanishi, 1992) and is found in high concentrations in the central nervous system (Zigmond *et al.,* 1999). Glutamate is produced from glucose through the Krebs cycle and transamination of α-ketoglutarate, an intermediate in the tricarboxylic acid cycle of intermediary metabolism (Figure 1.3a, Zigmond *et al.,* 1999). Glutamate is also formed directly from glutamine which is synthesised in glial cells through the action of an enzyme glutaminase (Figure 1.3b, Zigmond *et al.,* 1999). Glutamate released into the synapse is taken up into glial cells where it is converted to glutamine by the enzyme glutamine synthase (Kandel *et al.,* 1999). Glutamine is taken up into glutamatergic neurons where it is converted to glutamate by the enzyme glutaminase (Zigmond *et al.,* 1999).

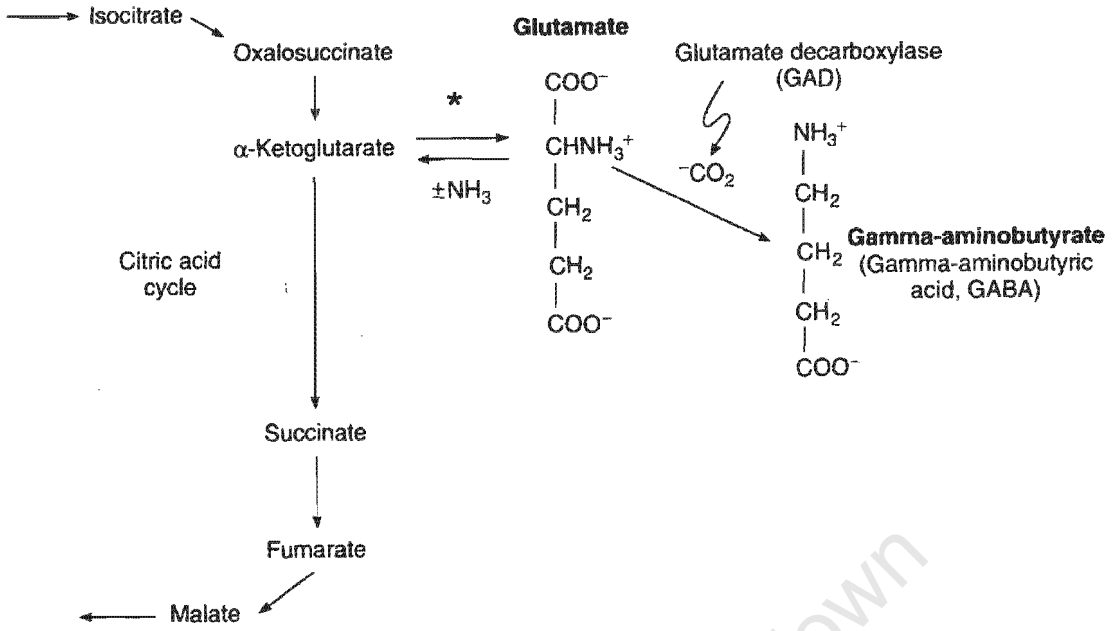

*Figure 1.3a Formation of glutamate and GABA from α-Ketoglutarate by transamination process * indicates glutamic acid dehydrogenase (Adapted from Ganong, 1999).*

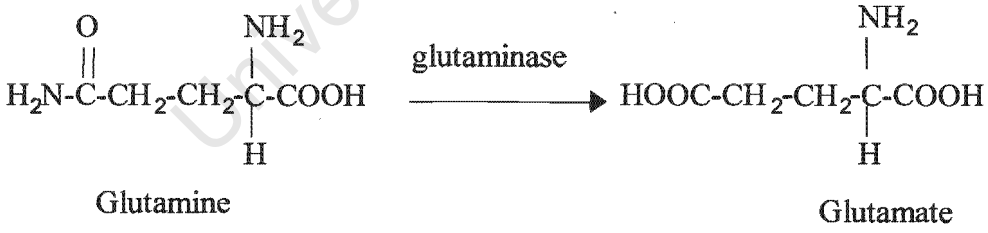

Figure 1.3b Formation of glutamate from glutamine (Adapted from McGeer et al., 1986)

Classification of Glutamate receptors

Spiny layer IV neurons in the barrel cortex are connected by glutamatergic synapses (Egger *et al.,* 1999). The effects of glutamate are mediated by glutamate receptors which are divided into two major classes, namely the metabotropic glutamate receptors (mGluRs) and the ionotropic glutamate receptors (Zigmond *et al.,* 1999). At ionotropic receptors glutamate is excitatory while at metabotropic receptors it is modulatory (Kandell *et al.,* 1999). Glutamate acts on both ionotropic and metabotropic receptors with similar efficiency indicating that metabotropic glutamate receptors share important roles in glutamate transmission with the ionotropic receptors (Nakanishi, 1994).

Metabotropic Glutamate receptors

Metabotropic glutamate receptors (Figure 1.4) are 7 trans-membrane domain proteins like other G protein-coupled receptors and share more than 40% amino acid sequence homology (Nakanishi, 1992). Despite their overall similarity with other G protein coupled receptors, the metabotropic glutamate receptor family seems to be quite distinct evolutionarily, since they show no sequence similarity to a vast majority of the G protein-coupled receptors (Nakanishi, 1994). They also possess an unusually long extracellular domain consisting of about 550 amino acids following the N-terminal signal peptide (Nakanishi, 1994). The large extracellular domain of metabotropic glutamate receptors is responsible for glutamate binding while receptors for ligands such as dopamine, epinephrine and acetylcholine, have transmembrane pockets that are used as ligand binding sites (Nakanishi, 1994). Compared to ionotropic receptors, metabotropic glutamate receptors mediate relatively slow

glutamate responses by coupling to intracellular signal transduction via G-proteins (Nakanishi, 1994). Activation of different groups of metabotropic glutamate receptors can have either excitatory or inhibitory effects on neuronal activities (Ozawa *et al.*, 1998).

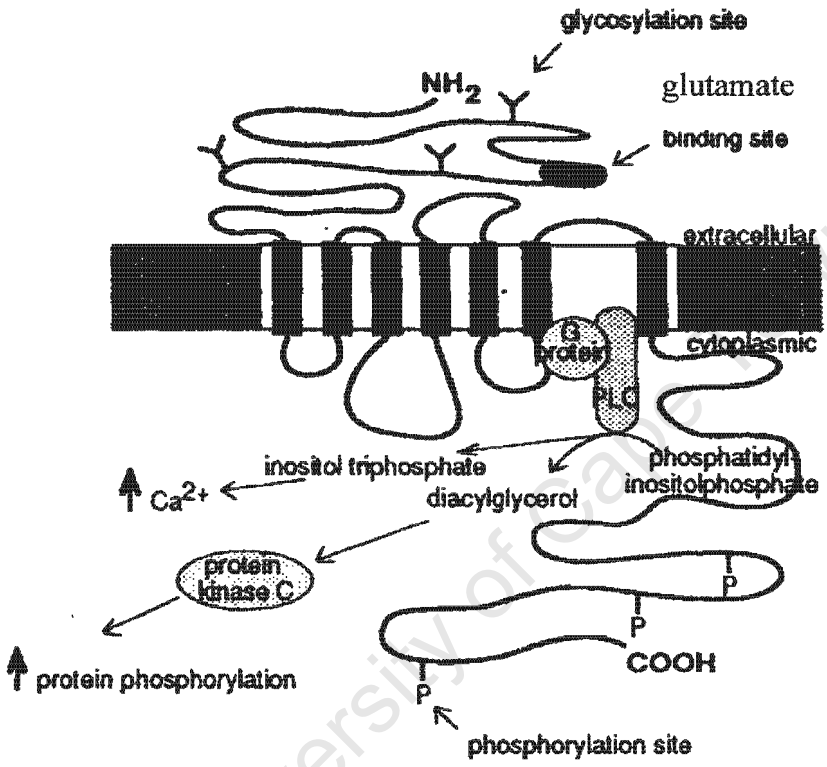

Figure 1.4: Schematic representation of a metabotropic glutamate receptor showing sites for various agonists, antagonists and modulators and for secondary modification (Hollmann and Heinemann, 1994). Abbreviation: PLC phospholipase C

Metabotropic glutamate receptors consist of at least 8 subtypes (mGluR1 – mGluR8) and are classified into three groups (Janssens and Lesage, 2001) according to their sequence similarities, signal transduction mechanisms and agonist selectivities (Nakanishi, 1994). Group 1 consists of mGluR1 and mGluR5, and they act by

stimulating phospholipase C (Janssens and Lesage, 2001) which in turn hydrolyses phosphatidylinositol phosphates (PIPs) to give inositol triphosphate (IP_3) and diacylglycerol (DAG) (Kennedy, 1989). The increase of inositol triphosphate and diacylglycerol leads to release of Ca^{2+} from intracellular stores (Ozawa *et al.*, 1998) and activation of Ca^{2+} dependent kinases respectively (Zigmond *et al.*, 1999). They respond strongly to quisqualate which is a glutamate agonist (Nakanishi, 1992).

Group 2, consists of mGluR2 and mGluR3 while group 3 consists of mGluR4, -6, -7 and –8. These two groups act by inhibiting adenylyl cyclase (Janssens and Lesage, 2001). Group 2 mGluRs show strong inhibition of forskolin-induced cyclic adenosine monophosphate (cAMP) formation (Ozawa *et al.*, 1998). Maximal inhibition of cAMP formation was somewhat smaller for the group 3 receptors (Ozawa *et al.*, 1998). Group 2 and 3 are strongly inhibited by pertusis toxin, suggesting that the G-proteins involved in coupling are of the Gi family (Ozawa *et al.*, 1998). Despite a known classification of glutamate as an excitatory neurotransmitter, the activation of certain groups of metabotropic glutamate receptors is known to cause inhibitory effects (Nakanishi, 1994).

Metabotropic glutamate receptors regulate neuronal excitability by inducing a slow depolarization accompanied by an increase in firing rate in many neurons (Ozawa *et al.*, 1998). These excitatory effects could be attributed to direct actions on several K^+ channels (Ozawa *et al.*, 1998). In addition to direct excitatory postsynaptic effects mGluR activation was shown to suppress both excitatory and inhibitory transmission at synapses by presynaptic mechanisms (Ozawa *et al.*, 1998). These presynaptic mGluRs may play important roles in activity-dependent regulation of synaptic

functions since they have been reported to not only serve as 'autoreceptors' to suppress excitatory transmission but also induce plasticity due to a presynaptic mechanism (Ozawa *et al.*, 1998).

Ionotropic glutamate receptors

Ionotropic glutamate receptors are oligomeric assemblies of membrane proteins which form cation-selective ion channels and mediate most excitatory neurotransmission in the mammalian central nervous system (Ripellino *et al.*, 1997). They have been characterised as four trans-membrane domain proteins (Bettler and Mulle, 1995). The putative channel lining segment M2, loops into the membrane without traversing it (Bettler and Mulle, 1995). All mammalian ionotropic receptors are encoded by sequence related genes (Bettler and Mulle, 1995). There is however no significant sequence homology between glutamate receptors and other ligand-gated ion channels including $GABA_A$, nicotinic, acetylcholine or serotonin receptors (Bettler and Mulle, 1995). Ionotropic glutamate receptors are rapid acting, ligand-gated and have been classified into three distinct subtypes, the α-amino-3-hydroxy-5-methyl-4-isoxazole propionic acid (AMPA) receptors, kainate receptors (sometimes referred to as non-NMDA receptors) and N-methyl-D-aspartate (NMDA) receptors according to their structure and pharmacology (Varju *et al.*, 2001).

non-NMDA Receptors

AMPA Receptors

AMPA receptors are widely and abundantly distributed throughout the entire vertebrate nervous system (Bettler and Mulle, 1995) although regional differences are

conspicuous (Ozawa *et al.,* 1998). Brain regions that are rich in high affinity [^{3}H]AMPA binding include the hippocampus and cerebral cortex (Ozawa *et al.,* 1998). Intermediate levels are found in the deeper layers of the cortex and in the caudate-putamen while lower levels are found in the diencephalon, midbrain and brainstem (Ozawa *et al.,* 1998).

AMPA receptors are found in the majority of excitatory synapses where they mediate the majority of all fast excitatory neurotransmission (Seeburg, 1993). Their rapid kinetics render them ideally suited for this purpose (Seeburg, 1993). The generally very low Ca^{2+} permeability of AMPA receptor channels means that glutamate-activated ionic currents mediated by these channels do not carry sufficient Ca^{2+} ions into cells to initiate biochemical and cell biological processes triggered by an increase in intracellular Ca^{2+} levels (Seeburg, 1993).

AMPA receptors are formed from subunit proteins GluRs 1 – 4 encoded by a family of genes (Ripellino *et al.,* 1997). AMPA receptor subunits co-localise within cell bodies, dendrites or dendritic spines and are found to be clustered at postsynaptic sites consistent with the function of glutamate in synaptic transmission (Bettler and Mulle, 1995). Some AMPA receptors are Ca^{2+} permeable while some are impermeable (Wollmuth and Sakmann, 1998). Ca^{2+} impermeable AMPA receptors contain the edited form of the GluR – 2 subunit termed GluR –2 (R) which contains an arginine (R) at the functionally critical Q/R site (Wollmuth and Sakmann, 1998). AMPA receptor channels containing only the GluR –1, –3 or –4 subunits, which contain a glutamine (Q) at this position, are Ca^{2+} permeable (Wollmuth and Sakmann, 1998) and show high but not exclusive selection of Ca^{2+} over monovalent alkali cations like

K^+ and Na^+ (Wollmuth and Sakmann, 1998). A role has yet to be assigned to the Ca^{2+} permeability of AMPA receptor channel activation following synaptic release of glutamate (Bettler and Mulle, 1995). It has been proposed that long term potentiation (LTP) is due to both an increase in neurotransmitter release and to an increase in the postsynaptic AMPA/kainate response (Bettler and Mulle, 1995). Although the molecular mechanism is not understood, AMPA receptor function is decreased in long term depression (LTD). It has been proposed that increased activation of protein kinase C (PKC) may be accountable (Bettler and Mulle, 1995). AMPA receptors have at least three separate binding sites at which agonists or antagonists can bind: glutamate binding site, desensitization site and the intra-ion channel binding site (Ozawa *et al.*, 1998).

Kainate receptors

Kainate, a potent agonist of AMPA receptors, also activates a distinct class of GluRs, the kainate preferring receptors (Ozawa *et al.*, 1998) hence the name, kainate receptors. Kainate receptor channels are formed from two families of genes GluRs 5-7; KA1 and KA2 (Ripellino *et al.*, 1997). GluR 5 – 7 subunits are of similar size and share 75 – 80% amino acid sequence identity with each other and approximately 40% identity with AMPA receptor subunits GluR1 – GluR4 (Ozawa *et al.*, 1998). GluRs 5-7 subunits form low affinity kainate receptors (Ozawa *et al* 1998, Bettler and Mulle, 1995). KA1 and KA2 subunits are somewhat larger than GluR 5 – 7and share 70% amino acid sequence identity with each other and about 40% with either GluR1 – GluR 4 or GluR 5- GluR 7 (Ozawa *et al.*, 1998). KA1 and KA2 subunits form high affinity kainate receptors (Ozawa *et al.*, 1998, Bettler and Mulle, 1995). No direct involvement of kainate receptors in synaptic transmission has been demonstrated,

hence it has been proposed that kainate receptors might have a modulatory role at the synapse (Bettler and Mulle, 1995).

Each subunit that forms kainate receptors is differentially distributed in the CNS (Ozawa *et al.,* 1998). The KA1 mRNA occurs mainly in the hippocampus while the KA2 mRNA is almost universally distributed (Ozawa *et al.,* 1998). The GluR5 mRNA is found in the cingulate and pirifiorm cortex, the subiculum, various septal nuclei and cerebellar purkinje cells (Ozawa *et al.,* 1998). The GluR6 mRNA is most abundant in cerebellar granule cells with lower levels in caudate-putamen and hippocampus (Ozawa *et al.,* 1998). GluR7 transcripts are present in the deep cerebral cortex, cingulate cortex, subiculum, caudate-putamen, reticular thalamus and stellate basket cells in the cerebellum (Ozawa *et al.,* 1998).

Kainate receptors also have important functions in development (Ripellino *et al.,* 1997). Focal application of glutamate or kainate slows the rate of neuronal growth cone extension (Ripellino *et al.,* 1997). Their activation also alters neurite development in cerebellar granule cells and may in part regulate the number of neurons in the developing cerebellum (Ripellino *et al.,* 1997).

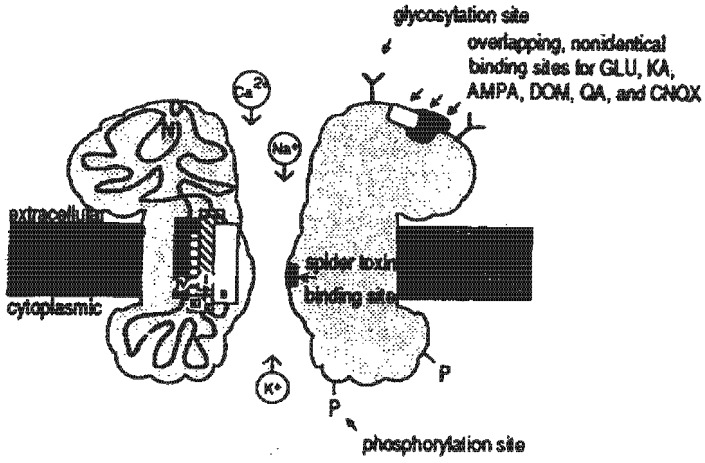

Figure 1.5

Schematic representation of an AMPA/KA receptor indicating sites for various agonists, antagonists and modulators (Hollmann and Heinemann, 1994). Abbreviations: GLU glutamate; KA kainate; AMPA, α-amino-3-hydroxy-5-methyl-4-isoxazole propionic acid; DOM domoic acid, QA quisqualate; CNQX 6-cyano-7-nitroquinoxaline-2,3-dione

NMDA receptors

The NMDA receptor is a rapid acting ligand-gated cation channel with a high permeability to Ca^{2+}(Chazot *et al.*, 1994). The NMDA receptor channel differs in fundamental ways from the non-NMDA receptor channels, and these properties relate directly to its physiological roles (Mori and Mishina, 1995). Molecular studies led to the identifying of 2 subunit families of the rat NMDA receptor designated as NMDAR1 (NR1) and NMDAR2 (NR2) subunit families (Mori and Mishina, 1995). NMDA receptors are heteromeric assemblies of subunits of which NR1 is required for functional receptors and at least one of the four NR2 subunits (NR2A, NR2B, NR2C,

Overactivaton of NMDA receptors on the other hand has been associated with a number of clinical conditions like cerebral hypoxia/ischemia, hypoglycemia, seizure disorders and traumatic brain injury (Wilson *et al.,* 1998). Overactivation of NMDA receptors causes necrotic neuronal death (Gasull *et al.,* 2001).

NMDA receptors and exposure to an enriched environment

It has been suggested that the NMDA receptor channel is involved in synaptic plasticity during development (McDonald and Johnston, 1990). Plasticity refers to the ability of the brain to change its structure and function (Kolb and Whishaw, 1998). Experience is the major stimulant of brain plasticity in animal species as diverse as insects and humans (Kolb and Whishaw, 1998). There are large neural changes associated with experience. These include increases in brain size, cortical thickness, neuron size, dendritic branching, spine density, synapses per neuron, and glial numbers (Kolb and Whishaw, 1998). Experience can either be in the form of exposure to an enriched environment or task specific training (Kolb and Whishaw, 1998). Exposure to an enriched environment provides animals with informal learning opportunities (Rosenzweig and Bennett, 1996).

At the molecular and biochemical level, exposure to an enriched environment over a period of time was shown to cause increased higher order dendritic branching in the visual cortex of kittens (Volkmar and Greenough, 1972). Exposure to an enriched environment has also been shown to increase brain weights (Por *et al.,* 1982, Rosenzweig *et al.,* 1968) and to increase both acetylcholine esterase activity and choline esterase activity (Rosenzweig *et al.,* 1968). Increases in expression of early

immediate genes in rat barrel cortex have been reported after exposure to an enriched environment (Filipkowski *et al.,* 2000, Staiger *et al.,* 2000a) and after direct stimulation of whiskers in rats (Filipkowski *et al.,* 2000). On the other hand prior exposure of rats to an enriched environment did not have an effect on dopamine/serotonin, α or β adrenergic, muscarinic/cholinergic or GABA receptor levels when compared to rats reared in the normal environment (Por *et al.,* 1982). Exposure to an enriched environment did not have an effect on dopamine D1 and D2 receptor densities in the nucleus accumbens either (Bardo and Hammer, 1991).

Environmental enrichment is described, in an experimental setting, as enriched in relation to the standard housing conditions in the laboratory where animals are always kept (Van Praag *et al.,* 2000). The animals in an enriched environment are kept in larger cages containing a variety of novel objects such as toys, nesting materials, and tunnels which are changed routinely (Kolb and Whishaw, 1998, Van Praag *et al.,* 2000). In addition the animals are placed in large numbers in the cage to allow for more complex social interaction (Van Praag *et al.,* 2000). A combination of the novel objects and the social interaction then gave rise to the description of the enriched environment as a combination of inanimate and social stimulation (Van Praag *et al.,* 2000).

As earlier mentioned, NMDA receptors are important in learning and memory (Mori and Mishina, 1995). Exposure to an enriched environment improved the animals' ability to learn and solve problems (Rosenzweig, 1996). It was found that animals with prior exposure to an enriched environment perform better than animals from a normal cage when presented with complex tasks (Rosenzweig, 1996). However it

was found that the animals from an enriched environment did not maintain their dominance over animals from the impoverished rearing conditions, the latter tended to catch up after a series of trials (Rosenzweig, 1996). It has been shown that experience is necessary for full growth of the brain in different species of the crow family (Rosenzweig, 1996). Species that cache food in a variety of locations for future use were found to have larger hippocampal formations than related species that do not cache food (Sherry *et al.,* 1989 in Rosenzweig, 1996). When animals were trained in specific tasks, specific changes were demonstrated in the dendritic fields of specific neurons associated with that task (Kolb and Whishaw, 1998). For example when one eye was occluded and rats were trained in a visual maze, the dendritic fields of the neurons of the trained eye were larger compared to the dendritic fields of the neurons of the non-trained eye. Depriving one eye of light in a young animal, starting at the age at which the eyes first open, reduced the number of cortical cells responding to subsequent stimulation of that eye (Rosenzweig, 1996). It was also found that olfactory deprivation not only led to restricted morphological development but resulted in reductions in neuronal number in the olfactory system whereas olfactory training or olfactory enrichment (enriched ordor exposure) led to enhanced development i.e increased neuron numbers (Kolb and Whishaw, 1998). Training and enriched environment experience helps in recovery from or compensates for effects of brain damage (Rosenzweig, 1996).

Experience-dependent change in the brain is modulated by several factors including sex hormones, neurotrophins, stress, injury and ageing (Kolb and Wishaw, 1998). There is evidence that male and female brains are different in their structure and that they respond differently to experience (Kolb and Wishaw, 1998). Neurotrophins,

chemicals known to have growth properties in the nervous system, influence dendritic structure (Kolb and Wishaw, 1998). Stress on the other hand has effects on the neuroendocrine system and this in turn has been shown to affect cell morphology (Kolb and Wishaw, 1998).

NMDA receptors and Ageing

During ageing there is both death of neurons and regression of dendrites of cells that have not yet died (Buell and Coleman, 1979). Regression of dendrites can be seen in some cells while dendrites of other cells are growing and growth of dendrites is the dominant observation (Buell and Coleman, 1979). There are two populations of neurons in the normal ageing cortex, one a group of dying neurons with shrinking dendritic trees, the other a group of surviving neurons with expanding dendritic trees (Buell and Coleman, 1979). In normal ageing the latter group prevails (Buell and Coleman, 1979). The process of ageing not only affects the number of neurons or dendritic branches, it is accompanied by several changes that occur in central neurotransmitter systems (Ossowska *et al.,* 2001). These changes include among others, decreases in the dopamine levels, decreases in the number of dopamine neurons and D1 and D2 receptors (Ossowska *et al.,* 2001). The process of ageing is also marked by a decline in the density of NMDA receptors in the hippocampus (Tremblay *et al.,* 1988, Wenk and Barnes, 2000), the cerebral cortex (Serra *et al.,* 1993) and in the inner frontal and entorhinal cortices of rats (Mitchell and Anderson, 1998). The decline in the NMDA receptor levels of rats has been shown to be responsible for the decline in motor function associated with ageing (Ossowska *et al.,* 2001).

Calcium and its role in neurotransmission

Calcium is an important signalling molecule in the central nervous system and has a dual role as a carrier of electrical current and as a second messenger (Zigmond *et al.*, 1999). Influx of calcium mediates a variety of processes at the level of the cell membrane and in the cytosol (Kennedy, 1989). At the membrane level Ca^{2+} directly regulates certain potassium channels, cation-selective channels and chloride channels (Kennedy, 1989). The rise in intracellular calcium concentration $[Ca^{2+}]_i$ causes activation of phospholipase C (PLC) and phopholipase A2 which in turn produce second messengers (Kennedy, 1989). Transient increases in the intracellular concentration of Ca^{2+} are required for neurotransmitter release from presynaptic neurons to occur (Fossier *et al.*, 1999). In the cytosol Ca^{2+} activates protein kinase C which in turn moves to the membrane where it regulates electrical excitability by phosphorylating certain ion channels (Kennedy, 1989). Ca^{2+} activates a group of neutral proteases called calpains that are implicated in the regulation of membrane proteins and the cytoskeleton (Kennedy, 1989). Finally, in the cytosol Ca^{2+} binds to calmodulin (CaM) which is a ubiquitous Ca^{2+} binding regulatory protein. In its Ca^{2+}-bound form CaM binds to specific proteins with different affinities and alters their properties (Kennedy, 1989). An example of the proteins is type II CaM kinase which has a "switch-like" regulation by autophosphorylation that suggests that it could play a role in the generation of long-lasting forms of synaptic plasticity such as long term potentiation (Kennedy, 1989). Another protein activated by the Ca^{2+} bound form of CaM is calcineurin which is a phosphatase that desensitises the L-type voltage dependent Ca^{2+} channels (Kennedy, 1989). Also Ca^{2+} mediates gene expression (Melena and Osborne, 2000) as transient changes in $[Ca^{2+}]_i$ trigger the transcription of immediate early genes such as c-fos and c-jun in the nucleus (Kennedy, 1989). These

genes encode DNA-binding proteins that initiate or modulate the expression of other genes leading to long term changes in neuronal function (Kennedy, 1989).

Calcium plays an important role in development of the central nervous system as it has been shown that depletion of intracellular calcium strongly decreased the density of filopodia, arrested axonal outgrowth and strongly decreased dendritic branching (Ramakers *et al.,* 2001). Prevention of calcium influx through L-type voltage-sensitive calcium channels decreased dendritic branching (Ramakers *et al.,* 2001). For actively elongating neurites and motile growth cones, the $[Ca^{2+}]_i$ has to be in the range of 100 to 300 nM (Kennedy, 1989) and any concentration below or above this range is associated with arrest of neurite elongation and cessation of movement of the growth cone (Kennedy, 1989). Calcium is found in very low concentrations of approximately 100 nM in cells (Ghosh and Greenberg, 1995).

For calcium to fulfill its functions within cells its concentration has to rise to about 0.5 - 1 μM (Zigmond *et al.,* 1999). The rise in intracellular calcium is caused by either an influx from the extracellular medium or release from intracellular stores. Influx from the extracellular medium occurs through a variety of mechanisms like the voltage-sensitive calcium channels (Saadoun *et al.,* 1997), ligand-gated receptors and the Ca^{2+} leak pathways (Triggle, 1990). The opening of voltage-sensitive calcium channels is regulated by the local membrane potential (Gosh and Greenberg, 1995). The voltage-sensitive calcium channels have been classified into a number of subtypes according to electrophysiological criteria, sensitivity to pharmacological agents (Gosh and Greenberg, 1995, Triggle, 1990) as well as permeation selectivity (Triggle, 1990). In the central nervous system neurons most of the voltage-sensitive calcium channels

current appears to be carried by the L-, N- and P-type calcium channels (Gosh and Greenberg, 1995). Influx from the extracellular medium can also be through the ligand-gated receptors like the NMDA receptors and to some extent the calcium permeable AMPA and kainate receptors (Gosh and Greenberg, 1995).

Another mechanism of raising intracellular calcium concentrations is via release from intracellular stores of which there are two pools. The first is the endoplasmic reticulum (Gosh and Greenberg, 1995) and the other is the mitochondria (Triggle, 1990). Release from the endoplasmic reticulum is mediated by two distinct mechanisms (Gosh and Greenberg, 1995, Mattson *et al.,* 2000). The first mechanism of release from endoplasmic reticulum happens in response to agonists that activate G-protein coupled receptors and subsequent activation of PLC leading to the production of diacylglycerol and IP_3, subsequently the binding of IP_3 to its receptors leads to channel opening in the endoplasmic reticulum (Mattson *et al.,* 2000, Gosh and Greenberg, 1995). The other mechanism of release from endoplasmic reticulum stores is regulated by the activation of the ryanodine receptor (Gosh and Greenberg, 1995, Mattson *et al.,* 2000). Release from mitochondria is via the mitochondiral Na^+/Ca^{2+} exchange (Triggle, 1990).

In order to maintain the low intracellular calcium concentration, the cell uses two mechanisms. Firstly calcium can be pumped out of the cell via the Ca^{2+}/Na^+ exchange mechanism which extrudes one calcium molecule while transporting two Na^+ molecules into the cell (Triggle, 1990). Secondly the cell uses the ATP- and calmodulin dependent Ca^{2+} transport across the plasma membrane to transport calcium out of the cell (Saadoun *et al.,* 1997, Triggle, 1990). These pumps act against

a steep concentration gradient provided by the high calcium concentration in the extracellular space.

Another mechanism used by cells to maintain the low intracellular calcium levels is the uptake of calcium into internal stores, namely, the endoplasmic reticulum and mitochondria. Uptake into endoplasmic reticulum occurs via an ATP dependent pump (Mattson *et al.,* 2000, Triggle, 1990) called SERCA (smooth ER Ca^{2+} ATPase) (Mattson *et al.,* 2000) while uptake into mitochondria occurs through either a Ca^{2+}/Na^{+} exchange (Triggle, 1990) or through a calcium uniporter (Kannurpatti *et al.,* 2000, Peng and Greenamyre, 1998). In addition to serving as the neuron's primary source of energy, mitochondria act as important buffers of cytosolic calcium and help to prevent excessive and prolonged elevation of the internal calcium concentration (Peng and Greenamyre, 1998). The huge electrochemical proton gradient across the inner mitochondrial membrane, generated by active extrusion of protons along the electron transport chain, provides a strong driving force of calcium uptake through a calcium-selective uniporter (Peng and Greenamyre, 1998). Indeed, Peng and Greenamyre, (1998) have shown that calcium influx through NMDA receptors has privileged access to mitochondria compared to calcium coming from other sources and suggested two possible reasons: (1) NMDA receptors allow more Ca^{2+} to enter the cell in a short time, (2) it is possible that mitochondria are in closer proximity to NMDA receptors than other routes of entry (Peng and Greenamyre, 1998). Calcium taken into mitochondria and endoplasmic reticulum forms intracellular stores of calcium which can also be used to increase the intracellular calcium concentration when the need arises (Zhang and Lipton, 1999).

The regulation and homeostasis of calcium is summarised in Figure 1.7

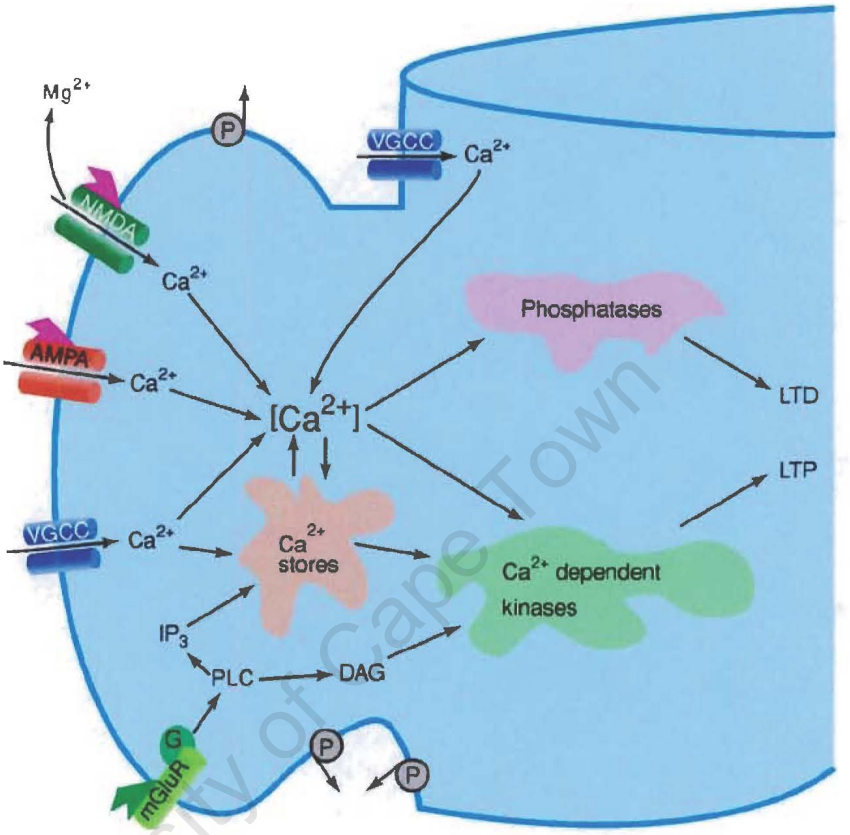

Figure 1.7

Schematic diagram depicting a postsynaptic spine showing Ca^{2+} entry through AMPA and NMDA receptors (after removal of Mg^{2+} block) and entry through voltage-gated calcium channels (VGCCs). Also shown is uptake into and release from internal stores as well as processes in which calcium is involved (LTP and LTD). (Zigmond et al., 1999). Abbreviations: AMPA α-amino-3-hydroxy-5-methyl-4-isoxazole propionic acid; DAG diacylglycerol; G g-protein; LTD long term depression; LTP long term potentiation; mGluR metabotropic glutamate receptor; NMDA N-methyl-D-aspartate; IP_3 inositol triphosphate; PLC phopholipase C; VGCC voltage-gated calcium channels

NMDA receptor toxicity

Depending on the mode of entry into the cell the influx of calcium can have different effects. For example influx through voltage-sensitive calcium channels can lead to increased survival of embryonic neurons from the central and peripheral nervous system (Ghosh and Greenberg, 1995) while influx through NMDA receptors mediates excitotoxic cell death (Ghosh and Greenberg, 1995).

There is evidence that excessive activation of NMDA receptors leads to brain damage associated with anoxia, hypoglycemia, epilepsy and neurodegenerative disorders like Huntington's disease (Rothman and Olney, 1987). Prolonged stimulation of ionotropic glutamate receptors, both NMDA and non-NMDA, results in the death of most central neurons (Rothman and Olney, 1987). Brief periods of intense NMDA receptor activation as well as long periods of exposure to low NMDA (20 μM) concentrations are sufficient to trigger neurodegeneration (Lu *et al.*, 1996). Neuronal injury due to intense kainate exposure was less than that produced by relatively low NMDA exposure but both NMDA and kainate-induced neurotoxicity increased with increasing external calcium concentration (20 μM lowest NMDA concentration) (Lu *et al.*, 1996). This comes as a result of prolonged depolarisation caused by glutamate or its agonist NMDA at postsynaptic dendrosomal receptor sites (Rothman and Olney, 1987), an action assumed to result in pathological membrane changes and impaired ion homeostais (Rothman and Olney, 1987). AMPA receptors have a lower affinity for L-glutamate than NMDA receptors and desensitise rapidly, therefore raised extracellular concentration of glutamate would be expected to primarily cause desensitisation of AMPA receptors (Kidd and Isaac, 2000).

The first component of glutamate excitotoxicity is mediated by excessive activation of non-NMDA receptors (McDonald and Johnston, 1990). It is characterised by influx of Na^+ followed by passive influx of chloride ions into neurons down an electrochemical gradient; chloride entry results in further cation influx to maintain electroneutrality and the chloride and cation entry draws water into cells (Rothman and Olney, 1987). These processes lead to swelling and sometimes osmotic lysis of dendrites and neuronal somata accompanied by clumping of nuclear chromatin although some neurons display dark-cell vacuolar degeneration (Rothman and Olney, 1987). These are acute events occurring within hours of exposure to excitatory amino acid agonists (McDonald and Johnston, 1990).

The second, more prominent component of glutamate excitotoxicity is produced by overactivation of NMDA receptors, which leads to a rise in intracellular Ca^{2+} concentration (McDonald and Johnston, 1990). A sustained rise in intracellular Ca^{2+} may trigger a biochemical cascade of events that lead to neuronal injury and death (McDonald and Johnston, 1990). Excess intracellular Ca^{2+} causes activation of second messenger systems, mobilisation of internal Ca^{2+} stores, triggers activation of intracellular proteases and lipases, generation of free radicals, depletion of energy reserves by activation of Ca^{2+} ATPase and impairment of mitochondrial oxidative phosphorylation (McDonald and Johnston, 1990, Choi, 1988). These cellular derangements lead to destruction of neuronal, cytoskeletal and membrane components and ultimately death (McDonald and Johnston, 1990). Glutamate mediated toxicity in vivo is usually manifested when the presynaptic uptake system is overloaded or suppressed (McDonald and Johnston, 1990). This may be a result of ineffective

removal of glutamate from the synapse (Kidd and Isaac, 2000). The extracellular concentration of glutamate in the rat frontoparietal cortex measured by *in vivo* microdialysis was found to be 626 ± 165 nmol (Herrera-Marschitz *et al.*, 1996). Glutamate regulation in the extracellular space is of vital importance and is achieved by action of high affinity glutamate transporters (Kidd and Isaac, 2000). These high affinity transporters take up glutamate into the glial cells where it is converted to glutamine which can then be taken up into neurons to be reused (Zigmond *et al.*, 1999). Under conditions of metabolic stress or depleted cellular energy, high affinity uptake of glutamate is compromised, because this process is highly energy dependent (McDonald and Johnston, 1990). This results in accumulation of glutamate in the synaptic cleft leading to prolonged activation of glutamate receptors producing sustained membrane depolarisation and leading to large ion fluxes (McDonald and Johnston, 1990).

Excessive NMDA receptor activation leads to an influx of Ca^{2+} from the extracellular space with subsequent Ca^{2+} overload causing certain types of cell death (Choi, 1988). Excessive Ca^{2+} influx appears to be the primary determinant of neuronal injury (Lu *et al.*, 1996). It has been shown that excessive Ca^{2+} influx contributes to invertebrate muscle cell injury induced by excess exposure to glutamate; injury to cardiac cell injury induced by excess exposure to catecholamines and skeletal muscle cells induced by excess exposure to cholinergic agonists (Choi, 1988). Although it is suggested that the major route for lethal Ca^{2+} entry is via the NMDA receptors there are other routes that contribute to influx of lethal Ca^{2+} concentrations in cells (Choi, 1988). The second route is the voltage-sensitive calcium channels activated by the glutamate induced membrane depolarisation (Choi, 1988). A third possible route is

the Na^+/Ca^{2+} exchanger, a mechanism that normally extrudes Ca^{2+} but might operate in reverse mode under conditions of elevated cytosolic Na^+ concentration (Choi, 1988). A fourth possible entry is via the non-specific membrane leak pathways enhanced by membrane distortion associated with excitotoxic swelling (Choi, 1988). Ca^{2+} entry amplifies the ongoing level of NMDA receptor activation through increased release of glutamate and/or NMDA activated expression of receptor (Rothman and Olney, 1987). This increase in NMDA activation may lead to further ion fluxes and subsequent cell death (Rothman and Olney, 1987). Since energy is required to extrude Ca^{2+} from the cell and maintain ionic balances across neuronal membranes, excessive neuronal activation will exacerbate any imbalance between cellular energy requirements and energy availability (McDonald and Johnston, 1990).

NMDA Receptors and neurological disorders

NMDA receptors have been implicated in the pathophysiology of both acute and chronic neurological diseases (Rothman and Olney, 1987). It has been shown that application of NMDA receptor antagonists reduced several types of brain damage like anoxic-ischemic brain damage, hypoglycemic brain damage and seizure-mediated brain damage (Rothman and Olney, 1987). This shows that NMDA receptors are involved in the different processes of brain damage (Rothman and Olney, 1987).

Attention Deficit Hyperactivity Disorder/Spontaneously Hypertensive Rat

Attention-deficit hyperactivity disorder (ADHD) is one of the most common psychiatric disturbances in childhood (Moll *et al.*, 2000). ADHD disorder is characterised by abnormal attention being paid to distracting stimuli, so much so that patients with attention deficit disorder cannot focus attention for long periods of time

(Oosterlaan and Sergeant, 1998; Sagvolden and Sergeant, 1998, Sagvolden *et al.*, 1989; Solanto, 1998). The major symptoms of ADHD are impulsiveness, poorly sustained attention and increased motor activity (Sergeant, 2000). Impulsiveness is characterised by inability to withhold a planned response, interruption of a response that has been started, failure to protect an ongoing activity from interfering activities and failure to delay a response (Sagvolden and Sergeant, 1998). Descriptions of poorly sustained attention are global (Taylor, 1998). Some relate to problems in sustaining attention and being distracted by extraneous stimuli that imply an observable style of brief and rapidly changing sequences of behaviour (Taylor, 1998). Other descriptions of poorly sustained attention involve a dislike of activities requiring sustained mental effort and a failure to give close attention to detail (Taylor, 1998). Increased motor activity means an excess of movements made by different parts of the body without any intercorrelation (Taylor, 1998). Actometers strapped on to various parts of the body, stabilimeter chairs and interruption of ultrasonic beams around a room have been used to detect movement (Taylor, 1998). Careful studies using truncal actometers have shown that children with ADHD are more active than normal children during nearly all daytime activities as well as during sleep (Solanto, 1998).

There is evidence of increased motor activity in ADHD patients (Taylor, 1998, Solanto, 1998). The spontaneously hypertensive rat (SHR), is the most frequently used ADHD model (Sagvolden and Sergeant, 1998). The SHR has been bred from the Wistar-Kyoto rats (WKY) for its hypertensive trait, a feature which makes it the most widely used model for essential human hypertension (Hendley, 2000). Genetic strains of hypertensive animals offer certain advantages as experimental models of

hypertension, as the hypertension develops without the intervention of either surgery or other manipulatory practices (Udenfriend and Spector, 1972). SHR appears to be an excellent model of human hypertension in that hypertension has a hereditary component and does not appear to be of primary renal or simple neurogenic origin (Udenfriend and Spector, 1972).

In addition to the hypertensive trait, the SHR strain has other behavioural abnormalities, which come as unintended consequences of inbreeding (Hendley, 2000). Most prominent among the behavioural abnormalities is that SHR are hyperactive in a novel environment and hyper-reactive to stress, when compared to controls (Hendley, 2000). It is because of its hyperactive trait that SHR is used as a model for ADHD, (Sagvolden, 1998). An animal model to be used in studying ADHD has to have the following characteristics; (a) to best mimic although in a simpler form than the full blown clinical case, the fundamentals of the behavioural characteristics of ADHD, (b) has to conform with a theoretical rationale for ADHD and finally (c) is able to predict aspects of ADHD behaviour, genetics and neurobiology previously uncharted in the clinics (Sagvolden, 1998). A major disadvantage of considering the SHR as a model for hyperactive disorders is that hypertension coexists with their behavioural abnormalities (Hendley, 2000).

Because of the increased motor activity in SHR which is used as a model for ADHD, the barrel cortex would be an ideal brain area to investigate since it is the major sensory input area of the brain. Also because glutamate is the major excitatory neurotransmitter in the barrel cortex (Keller, 1995), it is possible that the function of the NMDA subtype of glutamate receptors might be altered in the barrel cortex of

SHR. It will be appropriate to investigate possible NMDA receptor malfunction in this region of the brain in the SHR model. A decline in motor function with ageing has been shown to be associated with a decline in NMDA receptor levels (Ossowska *et al.*, 2001) and it is possible that with increased motor activity seen in ADHD patients (Solanto, 1998), NMDA receptor function might also be altered in SHR barrel cortex. Very little is known about the nature and function of glutamate receptors in the barrel cortex. The first aim of the present study was to develop a method to evaluate glutamate receptor function in rat barrel cortex slices. The second aim of this study would be to use the developed method to determine whether glutamate receptor function is abnormal in the barrel cortex of a rat model for ADHD, the SHR.

Chapter 2 Materials and Methods

2.1 Materials

2.1.1 Animals

A total of 32 Long Evans rats, 39 Spontaneously Hypertensive Rats (SHR) and 43 Wistar-Kyoto (WKY) were used in this study. The rats were obtained from the University of Cape Town animal unit and their use in these experiments was approved by the University of Cape Town animal ethics committee. These animals were housed in the animal house of the physiology department. They were exposed to a normal 12hour light-dark cycle and allowed free access to commercial pellets and tap water.

The SHR and WKY were housed in a separate room with an infra-red light under which their behaviour following exposure to novel items was observed according to the methods of Filipkowski *et al.,* (2000) and Staiger *et al.,* (2000a). The rats were exposed to a normal 12hour light-dark cycle and allowed free access to commercial pellets and tap water. For some studies the age-matched animals were divided into two groups (of 2 to 6 SHR and 2 to 6 WKY), one group was exposed to a novel environment while another group was left in normal cages. The novel environment consisted of a variety of items such as PVC pipes, metal pipes, a PVC bend, metal ladders (straight and circular) and metal boxes. The items were introduced to the cage at the same time (5.00pm) each day and replaced after 24 hours. There were two sets of items so that the SHR and WKY could be exposed to the same items at the same time. For another set of experiments the animals 4 SHR and 4 WKY were exposed to

a novel environment consisting of the different items in the cage at the same time for 12 weeks. The night prior to the experiment each test rat was introduced to a cage containing a self-made polystyrene maze for ± 16hours. The rats were then sacrificed at 9:30 – 10:30 the following morning. The control rats were left in the cage that did not contain any novel objects with their littermates. For prefrontal cortex studies the animals were left in the normal cage and prior to an experiment some rats were transferred to a new cage containing a polystyrene maze and were referred to as tests while other animals that were sacrificed without exposure to a maze were referred to as controls.

2.1.2 Chemicals and Reagents

All reagents were of analytical grade obtained from Merck Darmstadt, Germany except $^{45}CaCl_2$ which was obtained from NEN Life Science Products Inc, Boston, Scintillation fluid, obtained from Zinsser Analytic Berkshire UK, N[2-Hydoxyethyl]piperazine-N'-[2-ethanesulfonic acid] (HEPES) and NMDA, obtained from Sigma Chemical Corp. St. Louis MO USA, Bovine Serum Albumin (BSA), obtained from Miles Laboratories RSA, and Na_2CO_3, Na^+K^+-tatrate obtained from BDH Chemicals England.

2.1.2.1 Drugs

A selective glutamate receptor agonist N-Methyl-D-Aspartate (NMDA) was obtained from Sigma Chemical Corp. St. Louis MO USA.

The NMDA receptor antagonist MK 801 was obtained from Research Biochemicals Incorporated.

2.1.2.2 Disposables

Gilson pipette tips – white, blue and yellow

Finntip pipette 50ml tips

Blades – platinum blades for slicing in the vibratome

Surgical blades for dissection

Eppendorf vials

Loctite glue 406 – for gluing wet brain block to chuck

5ml Teflon vials and 20ml polyethylene vials for scintillation counting

Vinyl gloves

Filter paper

2.1.2.3 Novel objects used to provide an enriched environment

PVC pipe length 23cm diameter 3.5cm

Metal pipe length 17.5cm diameter 4.5cm

Metal box width 12cm, breadth 14cm height 14cm, (open box with an intermediate level 6cm above floor level)

Metal ladder height 11cm, width 4cm, stair distance 1cm,

PVC bend length 6cm, diameter 5.0cm

Circular metal ladder diameter 12cm, width 4cm, stair distance 1cm

2.1.2.4 Preparation of solutions

2.1.2.4.1 Stock solutions

1 litre stock solutions of NaCl (1.2 M or 600 mM), KCl (50 mM, 33.6 mM, 100 mM or 625 mM), $MgCl_2$ (10 mM), $CaCl_2$ (20 mM), D-Glucose (100 mM) and $LaCl_3$ (100 mM) were prepared ten fold more concentrated than required. The appropriate masses of the chemicals were weighed carefully, dissolved in a small volume of distilled water and made up to 1 litre in a volumetric flask. A one litre stock solution of HEPES (200 mM) was prepared by dissolving 47.66 grams in approximately 800ml of distilled water and by adding one drop at a time of 5 M NaOH, the pH was adjusted to 7.4 before being made up to 1L.

A 1 mM MK-801 stock solution was prepared by weighing accurately 0.33 mg of MK-801 (MW 337.37g.mol^{-1}) and dissolving it in 1ml of distilled water.

A 100 mM NMDA (MW 147.13g.mol^{-1}) stock solution was prepared by weighing accurately 1.47 mg NMDA and dissolving it in 90 µl of distilled water + 10 µl of 5 M NaOH to adjust the pH to about 7 and also to aid in dissolving the NMDA. The solution was wrapped in tin foil (to avoid exposure to light) and stored at 4°C and it was used for a maximum of 2 weeks.

A 10 mM glycine (MW 75.07g.mol^{-1}) stock solution was prepared by dissolving 7.507 mg of glycine in 10 ml of distilled water to give a final concentration of 10 mM.

2.1.2.4.2 HEPES Buffer

On the day of the experiment 500 ml of HEPES buffer was made by adding 50 ml of each of the stock solutions to a volumetric flask and the final volume made up to 500 ml with distilled water (final concentrations of NaCl (120 mM), KCl (5 mM or 3.36 mM), $MgCl_2$ (1 mM), $CaCl_2$ (2 mM or 1.2 mM), D-Glucose (10 mM) and HEPES (20

mM). Another 500 ml of HEPES buffer was prepared the day preceding the experiment and frozen in an ice tray to prepare HEPES buffer "slush" for immersion of the brain during slicing.

2.1.2.4.3 Incubation buffer

Incubation buffer was prepared by adding 1ml of each of the stock solutions of the above HEPES buffer to two 10ml volumetric flasks and making up to the mark with distilled water to give a 1:10 dilution of each. In a separate glass vial 2.2µl of $^{45}Ca^{2+}$ was added to 2.2 ml of $CaCl_2$ (20 mM) to give a final concentration of 1 µCi/µl. A 1 ml aliquot of the mixture of cold and hot Ca^{2+} was then added to each of the two 10 ml volumetric flasks to give a final concentration of 2 mM $CaCl_2$ so that both the test and control solutions had the same amount of radioactivity. To get a final concentration of 1.2 mM $CaCl_2$, 1 .5 µl of $^{45}Ca^{2+}$ was added to 1.5 ml of $CaCl_2$ (20 mM) to give a final concentration of 1 µCi/µl. A 600 µl aliquot of the mixture of cold and hot Ca^{2+} was then added to each of the two 10 ml volumetric flasks to give a final concentration of 1.2 mM $CaCl_2$

2.1.2.4.4 Lanthanum chloride wash buffer

A lanthanum chloride wash was prepared by substituting $LaCl_3$ 100 mM for $CaCl_2$ 20 mM in the HEPES buffer described in section 2.1.2.4.2. Twenty (20 ml) millilitres of each of the stock solutions was added to a volumetric flask and the volume made up to 200 ml with distilled water. The final concentrations were the same as for the HEPES buffer with the final concentration of $LaCl_3$ being 10 mM.

2.1.2.4.5 KCl Stimulation Solution

The potassium chloride stimulation solution was prepared from stock solutions of $MgCl_2$ (10 mM), $CaCl_2$ (20 mM), D-Glucose (100 mM), HEPES (200 mM), as above as well as from stock solutions of KCl (625 mM) and NaCl (600 mM). The KCl stimulation solution was prepared by adding 1 ml of each of the stock solutions to a volumetric flask and making the volume up to 10 ml with distilled water to give final concentrations of KCl (62.5 mM), NaCl (60 mM), $MgCl_2$ (1 mM), $CaCl_2$ (1.2 or 2.0 mM), D-Glucose (10 mM) and HEPES (20 mM). To get a final concentration of 1 $\mu Ci/^{45}Ca^{2+}\mu l$ in the KCl stimulation buffer the procedure described in section 2.1.2.4.3 was followed.

2.1.2.4.6 NMDA-stimulation buffer

NMDA-stimulation buffer was prepared by adding 1ml of each of the stock solutions of the above HEPES buffer (section 2.1.2.4.3) to a 10ml volumetric flask and making up to the mark with distilled water to give a 1:10 dilution of each. In addition 10 µl of 100 mM NMDA stock solution (section 2.1.2.4.1) was added to one of the volumetric flasks to obtain a final concentration of 100 µM in 10 ml. In a separate glass vial 1.5 µl of $^{45}Ca^{2+}$ was added to 1.5 ml of $CaCl_2$ (20 mM) to give a final concentration of 1 µCi/µl. A 600 µl aliquot of the mixture of cold and hot Ca^{2+} was then added to each of the two 10 ml volumetric flasks to give a final concentration of 1.2 mM $CaCl_2$ so that both the test and control solutions had the same amount of radioactivity.

2.1.2.4.7 Glycine buffer

To get a final concentration of 1 mM glycine in the incubation buffer 1 ml of the stock solution (section 2.1.2.4.1) was added together with 1ml of each of the components of

the HEPES buffer (section 2.1.2.4.2) in a volumetric flask and made up to 10 ml with distilled water. In a separate glass vial 1.5 µl of $^{45}Ca^{2+}$ was added to 1.5 ml of $CaCl_2$ (20 mM) to give a final concentration of 1 µCi/µl. A 600 µl aliquot of the mixture of cold and hot Ca^{2+} was then added to each of the two 10 ml volumetric flasks to give a final concentration of 1.2 mM $CaCl_2$ so that both the test and control solutions had the same amount of radioactivity.

2.1.2.4.8 MK 801 buffer

To get a final concentration of 10 µM MK-801 in the pre-incubation buffer, 50 µl of MK-801 stock solution was added to 5 ml of HEPES buffer (section 2.1.2.4.2) while 20 µl was added to 2 ml incubation buffer (section 2.1.2.4.3).

2.1.2.4.9 K^+ Buffers for NMDA stimulation

The 3.36 mM K^+ buffer was prepared by adding 1 ml of a 33.6 mM stock solution to 10 ml volumetric flask together with other components of the buffer while 20 mM K^+ solution was prepared by adding 2 ml of a 100 mM stock solution to a 10 ml volumetric flask together with the other components of the incubation buffer, the two were made up to 10 ml with distilled water. In a separate glass vial 1.5 µl of $^{45}Ca^{2+}$ was added to 1.5 ml of $CaCl_2$ (20 mM) to give a final concentration of 1 µCi/µl. A 600 µl aliquot of the mixture of cold and hot Ca^{2+} was then added to each of the two 10 ml volumetric flasks to give a final concentration of 1.2 mM $CaCl_2$ so that both the test and control solutions had the same amount of radioactivity. A 1 in 100 dilution of the NMDA stock solution was made in order to give a final concentration of 1 mM. From the dilute NMDA stock solution 20µl was pipetted to give 10 µM NMDA, 25 µl

was pipetted to give 12.5 μM NMDA while 50μl was pipetted to give 25μM NMDA. These volumes were pipetted directly into the incubation wells containing 2ml of incubation buffer with either 3.36 mM K^+ or 20 mM K^+ and mixed gently.

2.2 Methods

2.2.1 Tissue Preparation.

On the day of the experiment, a 4 to 6 week old (or adult) rat was transported to the laboratory, killed by cervical dislocation and rapidly decapitated. The skin on the midline of the skull was cut using a surgical blade and deflected to the sides to expose the skull. An angled pair of scissors was inserted into the foramen magnum and the base of the skull cut through to the left and right to facilitate detachment of the skull from its base and therefore complete opening of the skull. The angled pair of scissors was then used to cut the skull from posterior to anterior along the midline towards the bregma. From bregma the pair of scissors was angled downwards first right and then left to make transverse cuts of the skull just posterior to the orbit of the eye. The skull, with the brain still intact was then immersed in a beaker containing HEPES buffer "slush" (made from crushed frozen HEPES buffer and liquid HEPES buffer, section 2.1.2.4.2) for one minute to cool the brain. Cooling the brain reduced metabolic activity and made the brain more rigid and stable for slicing. The above procedure took less than 1 minute on average, the emphasis being on precision and speed.

After 1 minute the dorsal surface of the skull was carefully broken away using a forceps to expose the brain. The brain was gently removed from the cranium using a

small rounded spatula and transferred to another beaker containing fresh continuously oxygenated HEPES buffer and allowed to stand for two minutes. The brain was then transferred to a dampened piece of filter paper in a large petri dish (kept on ice) to prepare it for slicing in a vibratome. For barrel cortex studies the first cut in the coronal plane was made anteriorly approximately 5mm from the most anterior point on the dorsal surface of the brain. The second cut was made posteriorly on the dorsal surface where the two cortices meet hence the cerebellum and the most caudal part of the cortex were removed using a surgical blade. The remaining part of the brain was termed the brain block. For the prefrontal cortex studies only the posterior cut was made approximately 5mm anterior to the point where the two cortices meet so that the pre-frontal cortex was left intact and also the brain block could fit under the blade in the vibratome. A small cut was made on the ventral side of the brain block either on the left or right side of the brain in order to distinguish the slices from the two hemispheres. The posterior surface of the brain block was then glued onto a cutting stage with a thin layer of glue (Loctite 406) to hold it secure during slicing. The amount of glue had to be carefully controlled to ensure uniform gluing of the base of the brain block and ensure that excess glue would not run up the side surfaces of the block thereby interfering with slicing. The brain block was then ready for cutting in a vibratome.

2.2.2 Preparing the vibratome

The vibratome (Series 1000 Sectioning System, ARH Horwell) was prepared by fitting a new blade (Minora platinum blades), cleaned with absolute ethanol, into the holder (the blade inclination had to be between 10 and 15 degrees and was measured with the blade angle indicator apparatus provided with the vibratome and adjusted

accordingly). The vibratome bath was filled with ice-cold HEPES buffer slush (section 2.1.2.4.2) that was continuously oxygenated. The cutting stage was inserted into the vibratome chuck and clamped into position. The brain was positioned in the vibratome with the ventral surface of the brain positioned slightly at an angle from the perpendicular position so that the brain was sliced from the ventral side towards the cortex. The advance mechanism was set to cut slices at a slow speed (approximately 36mm/min). The first slice was made to be 0.5mm in order to straighten the block and was discarded. A second slice was 350μm thick and was also discarded due to the distortion caused by the cutting of the first thick slice. The rest of the slices were 350μm.

As the slices were produced they were gently transferred to a plastic tissue container (kept on ice) filled with continuously oxygenated HEPES buffer using a small paintbrush. The plastic tissue container was made from a rectangular perspex plate with small holes drilled on the cavities containing the slices to allow oxygen to reach the slices. This was immersed in a larger glass container containing continuously oxygenated HEPES buffer. The larger container was in turn placed in a tray filled with ice to maintain the temperature at 4°C. The slicing procedure took between 40 and 60 minutes.

2.2.3 Dissection of Barrel cortex

The somatosensory cortex corresponding to area 1 of the parietal cortex was dissected from slices approximately corresponding to antero-posterior co-ordinates 8.70 to 4.84 mm (Paxinos and Watson 1986) with reference to the interaural line, using a curved

blade attached to a pair of scissors. The somatosensory cortex was divided into rostral, middle and caudal regions, each division having a maximum of four slices.

The rostral region began at stereotaxic co-ordinates of approximately 8.7mm from the interaural line and ended at stereotaxic co-ordinates of approximately 7.2mm from the interaural line. This was marked physically by the appearance of the anterior commissure posterior across the slice to just before the appearance of the hippocampus.

The middle region began at stereotaxic co-ordinates of approximately 7.2mm from the interaural line and ended at stereotaxic co-ordinates of approximately 6.2mm from the interaural line. This was marked physically by the appearance of the hippocampus and ended where the hippocampus began to fold downwards.

The caudal region consisted of the four most posterior sections cut from the brain block. The caudal region started at stereotaxic co-ordinates of approximately 5.8 mm from the interaural line and ended at stereotaxic co-ordinates of approximately 4.8 mm from the interaural line. This was marked physically by the beginning of the folding of the hippocampus and it ended just before the appearance of the hippocampus on the ventral side of the slice. The physical landmarks were the ones used because sometimes it was not easy to match the actual slices with pictures in the atlas.

2.2.4 Dissection of the prefrontal cortex

The prefrontal cortex was dissected from stereotaxic co-ordinates 14.20 mm from the interaural line to stereotaxic co-ordinates 12.20 mm from the interaural line (Paxinos and Watson 1986). This included both the frontal cortex and the cingulate cortex. The landmark used was the appearance of area 2 of the frontal cortex and ended with

the appearance of the forceps minor corpus callosum. The area containing the pre-frontal cortex (landmark used was halfway through the upper part of the slice without the olfactory bulb) was dissected out using a curved blade attached to a pair of scissors. The slices were then divided into three regions (rostral, middle and caudal) each consisting of two slices and they were subjected to the same assay as the barrel cortex slices.

2.2.5 Assay

After dissecting out the desired area of the cortex the slices were transferred to mesh cylinders made of teflon tubes that had a mesh made of nylon stockings stretched across the base and held firmly to the bottom with an o-ring fitted to a groove at the base of the tube. These small vials were firmly held in a rack with six holes which enabled them to be transferred simultaneously to different sets of wells containing different media in subsequent phases of the assay. The wells were made of 20ml polyethylene vials filled with various incubation media. Each well was supplied with oxygen through a system of fine tubing made by heating 1ml syringes over a small bunsen flame and hand pulled to the desired diameter.

2.2.5.1 Stages of the incubation procedure

2.2.5.1.1 Equilibration phase

The first stage of the incubation assay was the equilibration stage where the slices were subjected to 45-minute equilibration at room temperature (±20°C). This step consisted of submersion of the cylinders containing brain tissue into 20 ml polyethylene vials filled with 5 ml of HEPES buffer (pH 7.4) attached to a polystyrene rack and immersed in a polystyrene container filled with tap water. The

polystyrene container helped keep the water temperature constant at room temperature for the duration of the equilibration phase. The slices were agitated frequently to expose all surfaces of the slices to HEPES buffer.

2.2.5.1.2 Pre-incubation phase

The next step was a 5-minute pre-incubation phase at 35°C. Six 20ml polyethylene vials filled with 5ml of HEPES buffer were placed in a perspex holding rack in a constant temperature water bath which was thermostatically controlled using a flow-heater (Grant FH16D electric pump). The tubes were equilibrated for at least 20 minutes at 35°C in order to allow sufficient heating of the wells and their contents before 5-minute pre-incubation of the brain tissue. The wells were continuously oxygenated using fine tubes which were the same as the ones used in the equilibration phase.

2.2.5.1.3 Ca^{2+} uptake studies

The final stage was a 2-minute incubation in 2ml of incubation buffer containing (section 2.1.2.4.3) 1μCi of $^{45}Ca^{2+}$ also at 35°C. The incubation buffer was continuously oxygenated using a system of fine tubes described earlier. Potassium- or NMDA-stimulated calcium uptake into each region was measured according to the method of Feldman et al (1990) with modifications made by Govender (1999). Each stage was accurately timed by means of a timer and in between the different phases the tubes were blotted on paper towel to minimise the transfer of buffer from one set of wells to the next. During the final stage the slices were exposed to incubation buffer containing 1) High K^+, 2) NMDA, 3) a combination of glycine and NMDA and

4) a combination of MK-801 and NMDA. These were referred as tests while slices exposed to incubation buffer only were referred to as controls.

2.2.5.1.3.1 K^+-depolarisation induced $^{45}Ca^{2+}$ uptake

K^+-depolarisation induced $^{45}Ca^{2+}$ uptake into slices was achieved by incubating brain tissue slices from the right hemisphere in a high K^+ (62.5 mM) solution containing 1 μCi of $^{45}Ca^{2+}$ (10 mCi/mg) for 2 minutes at 35°C. In another set of experiments the Ca^{2+} concentration in both the HEPES and incubation buffer was reduced from 2 mM to 1.2 mM while in another set of experiments the concentration of K^+ in the incubation buffer was reduced from 5 mM to 3.36 mM. The slices from the left hemisphere were incubated in a low K^+ (5 mM or 3.36 mM) buffer also containing 1 μCi of $^{45}Ca^{2+}$. These were referred to as controls.

2.2.5.1.3.2 NMDA-Stimulated $^{45}Ca^{2+}$ uptake

The effect of NMDA on $^{45}Ca^{2+}$ uptake was determined by incubating test slices from the right hemisphere in 2 ml of incubation buffer (section 2.1.2.4.3) containing 100 μM NMDA for 2 minutes at 35°C. These slices were compared to slices from the left hemisphere, which were incubated in the equivalent incubation buffer that did contain NMDA. In another set of experiments the test slices were incubated in buffer containing either 10 μM, or 12.5 μM or 25 μM NMDA with the K^+ concentration being increased to 20 mM for certain samples. These test slices were compared to control slices that were incubated in the equivalent incubation buffer that did not contain NMDA.

2.2.5.1.3.3 Glycine

In another set of experiments a group of slices (from the left caudal and right middle region of the rat somatosensory cortex) was incubated with NMDA (100 μM). Another group of slices (from the left middle and right caudal region) was incubated with both NMDA (100 μM) and glycine (1 mM) in the incubation buffer while a third group of slices (from the rostral region both left and right) was incubated with neither NMDA nor Glycine.

2.2.5.1.3.4 MK 801

In another set of experiments a group of slices (from the left caudal and right middle region of the rat somatosensory cortex) was pre-incubated with MK-801 (10 μM) and then incubated with both NMDA (100 μM) and MK-801 (10 μM) in the incubation buffer. Another group of slices (from the left middle and right caudal region) was incubated with NMDA only, in the incubation buffer. A third group of slices (from the left rostral region) was incubated without NMDA but with MK-801 while a fourth group (from the right rostral region) was incubated in buffer containing neither NMDA nor MK-801. These were control slices (these experiments were done on female WKY rats). A comparison was then made between the three groups of slices.

2.2.5.1.4 Lanthanum Chloride Wash

After incubation, the slices were washed in a series of lanthanum chloride ($LaCl_3$) washes in tubes containing 10 ml HEPES buffer with $CaCl_2$ replaced by $LaCl_3$ 10 mM, solution. This was to remove any excess $^{45}Ca^{2+}$ from the surfaces of the slices. The series comprised a 10-second wash, followed by a 15-minute wash in tubes that

contained 10ml $LaCl_3$ solution. In between the washes the tubes containing the slices were blotted on paper towel to minimise transfer of radioactivity from one solution into the next wash. The final wash was in flat petri dishes also containing 10ml of $LaCl_3$ solution (placed on ice) in order to facilitate easy retrieval of the slices from the mesh. The tubes were not blotted on paper towel before transfer of slices to the petri dishes in order to prevent them from adhering strongly to the mesh. This is a modification of the Feldman (1990) method applied by Govender (1999) and used throughout this study. After washing, the slices were transferred using a small paintbrush to tubes containing 1 ml of distilled water placed on ice.

2.2.5.1.5 Quantification

2.2.5.1.5.1 Sonication

The slices were then sonicated for 3 minutes in an ultrasound sonicator (Heat Systems-Ultrasonics Inc. Ultrasonic Processor, W385) under settings, cycle time = 2 seconds, output control = 2; duty cycle = 50% to rupture the cells and release $^{45}Ca^{2+}$ taken up. The slices were sonicated while the test-tube was immersed in a beaker of ice-cold water to prevent temperature increase that would denature protein in the slices. This would in turn alter the results of the protein determination. Part of the sonicate (600 µl) was counted in a liquid scintillation counter while the remainder was used for protein determination.

2.2.5.1.5.2 Liquid Scintillation Counting

In order to determine the amount of radioactivity in the slices, 600 µl of the sonicate was mixed with 3.4 ml of scintillation fluid, mixed thoroughly by shaking and counted in a liquid scintillation counter (Packard 1900 CA Tri-carb Liquid

Scintillation Analyser). In addition to the samples, a quench curve was prepared by mixing different volumes of water i.e 0 ml, 50 µl, 250 µl, 600 µl, 1.0 ml, 1.5 ml and 2.0 ml with 20 µl of incubation media which contained radioactively labelled calcium in small vials. The quench curve was prepared so that the amount of quenching in the samples could be determined by comparison with the standards whose quench was known (Govender 1999). This was done for each experiment in order to take into account experimental day-to-day variation in conditions. Twenty microlitres of the incubation buffer gave an adequate number of counts per minute (CPMs) for the scintillation counter to analyse (Govender 1999). Scintillation fluid (3.4 ml) was added to the vials using a dispenser (eppendorf varispenser plus) and the contents of the vials were mixed thoroughly by shaking. The small vials were placed in larger counting vials and counted in a liquid scintillation counter. From the counts per minute (CPMs) of the quenched standards a curve of percentage efficiency (calculated) against tSIE was plotted (Govender 1999). The tSIE indicates the amount of quench and is calculated automatically by the machine for both the sample and the standards. The equation of the curve was then used to calculate the DPM of the samples.

Theory of liquid scintillation counting

The theory of liquid scintillation counting is based on the existence of an imbalance between the number of protons and neutrons in the nucleus of an element (Liquid Scintillation Analyzer, Operation manual, 1986). This imbalance leads to instability of the element and results in a radioactive event and energy release as radiation in the form of two particles namely a beta particle (β) and a neutrino (Liquid Scintillation Analyzer, Operation manual, 1986). These two particles are released simultaneously

and carry the decay energy from the nucleus. The energy is absorbed by the medium as either heat, ionization or excitation and the latter is the one used in liquid scintillation (Liquid Scintillation Analyzer, Operation manual, 1986). The presence of a beta particle is manifested by collisions with solvent molecules in the scintillation fluid and the excitation of many fluor molecules in the scintillation fluid (Liquid Scintillation Analyzer, Operation manual, 1986). This results in a photon of light being produced and this can then be measured using a photomultiplier tube. The photomultiplier tube functions by amplifying the light photons since they are very small to be detected (Liquid Scintillation Analyzer, Operation manual, 1986). In reality only the counts per minute are measured. The counts per minute differ from the expected DPM due to the effect of quenching. Quenching is a result of the transfer of β-particle energy to sample molecules that are not able to produce photons (Liquid Scintillation Analyzer, Operation manual, 1986). This leads to fewer photons being produced compared to the theoretically expected ones. Standard solutions of radioactively labelled compounds are used to draw up a quench curve to convert the cpm's to dpm's

2.2.5.1.5.3 Calculations

The standards and samples were analysed for a period of 10 minutes in the liquid scintillation counter (Packard 1900 CA Tri-carb Liquid Scintillation Analyser) in the region of the energy distribution spectrum for $^{45}Ca^{2+}$ spanning from 0 keV to 256 keV (A Govender 1999). In addition the machine also gave the tSIE which is the inverse of the quench in each sample prepared. The cpm's of the seven standards obtained from the counter showed a decrease with increasing volume of water though they contained the same amount of radioactivity and this shows that increasing volumes of

water provided increasing amount of quench (Govender 1999). The expected dpm's for the standards were calculated by multiplying the expected dpm in 20 µl of incubation media by the appropriate decay factor of $^{45}Ca^{2+}$ obtained from the decay table provided by the manufacturer (Govender 1999). The percentage counting efficiency was then calculated for each standard as the percentage of cpm over expected dpm.

% Efficiency = cpm/expected dpm x 100

A standard curve was plotted with amount of quench given as tSIE on the x-axis against % counting efficiency on the y-axis (Govender 1999). For each set of standards a linear regression trendline was prepared and the equation of the trendline was used to calculate the % efficiency of the samples by multiplying the tSIE of the sample by the x-coefficient of the equation and then adding the y-intercept. The % efficiency was then divided by the sample cpm and multiplied by 100 to give sample dpm. The sample dpm were multiplied by the number of nanomoles of Ca^{2+} in 20 µl of standard (calculated to be 24 nanomoles), and divided by the expected dpm to give the nanomoles of Ca^{2+} in the sample. To get the nanomoles per milligram of protein the nanomoles were divided by the milligrams of protein as determined in section 2.2.5.1.5.4. This was done in a separate spreadsheet for every assay.

2.2.5.1.5.4 Protein determination

Protein content of the slices was determined using Miller's modification of the Lowry method (Miller 1959) using bovine serum albumin (1 mg/ml) as a standard. Different volumes of a standard bovine serum albumin i.e 10 µl, 20 µl, 40 µl, 80 µl, 120 µl and 160 µl were made up to 1ml with distilled water in test tubes. One tube served as a blank and it did not contain any protein. At the same time different volumes of

sample were made up to 1 ml with distilled water. One millilitre of alkaline copper reagent (freshly prepared by mixing 1% $CuSO_4$ with 2% Na^+K^+-Tartrate in a 1:1 ratio to give final concentrations of 0.5% and 1% respectively) was mixed with 10 % Na_2CO_3 in 0.5 M NaOH in a 1:10 ratio. The tubes were allowed to stand for 10 minutes at room temperature. After 10 minutes, 3ml of Folin phenol reagent, (freshly made by diluting the original Folin phenol reagent in a 1:11 ratio) was added as forcefully as possible using a Finntip pipette and then mixed on a vortex mixer immediately to ensure adequate mixing. The tubes were immediately transferred to a constant temperature water bath where they were incubated for 10 minutes at 50°C after which they were allowed to cool to room temperature. The absorbances of the samples and the standards were then read at 650nm in a Model 35 spectrophotometer (Beckman USA). The standards were used to construct a standard curve from which the concentrations of the samples were calculated. The concentrations of the samples were then used to divide the nanomoles of $^{45}Ca^{2+}$ in the sample in order to obtain the nanomoles of $^{45}Ca^{2+}$ per milligram of protein.

2.2.5.1.6 Statistical Analysis

Data were analysed using either a one-way analysis of variance (ANOVA), multiple analysis of variance (MANOVA) followed by Newman-Keuls test for comparison between means or a t-test for dependent samples using a statistical package, Statistica and selecting ($p < 0.05$) as value of significance. Results are presented in the form of bar graphs and tables of the means of total and basal uptake and also as means of either K^+ or NMDA-stimulated Ca^{2+} uptake ± standard error of the mean (SEM).

Chapter 3 Results

The first phase of the study consisted of sets of experiments carried out on LE rats in order to establish a method to measure uptake of radioactively labelled calcium ($^{45}Ca^{2+}$) into rat barrel cortex slices. This included changing concentrations of important components of the HEPES buffer such as Ca^{2+} and K^+, and testing whether it was necessary to include glycine in the buffer. Another set of experiments was done to verify that NMDA-stimulated Ca^{2+} uptake was in fact due to opening of NMDA receptor channels and for this, the NMDA receptor antagonist MK-801 was used. The method was then used in the second phase where possible differences in NMDA receptor function between SHR and WKY were studied. A second application of the method was to test the effect of ageing and exposure to a novel environment on Ca^{2+} uptake into barrel cortex slices of SHR and WKY. The third application of the method was to measure Ca^{2+} uptake into prefrontal cortex slices of SHR and WKY.

3.1 OPTIMIZATION OF ASSAY CONDITIONS

3.1.1 Potassium-stimulated $^{45}Ca^{2+}$ uptake

Firstly the viability of slices was tested. This was achieved by exposing the rat barrel cortex slices from the right hemisphere to incubation buffer containing high K^+ (62.5 mM). These were compared to corresponding slices from the left hemisphere, which were incubated in buffer containing low K^+ (5.0 mM) as described in section 2.2.5.1.3.1 of the methods. The barrel cortex was divided into three regions namely rostral, middle and caudal according to co-ordinates described in section 2.2.3. The average uptake into the three regions was calculated and is referred to as uptake into the entire barrel cortex.

Statistical analysis (t-test for dependent samples, Appendix A 3.1.1) of the results shown in figure 3.1.1a shows that the average total $^{45}Ca^{2+}$ uptake into the entire barrel cortex was significantly higher than basal uptake ($n = 6$, $p < 0.01$). Total uptake into the rostral region was not significantly different from the basal uptake ($n = 6$, $p > 0.1$) while in the middle and caudal regions total uptake was significantly higher than basal uptake ($n = 6$, $p < 0.05$). K^+-stimulated uptake (figure 3.1.1b) into the entire barrel cortex was 28% above basal levels while uptake into the rostral, middle and caudal regions amounted to 15%, 24% and 45% above basal levels respectively. K^+-stimulated uptake into the rostral region was not significantly different from uptake into middle and caudal regions (figure 3.1.1b, $n = 6$, $p > 0.1$, Appendix A 3.1.1) while uptake into middle region was significantly lower than uptake into the caudal region (figure 3.1.1b, $n = 6$, $p < 0.01$).

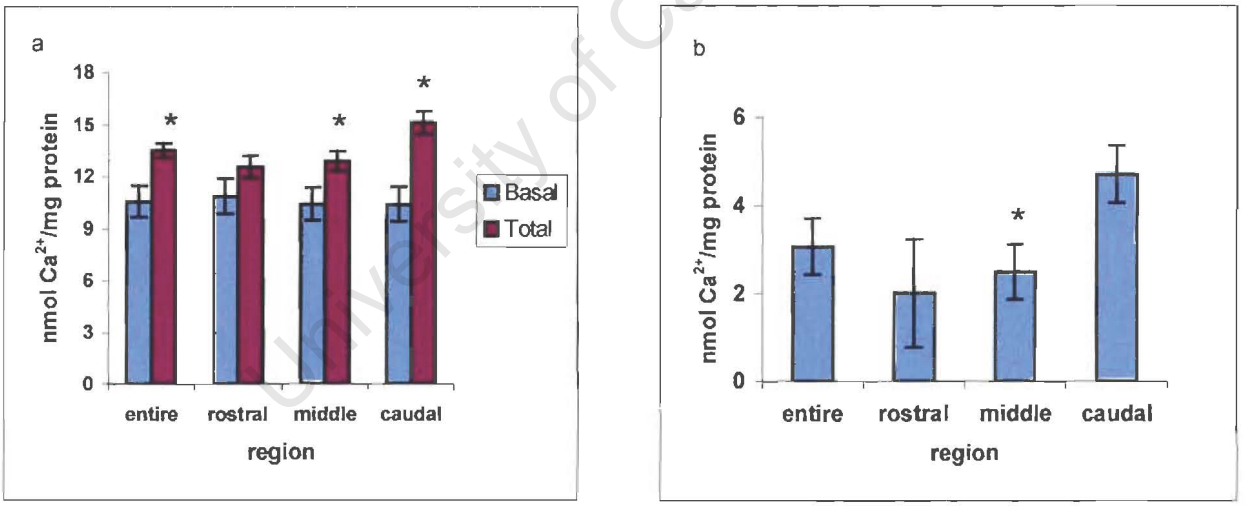

Figure 3.1.1

*a) Basal and total $^{45}Ca^{2+}$ uptake in the presence of 62.5 mM K^+ into barrel cortex slices incubated in buffer containing 2 mM Ca^{2+} and 5 mM K^+ ($n = 6$, * indicates significantly different from basal value, $p < 0.05$, t-test for dependent samples). Results are mean ± SEM*

*b) K^+-stimulated (total – basal) $^{45}Ca^{2+}$ uptake into barrel cortex slices incubated in buffer containing 2 mM Ca^{2+} and 5 mM K^+ (n = 6, * indicates significantly different from caudal region $p < 0.01$, t-test for dependent samples). Results are mean ± SEM*

Table 3.1.1a: Basal and total $^{45}Ca^{2+}$ uptake, following 2-minute exposure to 62.5 mM K^+, into barrel cortex slices incubated in buffer containing 2 mM Ca^{2+} and 5 mM K^+ (data depicted in figure 3.1.1a)

		Total (nmol Ca^{2+}/mg protein)			**Basal** (nmol Ca^{2+}/mg protein)		
Region	**N**	**Mean**	**SD**	**SEM**	**Mean**	**SD**	**SEM**
Entire	6	13.5	1.016	0.415	10.6	2.261	0.923
Rostral	6	12.6	1.549	0.632	10.9	2.470	1.009
Middle	6	12.9	1.402	0.572	10.4	2.270	0.927
Caudal	6	15.1	1.633	0.667	10.4	2.457	1.003

Table 3.1.1b: K^+-stimulated $^{45}Ca^{2+}$ uptake into barrel cortex slices incubated in buffer containing 2 mM Ca^{2+} and 5 mM K^+ (data depicted in figure 3.1.1b)

Region	**N**	**Mean** (nmol Ca^{2+}/mg protein)	**SD**	**SEM**
Entire	6	3.1	1.554	0.634
Rostral	6	2.0	3.012	1.230
Middle	6	2.5	1.51	0.619
Caudal	6	4.7	1.594	0.651

3.1.2 Decreased Ca^{2+} concentration in HEPES buffer

In an effort to improve the sensitivity of the assay, the Ca^{2+} concentration in both the HEPES and incubation buffer was reduced from 2 mM to 1.2 mM (section 2.2.5.1.3.1)

which is the physiological concentration of calcium in the rat cerebrospinal fluid (Davson *et al.,* 1987) while the potassium (K^+) concentration was not altered.

The results in figure 3.1.2a show that the average total uptake of $^{45}Ca^{2+}$ was significantly higher than basal uptake into barrel cortex slices ($n = 4$, $p < 0.01$, Appendix 3.1.2). Similar results were obtained for rostral, middle and caudal regions of the barrel cortex ($n = 4$, $p < 0.05$). Both total and basal uptake of $^{45}Ca^{2+}$ into rostral, middle and caudal regions was significantly decreased when the Ca^{2+} concentration was reduced from 2 mM to 1.2 mM (tables 3.1.1a and 3.1.2a, $n = 6$ and $n = 4$ respetively, $p < 0.05$, ANOVA, Appendix 3.1.4).

Results in figure 3.1.2b show significant K^+-stimulated $^{45}Ca^{2+}$ uptake into barrel cortex slices (average 37%). Uptake into rostral, middle and caudal regions amounted to 25%, 30% and 58% of basal values, respectively. K^+-stimulated uptake into the rostral area was significantly lower than uptake into the caudal region (figure 3.1.2b, $p < 0.01$, Appendix 3.1.2) while uptake into the middle region was not significantly different from uptake into both rostral and caudal regions (figure 3.1.2b, $p > 0.05$, Appendix 3.1.2).

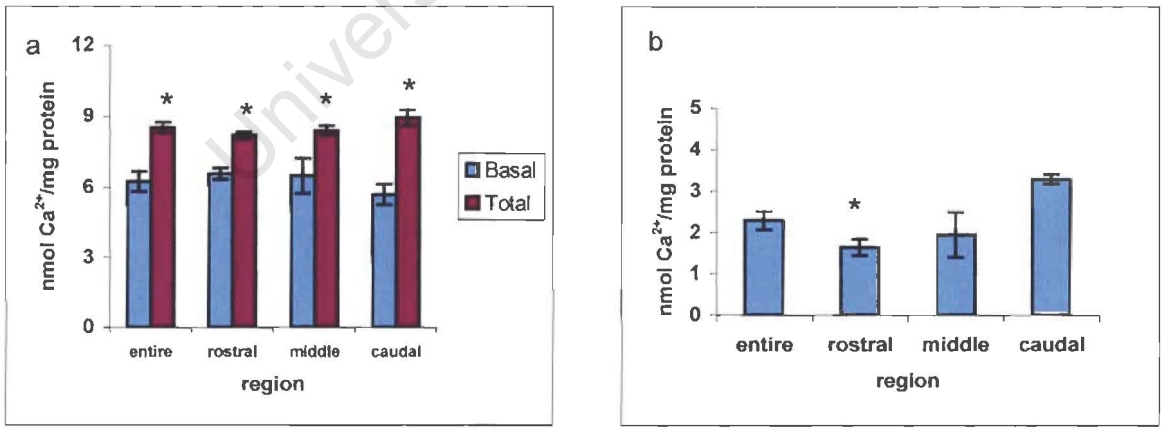

Figure 3.1.2a) Basal and total $^{45}Ca^{2+}$ uptake in the presence of 62.5 mM K^+ into barrel cortex slices incubated in buffer containing 1.2 mM Ca^{2+} and 5 mM K^+ (n = 4,

**indicates significantly different from basal value, $p < 0.05$, t-test for dependent samples). Results are mean ± SEM*

*b) K^+-stimulated (total – basal) $^{45}Ca^{2+}$ uptake into barrel cortex slices incubated in buffer containing 1.2 mM Ca^{2+} and 5 mM K^+ (n = 4, *indicates significantly different from caudal region, $p < 0.05$, t-test for dependent samples). Results are mean ± SEM*

Table 3.1.2a: Basal and total $^{45}Ca^{2+}$ uptake following 2-minute exposure to 62.5 mM K^+ into barrel cortex slices incubated in buffer containing 1.2 mM Ca^{2+} and 5 mM K^+ (data depicted in fig 3.1.2a)

		Total (nmol Ca^{2+}/mg protein)			**Basal** (nmol Ca^{2+}/mg protein)		
Region	**N**	**Mean**	**SD**	**SEM**	**Mean**	**SD**	**SEM**
Entire	4	8.5	0.428	0.214	6.3	0.882	0.441
Rostral	4	8.2	0.297	0.149	6.6	0.499	0.250
Middle	4	8.4	0.405	0.202	6.5	1.481	0.741
Caudal	4	8.9	0.673	0.336	5.7	0.891	0.445

Table 3.1.2b: K^+-stimulated (total – basal) $^{45}Ca^{2+}$ uptake into barrel cortex slices incubated in buffer containing 1.2 mM Ca^{2+} and 5 mM K^+ (data depicted in fig 3.1.2b)

Region	**N**	**Mean** (nmol Ca^{2+}/mg protein)	**SD**	**SEM**
Entire	4	2.3	0.458	0.229
Rostral	4	1.6	0.404	0.202
Middle	4	1.9	1.086	0.543
Caudal	4	3.3	0.231	0.115

3.1.3 Decreased K^+ concentration in HEPES buffer

In a further attempt to increase the sensitivity of the assay, the K^+ concentration in the HEPES buffer and control incubation medium was reduced from 5 mM to 3.36 mM (section 2.2.5.1.3.1) which is the physiological concentration of K^+ in the rat cerebrospinal fluid (Davson *et al.*, 1987). The Ca^{2+} concentration remained at 1.2 mM.

Statistical analysis (t-test for dependent samples, Appendix A 3.1.3) of the results in figure 3.1.3a showed that total uptake was significantly higher than basal uptake into barrel cortex slices ($n = 4$, $p < 0.01$). The same result was obtained when the rostral, middle and caudal regions were analysed separately ($n = 4$, $p < 0.05$). Figure 3.1.3b shows that exposure of barrel cortex slices to buffer containing high K^+ (62.5 mM) caused an average 42% increase in Ca^{2+} uptake above basal levels. K^+-stimulated $^{45}Ca^{2+}$ uptake into rostral, middle and caudal regions amounted to 29%, 40% and 56% respectively under these conditions. K^+-stimulated uptake into the rostral region was significantly lower than uptake into the middle region (figure 3.1.3b, $p < 0.05$) while uptake into both the rostral and middle regions was not significantly different from uptake into the caudal region (figure 3.1.3b, $p > 0.05$). There was no significant difference in basal or total uptake when the K^+ concentration was reduced from 5 to 3.36 mM (ANOVA appendix 3.1.4), although a p value of 0.065 suggests that the average total Ca^{2+} uptake into barrel cortex may be slightly greater in buffer containing the lower concentration of K^+. This favours the use of the 3.36 mM K^+ buffer in future experiments.

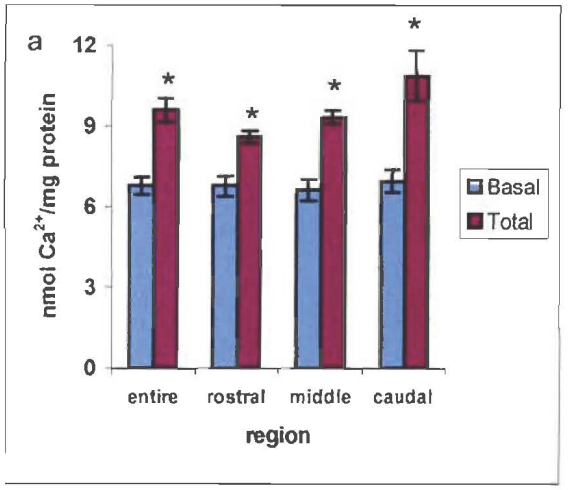

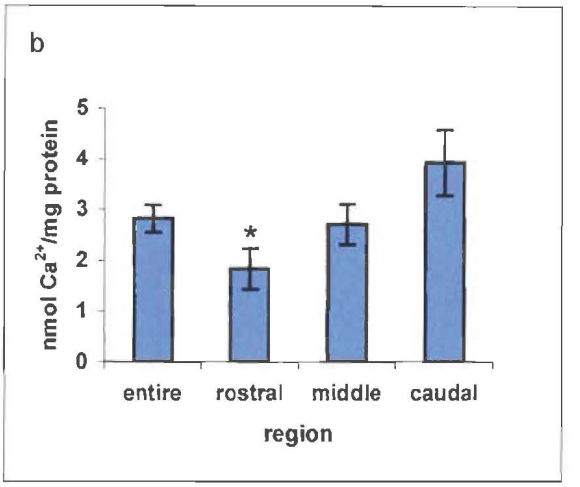

Figure 3.1.3

*a) Basal and total $^{45}Ca^{2+}$ uptake in the presence of 62.5 mM K^+ into barrel cortex slices incubated in buffer containing 1.2 mM Ca^{2+} and 3.36 mM K^+ (n = 4, *indicates significantly different from basal value, $p < 0.05$, t-test for dependent samples). Results are mean ± SEM*

*b) K^+-stimulated (total – basal) $^{45}Ca^{2+}$ uptake into barrel cortex slices incubated in buffer containing 1.2 mM Ca^{2+} and 3.36 mM K^+ (n = 4, *indicates significantly different from middle region, $p < 0.05$, t-test for dependent samples) Results are mean ± SEM*

Table 3.1.3a: Basal and total $^{45}Ca^{2+}$ uptake following 2-minute exposure to 62.5 mM K^+ into barrel cortex slices incubated in buffer containing 1.2 mM Ca^{2+} and 3.36 mM K^+ (data depicted in fig 3.1.3a)

		Total (nmol Ca^{2+}/mg protein)			**Basal** (nmol Ca^{2+}/mg protein)		
Region	**N**	**Mean**	**SD**	**SEM**	**Mean**	**SD**	**SEM**
Entire	4	9.6	0.885	0.442	6.8	0.673	0.337
Rostral	4	8.6	0.470	0.235	6.8	0.785	0.393
Middle	4	9.3	0.498	0.249	6.6	0.824	0.412
Caudal	4	10.9	1.855	0.928	6.9	0.859	0.429

Table 3.1.3b: K^+-stimulated $^{45}Ca^{2+}$ uptake into barrel cortex slices incubated in buffer containing 1.2 mM Ca^{2+} and 3.36 mM K^+ (data depicted in fig 3.1.3b)

Region	**N**	**Mean** (nmol Ca^{2+}/mg protein)	**SD**	**SEM**
Entire	4	2.8	0.534	0.267
Rostral	4	1.8	0.812	0.406
Middle	4	2.7	0.777	0.388
Caudal	4	3.9	1.295	0.647

Statistical analysis (ANOVA, appendix A 3.1.4) of the data from the three sets of experiments where different buffer conditions (namely 2 mM Ca^{2+}/5 mM K^+, 1.2 mM Ca^{2+}/5 mM K^+ and 1.2 mM Ca^{2+}/3.36 mM K^+) were used did not reveal any significant difference in the magnitude of K^+-stimulated uptake into the entire barrel cortex or into the rostral, middle and caudal regions ($p > 0.1$). The final concentrations of 1.2 mM Ca^{2+} and 3.36 mM K^+ were chosen as optimal for subsequent experiments, despite the fact that they did not significantly improve the K^+-evoked uptake of calcium. However they corresponded to the physiological concentrations of both ions in the rat cerebrospinal fluid (Davson *et al.*, 1987).

3.2 NMDA-stimulated $^{45}Ca^{2+}$ uptake

In another set of experiments the effect of neurotransmitter receptor activation on $^{45}Ca^{2+}$ uptake was tested by using the selective agonist, NMDA (100 μM) under optimised buffer conditions (1.2 mM Ca^{2+} and 3.36 mM K^+). The binding of NMDA to the receptor is required for the receptor to open and allow influx of Ca^{2+} into the cell. In this set of experiments slices from the right hemisphere of the brain were incubated in buffer containing NMDA (100 μM) while slices from the left hemisphere

were incubated in buffer that did not contain any NMDA (section 2.2.5.1.3.2) and served as controls.

The results in figure 3.2a and 3.2b show that NMDA (100 μM) caused a 45% increase in Ca^{2+} uptake into the entire barrel cortex. NMDA-stimulated Ca^{2+} uptake into rostral, middle and caudal regions amounted to 33%, 42% and 62% above basal levels respectively. Statistical analysis (t test for dependent samples, Appendix A 3.2) of the data shows that NMDA significantly increased $^{45}Ca^{2+}$ uptake above basal levels into all regions of the barrel cortex (figure 3.2a, $n = 5$, $p < 0.05$). There was no difference in NMDA-stimulated $^{45}Ca^{2+}$ uptake between the different regions of the barrel cortex (figure 3.2b, $n = 5$, $p > 0.1$).

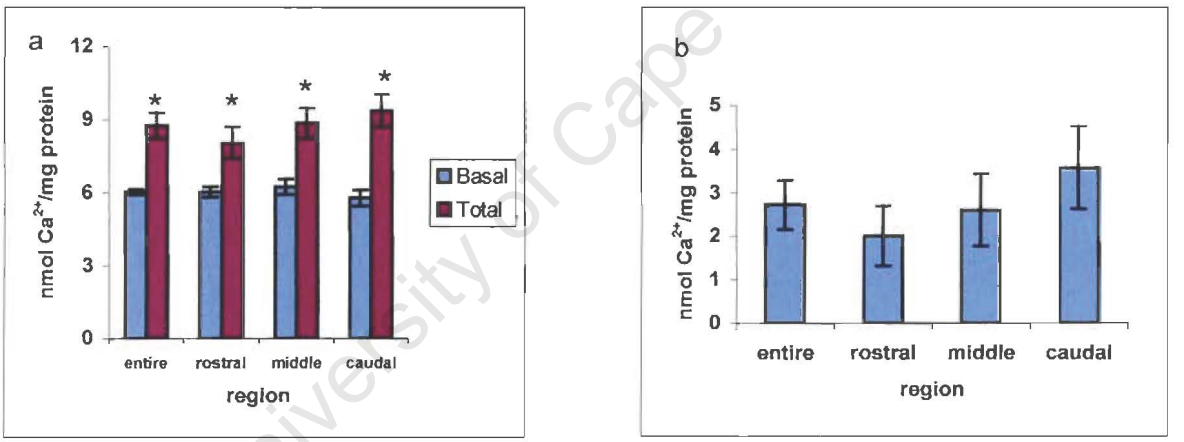

Figure 3.2

*a) Basal and total $^{45}Ca^{2+}$ uptake into barrel cortex slices in the presence of NMDA ($n = 5$, * indicates significantly different from basal value, $p < 0.05$, t-test for dependent samples). Results are mean ± SEM*

b) NMDA-stimulated $^{45}Ca^{2+}$ uptake into barrel cortex slices ($n = 5$). Results are mean ± SEM

Table 3.2a: Basal and total $^{45}Ca^{2+}$ uptake into barrel cortex slices in the presence of NMDA (data depicted in figure 3.2a)

		Total (nmol Ca^{2+}/mg protein)			**Basal** (nmol Ca^{2+}/mg protein)		
Region	**N**	**Mean**	**SD**	**SEM**	**Mean**	**SD**	**SEM**
Entire	5	8.7	1.173	0.524	6.0	0.241	0.108
Rostral	5	8.1	1.468	0.656	6.0	0.468	0.209
Middle	5	8.8	1.374	0.614	6.2	0.710	0.318
Caudal	5	9.4	1.493	0.668	5.8	0.750	0.335

Table 3.2b: NMDA-stimulated $^{45}Ca^{2+}$ uptake into barrel cortex slices (data depicted in figure 3.2b)

Region	**N**	**Mean** (nmol Ca^{2+}/mg protein)	**SD**	**SEM**
Entire	5	2.7	1.271	0.568
Rostral	5	2.0	1.543	0.690
Middle	5	2.6	1.859	0.832
Caudal	5	3.6	2.104	0.941

3.3 Effect of Glycine on NMDA-stimulated $^{45}Ca^{2+}$ uptake

Glycine is required for glutamate to activate NMDA receptors and allow calcium influx into cells. It was thought that the concentration of glycine may be too low in the slice preparation. In this set of experiments a group of slices (from the left caudal and right middle region of the rat barrel cortex) was incubated with NMDA (100 μM). Another group of slices (from the left middle and right caudal region) was incubated with both NMDA (100 μM) and glycine (1 mM) in the incubation buffer while a third group of slices (from the rostral regions of both left and right hemispheres) was incubated with buffer containing neither NMDA nor Glycine (section 2.2.5.1.3.3)

The results in figure 3.3a and 3.3b show that NMDA caused a significant increase in $^{45}Ca^{2+}$ uptake above control levels (31% and 28% for the left and right hemispheres, respectively, n = 5, $p < 0.05$, Appendix A3.3). Inclusion of glycine (1 mM) together with NMDA (100 μM) in the incubation buffer caused a significant increase (28%) in uptake above basal levels in both the left and right hemispheres (figure 3.3a, n = 5, $p < 0.05$). There was no difference in total Ca^{2+} uptake in the presence of NMDA alone compared to total uptake in the presence of NMDA plus glycine (figure 3.3a. n = 5, $p > 0.1$). Addition of glycine did not significantly increase NMDA-stimulated uptake of $^{45}Ca^{2+}$ into rat barrel cortex slices (figure 3.3b, n = 5, $p > 0.1$). The similar basal uptake shows that there were no interhemispheric differences in $^{45}Ca^{2+}$ uptake (figure 3.3a, n = 5, $p > 0.1$).

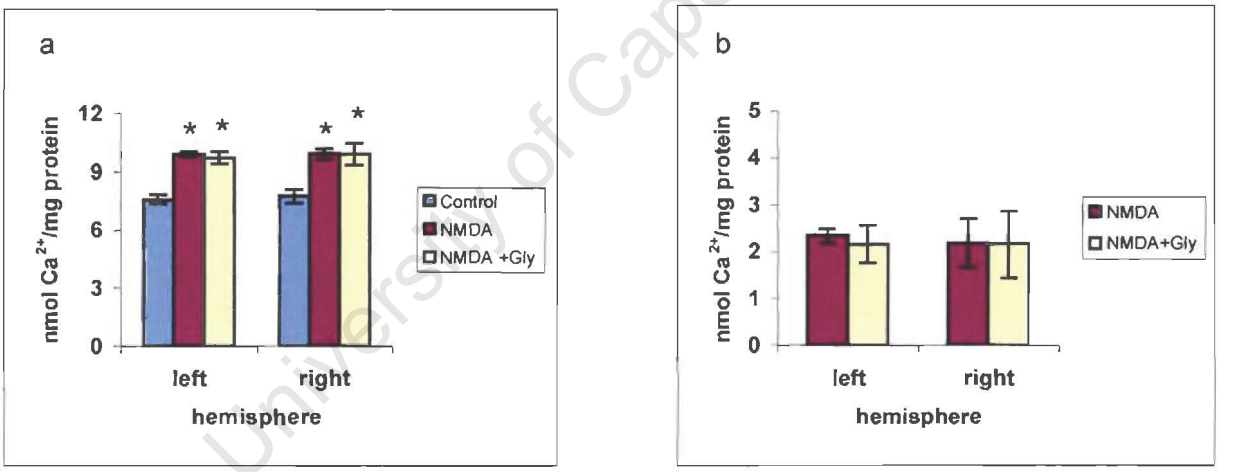

Figure 3.3

*a) Basal and total $^{45}Ca^{2+}$ uptake into barrel cortex slices in the presence of NMDA alone and total uptake in the presence of NMDA plus glycine. (n = 5, *indicates significantly different from basal values, $p < 0.05$ t-test for dependent samples) Results are mean ± SEM*

b) NMDA-stimulated (total - basal) $^{45}Ca^{2+}$ uptake into barrel cortex slices and the effect of NMDA plus glycine. Results are mean ± SEM

Table 3.3a: *Basal and total $^{45}Ca^{2+}$ uptake into barrel cortex slices in the presence of NMDA alone and in the presence of NMDA plus glycine (data depicted in figure 3.3a)*

		Basal			**NMDA**			**NMDA+ Glycine**		
Hemisphere	**N**	**Mean**	**SD**	**SEM**	**Mean**	**SD**	**SEM**	**Mean**	**SD**	**SEM**
Left	5	7.6	0.542	0.243	9.9	0.258	0.128	9.7	0.727	0.325
Right	5	7.8	0.766	0.343	9.9	0.583	0.261	9.9	1.282	0.573

Table 3.3b: *NMDA-stimulated $^{45}Ca^{2+}$ uptake into barrel cortex slices and the effect of NMDA plus glycine (data depicted in figure 3.3b)*

		NMDA (nmol Ca^{2+}/mg protein)			**NMDA+ Glycine**		
Hemisphere	**N**	**Mean**	**SD**	**SEM**	**Mean**	**SD**	**SEM**
Left	5	2.3	0.343	0.153	2.2	0.908	0.406
Right	5	2.2	1.168	0.522	2.1	1.592	0.712

3.4 Antagonising NMDA effect with MK-801

In this set of experiments a group of slices (from the left caudal and right middle regions of barrel cortex) was pre-incubated with MK-801 (10 μM) and then incubated with both NMDA (100 μM) and MK-801 (10 μM) in the incubation buffer. Another group of slices (from the left middle and right caudal barrel cortex) was incubated with NMDA only in the incubation buffer. A third group of slices (from the left rostral region) was incubated with no NMDA but with MK-801, while another group of slices (from the right rostral region) was incubated in buffer containing neither NMDA nor MK-801. These were control slices and were compared with each other to see if MK-801 had any effect on the slice preparation. These experiments were

done on female Wistar-Kyoto rats. A comparison was made between the different groups of slices. (Section 2.2.5.1.3.4)

When MK-801 (10 μM) was included in the pre-incubation buffer together with NMDA (100 μM), $^{45}Ca^{2+}$ uptake was not significantly different from controls (figure 3.4a and 3.4b, $n = 3$, $p > 0.1$, Appendix A3.4) whereas NMDA (100 μM) alone significantly increased Ca^{2+} uptake above basal levels in the left hemisphere (figure 3.4a, $n = 3$; $p < 0.05$) but not in the right hemisphere (figure 3.4a, $n = 3$; $p > 0.1$). This shows that the NMDA effect was antagonised by MK-801. Also in the same experiments one control (rostral right hemisphere barrel cortex) was pre-incubated and incubated in buffer containing MK-801 while another control (rostral left hemisphere barrel cortex) was not exposed to MK-801 and the results show no difference between the two controls (figure 3.4a, $n = 3$, $p > 0.1$). This shows that MK-801 alone had no effect on basal $^{45}Ca^{2+}$ uptake into the slice preparation. NMDA-stimulated $^{45}Ca^{2+}$ uptake was significantly higher than $^{45}Ca^{2+}$ uptake in the presence of both NMDA plus MK-801 (figure 3.4b, $n = 3$, $p < 0.05$) in both hemispheres.

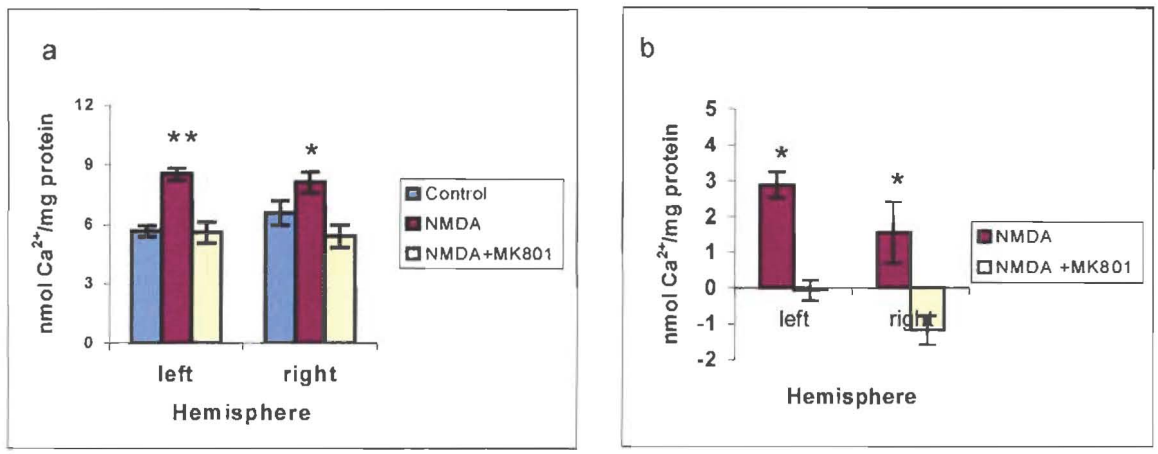

Figure 3.4

*a) Basal and total $^{45}Ca^{2+}$ uptake in the presence of NMDA alone and in the presence of NMDA together with MK-801 (n = 3, *indicates significantly different from NMDA + MK-801 value, ** indicates significantly different from basal and NMDA + MK-801 values, $p < 0.05$, t-test for dependent samples). Results are mean ± SEM*

*b) NMDA-stimulated $^{45}Ca^{2+}$ uptake above basal levels in the presence of NMDA alone and in the presence of NMDA together with MK-801 (n = 3, *indicates significantly different and NMDA + MK-801 values, $p < 0.05$ t-test for dependent samples). Results are mean ± SEM*

Table 3.4a: Basal and total $^{45}Ca^{2+}$ uptake in the presence of NMDA alone and in the presence of NMDA together with MK-801 (data depicted in figure 3.4a)

		Basal			**NMDA**			**NMDA+ MK-801**		
Hemisphere	**N**	**Mean**	**SD**	**SEM**	**Mean**	**SD**	**SEM**	**Mean**	**SD**	**SEM**
Left	3	5.7	0.493	0.285	8.6	0.563	0.352	5.6	0.927	0.535
Right	3	6.6	1.057	0.611	8.1	0.927	0.535	5.4	0.978	0.565

Table 3.4b: NMDA-stimulated $^{45}Ca^{2+}$ uptake above basal levels following exposure to NMDA alone and NMDA together with MK-801 (data depicted in figure 3.4b)

		NMDA			NMDA+ MK-801		
Hemisphere	**N**	**Mean**	**SD**	**SEM**	**Mean**	**SD**	**SEM**
Left	3	2.9	0.649	0.375	-0.1	0.499	0.288
Right	3	1.5	1.490	0.860	-1.2	0.697	0.402

3.5 Effect of different K^+ concentrations on NMDA–stimulated $^{45}Ca^{2+}$uptake

In this set of experiments barrel cortex slices were incubated with different concentrations of K^+ together with different concentrations of NMDA with the aim of testing whether an increase in external K^+ enhances the NMDA effect on $^{45}Ca^{2+}$ uptake. This was based on the premise that NMDA receptors require both depolarisation and binding of NMDA in order to open the ligand-gated ion channels. Therefore an elevated external K^+ concentration might be expected to cause a greater depolarisation of the membrane and removal of the Mg^{2+} block hence increase Ca^{2+} uptake via NMDA receptors. In these experiments slices were incubated with a combination of 3.36 mM K^+/25 µM NMDA (referred to as test T1, from middle left hemisphere), 20 mM K^+/10 µM NMDA (referred to as test T2, caudal left hemisphere), 20 mM K^+/12.5 µM NMDA (referred to as test T3, middle right hemisphere), 20 mM K^+/25 µM NMDA (referred to as test T4, caudal right hemisphere). In addition there were two controls, that were incubated with different concentrations of K^+ namely, 3.36 mM and 20 mM K^+ referred to as C1 from rostral left hemisphere and C2 from rostral right hemisphere respectively. (Section 2.2.5.1.3.2).

The results firstly show that increasing external K^+ concentration in the incubation buffer to 20 mM caused a tendency towards an increase but did not significantly increase Ca^{2+} uptake into barrel cortex slices compared to 3.36 mM K^+ (figure 3.5a, n = 5, p = 0.0619, Appendix A3.5). In the presence of 20 mM K^+ three different concentrations of NMDA namely 10 μM, 12.5 μM and 25 μM did not cause significant NMDA-stimulated Ca^{2+} uptake into barrel cortex slices compared to the control which contained 20 mM K^+ alone (figure 3.5b, n = 5, $p > 0.1$). Although there was a tendency towards an increase, 25 μM NMDA (test T1) did not cause a significant increase in uptake compared to the control that contained 3.36 mM K^+ (figure 3.5b, n = 5, p = 0.0629). In buffer containing 20 mM K^+, total $^{45}Ca^{2+}$ uptake in the presence of 25 μM was significantly higher than total uptake in the presence of 12.5 μM NMDA (figure 3.5a, t-test for dependent samples, $p < 0.01$).

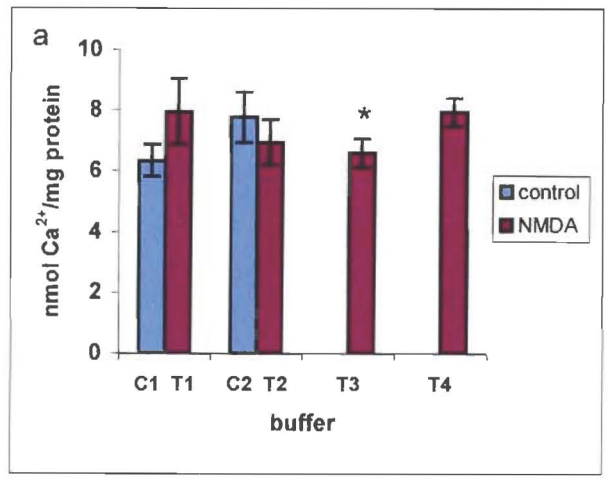

Figure 3.5a)

Total and basal $^{45}Ca^{2+}$ uptake under different K^+ and NMDA concentrations where:

C1 = basal uptake in the presence of 3.36 mM K^+ only

C2 = basal uptake in the presence of 20 mM K^+ only

T1 = total uptake in the presence of 3.36 mM K^+ plus 25 μM NMDA

T2= total uptake in the presence of 20 mM K^+ plus 10 μM NMDA

T3 = total uptake in the presence of 20 mM K^+ plus 12.5 μM NMDA

T4 = total uptake in the presence of 20 mM K^+ plus 25 μM NMDA

** indicates significantly different from T4 (Results are mean ± SEM)*

Table 3.5a: Total and basal $^{45}Ca^{2+}$ uptake under different K^+ and NMDA concentrations: (data depicted in figure 3.5a)

Buffer	**N**	**Mean** nmol Ca^{2+}/mg protein	**SD**	**SEM**
3.36 mM K^+ only	5	6.3	1.173	0.524
3.36 mM K^+ plus 25 μM NMDA	5	7.9	2.438	1.091
20 mM K^+ only	5	7.8	1.867	0.835
20 mM K^+ + 10 μM NMDA	5	6.9	1.694	0.757
20 mM K^+ plus 12.5 μM NMDA	5	6.6	1.047	0.468
20 mM K^+ plus 25 μM NMDA	5	7.9	1.045	0.467

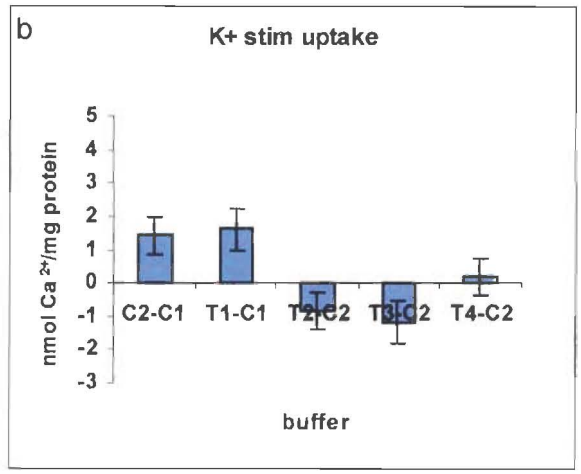

Figure 3.5b)

NMDA-stimulated $^{45}Ca^{2+}$ uptake at different K^+ and NMDA concentrations where:

C2-C1 = effect of 20 mM K^+ on Ca^{2+} uptake

T1-C1 =effect of 25 μM NMDA on Ca^{2+} uptake in the presence of 3.36 mM K^+

T2-C2 = effect of 10 μM NMDA on Ca^{2+} uptake in the presence of 20 mM K^+

T3-C2 =effect of 12.5 μM NMDA on Ca^{2+} uptake in the presence of 20 mM K^+

T4-C2 =effect of 25 μM NMDA on Ca^{2+} uptake in the presence of 20 mM K^+

(Results are mean ± SEM)

Table 3.5b: *$^{45}Ca^{2+}$ uptake under different K^+ and NMDA concentrations: (data depicted in figure 3.5b)*

Buffer	**N**	**Mean** nmol Ca^{2+}/mg protein	**SD**	**SEM**
Effect of 25 μM NMDA in 3.36 mM K^+	5	1.6	1.419	0.635
Effect of 20 mM K^+ alone	5	1.4	1.240	0.554
Effect of 10 μM NMDA in 20 mM K^+	5	-0.8	1.237	0.553
Effect of 12.5 μM NMDA in 20 mM K^+	5	-1.2	1.438	0.643
Effect of 25 μM NMDA in 20 mM K^+	5	0.2	1.193	0.534

3.6 Comparison between SHR and WKY

The aim of this set of experiments was to compare NMDA-stimulated calcium uptake (section 2.2.5 for methods) into barrel cortex slices of age-matched 4 to 6 week old SHR (n = 8) and WKY, (n = 11) strains. This is based on the fact that the two strains have different behavioural characteristics that suggest that NMDA receptor function may differ in the two strains. The housing and feeding conditions were kept similar for the two strains (section 2.1.1).

Results in figure 3.6.1 show that both total and basal uptake into barrel cortex slices were significantly lower in SHR compared to WKY (figure 3.6.2, $p < 0.05$, ANOVA, Appendix 3.6). Total Ca^{2+} uptake into the entire barrel cortex was significantly higher than basal uptake in both strains (figure 3.6.1, t test for dependent samples, $p < 0.001$).

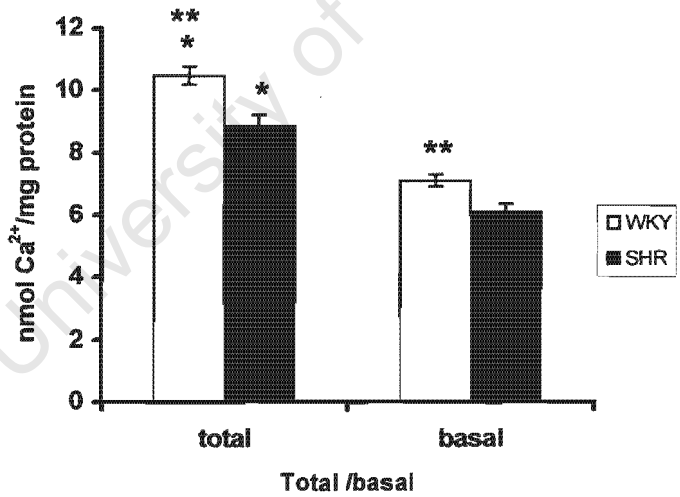

*Figure 3.6.1) Total, following 2-minute exposure to 100 μM NMDA, and basal uptake of $^{45}Ca^{2+}$ into barrel cortex slices of SHR and WKY (n = 8 and n = 11 respectively *indicates significantly different from corresponding basal value, ** indicates significantly different from corresponding SHR value, $p < 0.05$, ANOVA). Results are mean ± SEM*

Table 3.6.1: Total, following 2-minute exposure to 100 μM NMDA, and basal uptake of $^{45}Ca^{2+}$ into barrel cortex slices of SHR and WKY (data depicted in figure 3.6.1)

		Total (nmol Ca^{2+}/mg protein)			**Basal**(nmol Ca^{2+}/mg protein)		
Strain	**N**	**Mean**	**SD**	**SEM**	**Mean**	**SD**	**SEM**
SHR	8	8.8	1.032	0.365	6.1	0.756	0.267
WKY	11	10.5	0.970	0.292	7.1	0.656	0.198

Total Ca^{2+} uptake into the rostral, middle and caudal regions of the barrel cortex was significantly lower in SHR than in WKY (figure 3.6.2 ANOVA, $p < 0.05$). Basal uptake of $^{45}Ca^{2+}$ into rostral, and caudal regions of the barrel cortex of SHR was significantly lower than WKY (figure 3.6.2 ANOVA, $p < 0.05$) while basal uptake into the middle region of the barrel cortex was similar for both strains (figure 3.6.2, ANOVA, $p > 0.1$). Basal uptake into the different regions of SHR was not significantly different (figure 3.6.2, t-test for dependent samples, $p > 0.1$). Basal uptake into the middle region of WKY barrel cortex was significantly lower than basal uptake into rostral and caudal regions of WKY barrel cortex (figure 3.6.2, t-test for dependent samples, $p < 0.05$). Total uptake was significantly higher than basal uptake into the rostral, middle and caudal regions of the barrel cortex of both strains (t test for dependent samples, figure 3.6.2, $p < 0.01$).

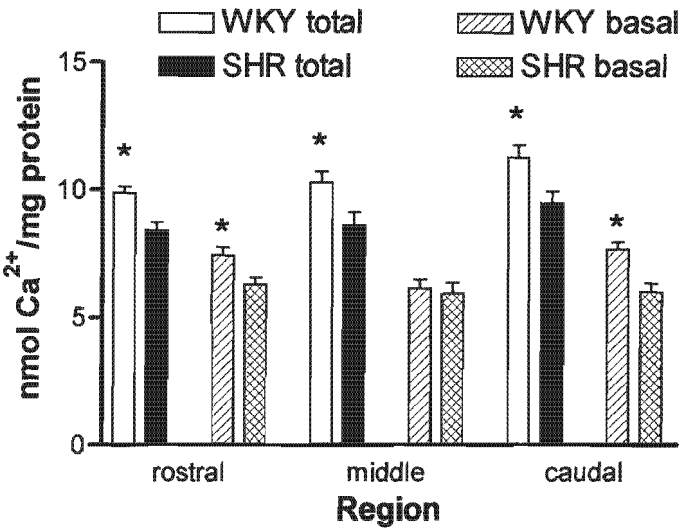

*Figure 3.6.2: Total, following 2-minute exposure to 100 μM NMDA, and basal $^{45}Ca^{2+}$ uptake into different regions of barrel cortex of SHR and WKY (n = 8 and n = 11 respectively *indicates significantly different from SHR value p < 0.05, ANOVA) Results are mean ± SEM*

Table 3.6.2: Total following 2-minute exposure to 100 μM NMDA, and basal $^{45}Ca^{2+}$ uptake into different regions of barrel cortex of SHR and WKY (data depicted in figure 3.6.2)

			Total (nmol Ca^{2+}/mg protein)			**Basal** (nmol Ca^{2+}/mg protein)		
Strain	**N**	**Region**	**Mean**	**SD**	**SEM**	**Mean**	**SD**	**SEM**
SHR	8	Rostral	8.4	0.961	0.340	6.3	0.805	0.285
		Middle	8.6	1.444	0.511	5.9	1.210	0.428
		Caudal	9.6	1.296	0.458	6.0	1.031	0.364
WKY	11	Rostral	9.9	0.880	0.265	7.4	1.101	0.332
		Middle	10.3	1.386	0.418	6.2	1.147	0.346
		Caudal	11.3	1.691	0.510	7.7	0.892	0.269

The results in figure 3.6.3a show that there was no significant difference between SHR and WKY in NMDA-stimulated Ca^{2+} uptake into barrel cortex slices (figure 3.6.3a, ANOVA, $p > 0.1$). When the rostral, middle and caudal regions were analysed separately, there was no significant difference between SHR and WKY in NMDA-stimulated Ca^{2+} uptake into rostral and caudal regions (figure 3.6.3b, $n = 8$ and $n = 11$ respectively, ANOVA, $p > 0.1$) while NMDA-stimulated Ca^{2+} uptake into the middle region of SHR was significantly lower than WKY (figure 3.6.3b, ANOVA, $p < 0.05$).

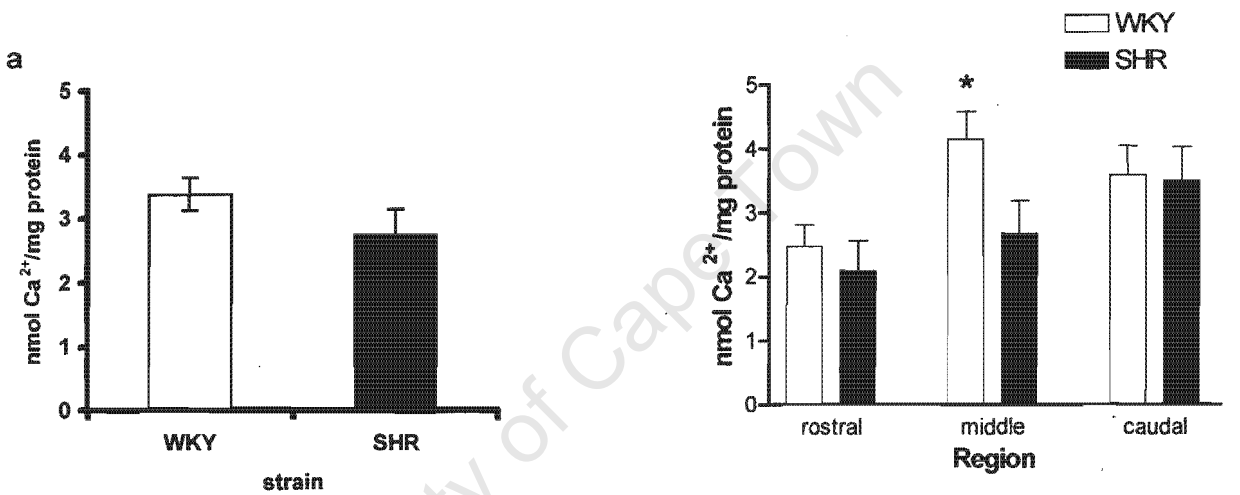

Figure 3.6.3

a) Average NMDA-stimulated Ca^{2+} uptake into entire barrel cortex of SHR and WKY ($n = 8$ and $n = 11$ respectively, t-test). Results are mean ± SEM

*b) NMDA-stimulated Ca^{2+} uptake into different regions of barrel cortex of SHR and WKY ($n = 8$ and $n = 11$ respectively *indicates significantly different from SHR value, $p < 0.05$, ANOVA) Results are mean ± SEM*

Table 3.6.3a: Average NMDA-stimulated uptake of Ca^{2+} into barrel cortex of SHR and WKY (data depicted in figure 3.6.3a)

Strain	**N**	**Mean** nmol Ca^{2+}/mg protein	**SD**	**SEM**
SHR	8	2.8	1.109	0.392
WKY	11	3.4	0.838	0.253

Table 3.6.3b: NMDA-stimulated Ca^{2+} uptake into different regions of barrel cortex of SHR and WKY (data depicted in figure 3.6.3b)

Strain	**Region**	**N**	**Mean** nmol Ca^{2+}/mg protein	**SD**	**SEM**
SHR	Rostral	8	2.1	1.319	0.466
	Middle	8	2.7	1.462	0.517
	Caudal	8	3.5	1.506	0.532
WKY	Rostral	11	2.5	1.118	0.337
	Middle	11	4.2	1.413	0.426
	Caudal	11	3.6	1.528	0.461

3.7 Effect of novel environment and age on NMDA stimulated $^{45}Ca^{2+}$ uptake

Another set of experiments was carried out where the two strains SHR and WKY, were exposed to a novel environment described in section 2.1.1 consisting of novel objects described in section 2.1.2.3 and these were compared to animals that were left in the normal cage. This was based on the method by Filipkowski *et al.,* (2000) and Staiger *et al.,* (2000a). The aim was to see whether exposure to a novel environment had an effect on NMDA receptor function and whether there is any interaction between strain and environment. The animals were divided into two groups; one group of 2 to 7 SHR and WKY was exposed to a novel environment in an enriched cage while the other group of 2 to 7 SHR and WKY was left in the normal cage. The same procedure was used for older and younger rats with one rat being sacrificed each day. At 5.00 pm on the day before the experiment one rat was removed from the enriched cage and transferred to a cage containing a self-made polystyrene maze. NMDA-stimulated Ca^{2+} uptake was measured according to section 2.2.5.3.2 of the methods.

During observation of the animals there were no visible differences in the way the two strains of rats reacted towards novel objects introduced to the cage. The animals began by first finding their way around the object, cautiously sniffing at it and after a brief period started exploring it more by touching and entering in the case of pipes and climbing in the case of ladders. This would be done at first by one rat while the others preferred to watch and follow later. There was no obvious preference to any object and there was also no object that was particularly disliked by the rats. As for the pipes the animals explored them by crawling into them and chasing each other through them. They were mostly found sleeping in them the next morning.

The animals also liked the polystyrene maze and in addition to exploring it (which was evidenced by the bedding that was strewn all over in the maze the next morning) they also preferred chewing it as was evident the next morning. This did not cause much damage to the maze in the case of younger rats but the maze had to be replaced more frequently with older rats. In contrast the animals in the normal cage only became active once the light went off and were playing and sometimes engaging in fights with their littermates in the cage as they did not have any novel objects to explore.

Statistical analysis (3-way MANOVA, appendix A 3.7a) of the results shows that there was no environmental effect on total and basal $^{45}Ca^{2+}$ uptake (figures 3.7.1a, b, 3.7.2a, b, c, and d, $p > 0.1$) and also no environmental effect on NMDA-stimulated $^{45}Ca^{2+}$ uptake into SHR and WKY barrel cortex slices (figures 3.7.3a, b, c, and d, $p > 0.1$). As a result the data from the novel and normal environment was pooled and analysed using a 2-way MANOVA (Appendix A3.7b)

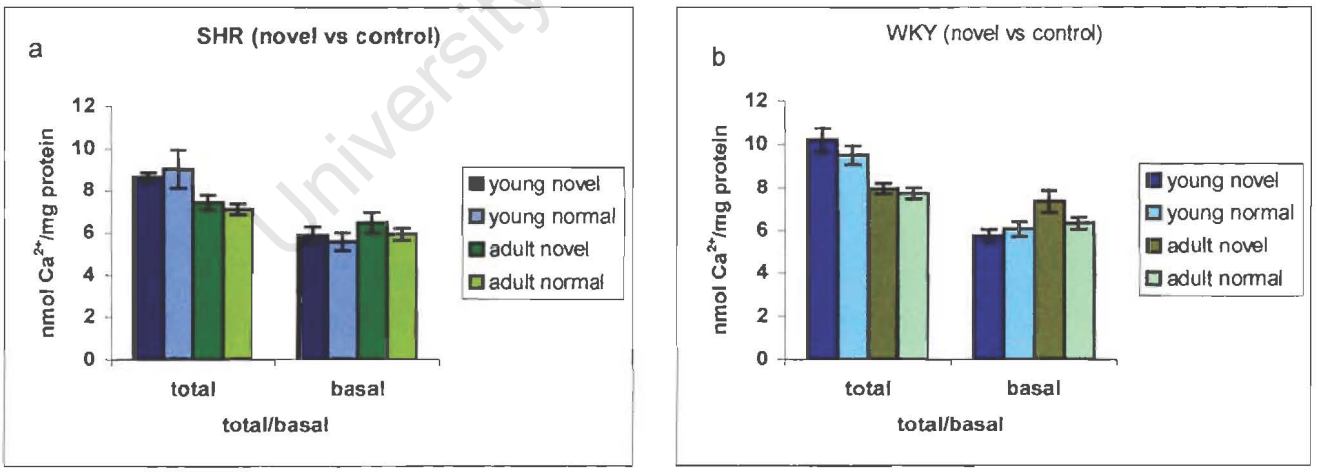

Figure 3.7.1

a and b) Total uptake, following 2-minute exposure to 100 μM NMDA, and basal $^{45}Ca^{2+}$ uptake into barrel cortex slices of SHR and WKY reared in a novel environment compared to controls. Results are mean ± SEM

Table 3.7.1:Total uptake, following exposure to NMDA, and basal $^{45}Ca^{2+}$ uptake into different regions of barrel cortex of young and adult SHR and WKY reared in a novel or a normal environment (data depicted in figures 3.7.1 a and b

		Total uptake			**Basal uptake**		
Strain/age/env	**N**	**Mean**	**SD**	**SEM**	**Mean**	**SD**	**SEM**
Young/SHR/novel	6	8.6	0.545	0.222	5.9	0.992	0.405
Young/SHR/normal	7	9.0	2.359	0.892	5.6	1.125	0.425
Adult/SHR/novel	4	7.4	0.702	0.351	6.5	0.962	0.481
Adult/SHR/normal	6	7.1	0.642	0.262	5.9	0.723	0.295
Young/WKY/novel	5	10.2	1.214	0.543	5.7	0.678	0.303
Young/WKY/normal	5	9.5	0.966	0.432	6.0	0.752	0.336
Adult/WKY/novel	4	7.9	0.500	0.250	7.3	1.037	0.519
Adult/WKY/normal	6	7.7	0.657	0.268	6.3	0.655	0.267

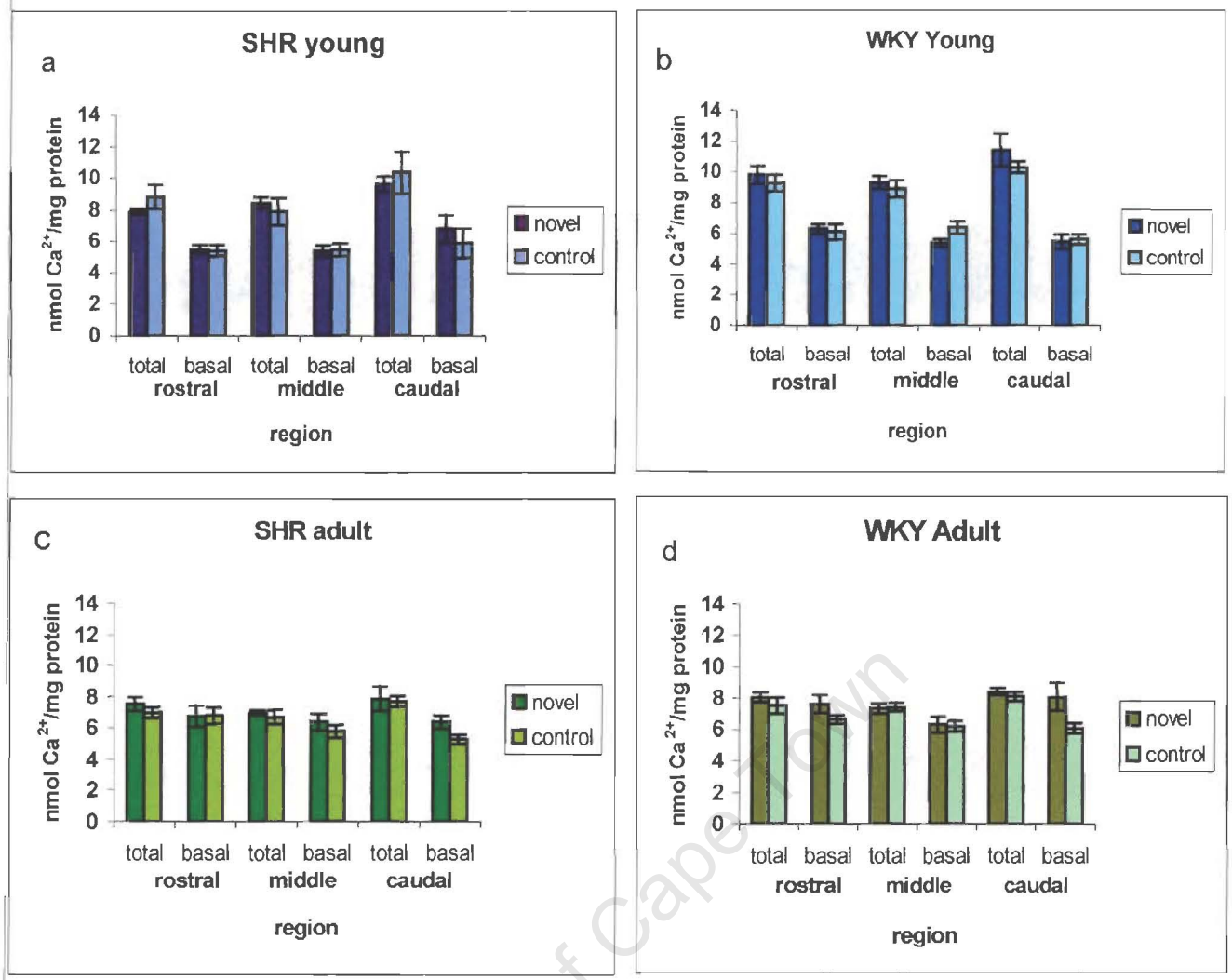

Figure 3.7.2

a) Total uptake, following 2-minute exposure to NMDA, and basal $^{45}Ca^{2+}$ uptake into different regions of barrel cortex of young SHR reared in a novel environment compared to controls (n = 5 novel and n = 5 control). Results are mean ± SEM

b) Total uptake, following 2-minute exposure to NMDA and basal $^{45}Ca^{2+}$ uptake into different regions of barrel cortex of young WKY reared in a novel environment compared to controls (n = 4 novel and n = 6 control). Results are mean ± SEM.

c) Total uptake, following 2-minute exposure to NMDA, and basal $^{45}Ca^{2+}$ uptake into different regions of barrel cortex of adult SHR reared in a novel environment compared to controls (n = 6 novel and n = 7 control). Results are mean ± SEM

d) Total uptake, following 2-minute exposure to NMDA, and basal $^{45}Ca^{2+}$ uptake into different regions of barrel cortex of adult WKY reared in a novel environment compared to controls (n = 4 novel and n = 6 control). Results are mean ± SEM

Table 3.7.2: Total uptake, following exposure to NMDA, and basal $^{45}Ca^{2+}$ uptake into different regions of barrel cortex of young and adult SHR and WKY reared in a novel or a normal environment (data depicted in figures 3.7.2 a, b, c and d)

			Total uptake			Basal uptake		
Strain/age/env	**Region**	**N**	**Mean**	**SD**	**SEM**	**Mean**	**SD**	**SEM**
Young/SHR/novel	Rostral	6	7.6	0.386	0.158	5.5	0.671	0.274
	Middle	6	8.4	0.880	0.359	5.4	0.821	0.335
	Caudal	6	9.6	1.143	0.466	6.8	2.171	0.886
Young/SHR/normal	Rostral	7	8.8	1.925	0.727	5.4	0.936	0.354
	Middle	7	7.9	2.236	0.845	5.5	1.069	0.404
	Caudal	7	10.4	3.587	1.356	5.9	2.542	0.961
Adult/SHR/novel	Rostral	4	7.5	0.925	0.463	6.7	1.356	0.678
	Middle	4	7.0	0.266	0.133	6.4	1.040	0.520
	Caudal	4	7.8	1.518	0.759	6.4	0.787	0.393
Adult/SHR/normal	Rostral	6	7.0	0.834	0.340	6.8	1.267	0.517
	Middle	6	6.7	1.006	0.411	5.8	0.950	0.388
	Caudal	6	7.7	0.861	0.352	5.2	0.820	0.335
Young/WKY/novel	Rostral	5	9.8	1.282	0.573	6.3	0.709	0.317
	Middle	5	9.3	0.932	0.417	5.4	0.583	0.261
	Caudal	5	11.4	2.368	1.059	5.5	1.038	0.464
Young/WKY/normal	Rostral	5	9.3	1.224	0.547	6.1	1.146	0.513
	Middle	5	8.9	1.234	0.552	6.4	0.881	0.394
	Caudal	5	10.3	0.817	0.365	5.6	0.766	0.343
Adult/WKY/novel	Rostral	4	8.1	0.605	0.302	7.6	1.121	0.560
	Middle	4	7.4	0.618	0.309	6.3	0.961	0.481
	Caudal	4	8.4	0.446	0.223	8.1	1.802	0.901
Adult/WKY/normal	Rostral	6	7.5	1.261	0.515	6.6	0.641	0.262
	Middle	6	7.4	0.688	0.281	6.2	0.780	0.318
	Caudal	6	8.1	0.720	0.294	6.1	0.822	0.336

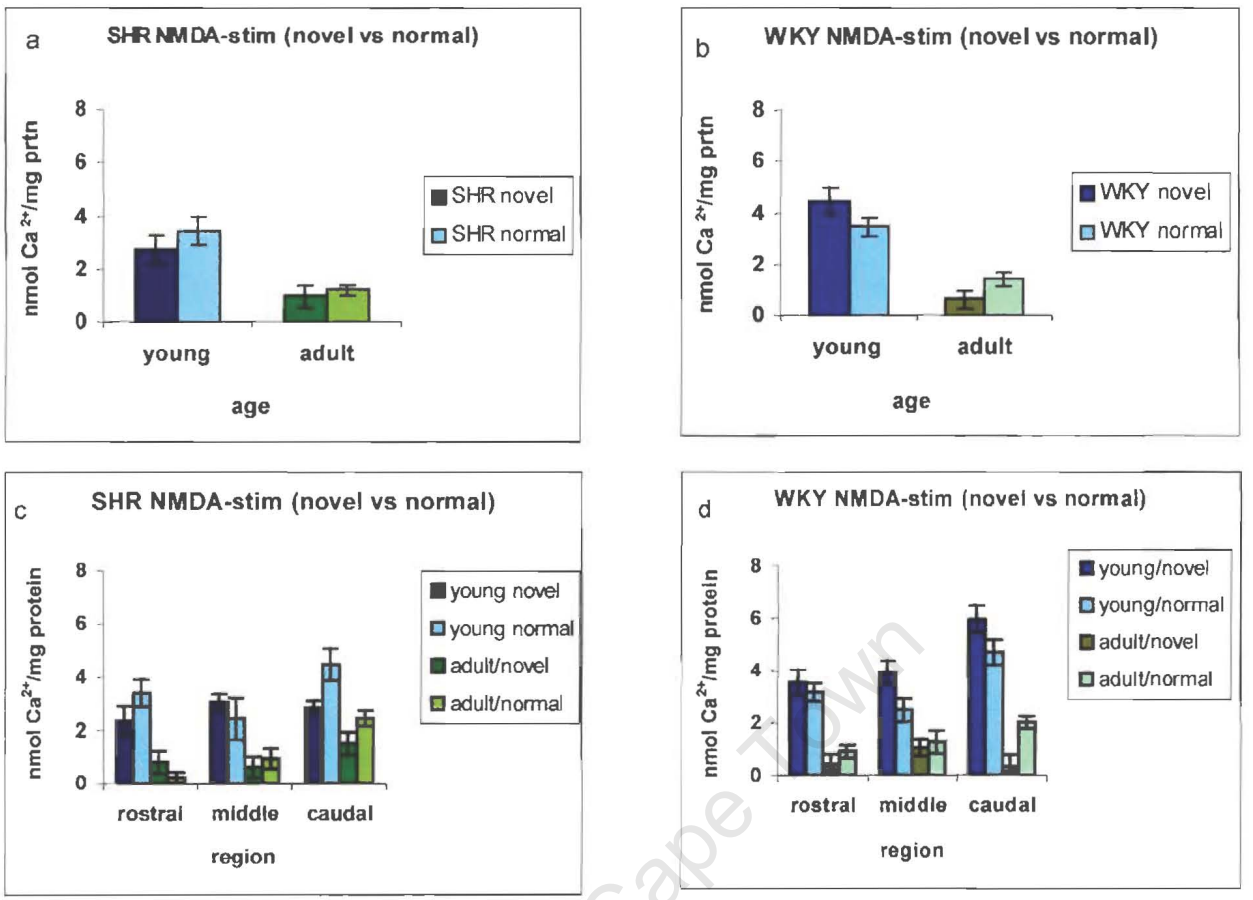

Figure 3.7.3

a) *Average NMDA-stimulated $^{45}Ca^{2+}$ uptake into entire barrel cortex of SHR (n = 6, young novel, n = 7 young normal, n = 4 adult novel, n = 6 adult normal) Results are mean ± SEM*

b) *Average NMDA-stimulated $^{45}Ca^{2+}$ uptake into entire barrel cortex of WKY (n = 5, young novel, n = 5 young normal, n = 4 adult novel, n = 6 adult normal) Results are mean ± SEM*

c) *NMDA-stimulated $^{45}Ca^{2+}$ uptake into different regions of barrel cortex of SHR (n = 6, young novel, n = 7 young normal, n = 4 adult novel, n = 6 adult normal) Results are mean ± SEM*

d) *NMDA-stimulated $^{45}Ca^{2+}$ uptake into different regions of barrel cortex of WKY (n = 5, young novel, n = 5 young normal, n = 4 adult novel, n = 6 adult normal) Results are mean ± SEM*

Table 3.7.3:NMDA-stimulated $^{45}Ca^{2+}$ uptake into barrel cortex and into different regions of barrel cortex of young and adult SHR and WKY reared in a novel or a normal environment (Data depicted in figures 3.7.3 a, b, c, and d)

Strain/age/env	Region	N	Mean	SD	SEM
Young/SHR/novel	Entire	6	2.8	1.312	0.536
	Rostral	6	2.4	0.775	0.316
	Middle	6	3.0	0.639	0.261
	Caudal	6	2.8	3265	1.333
Young/SHR/normal	Entire	7	3.4	1.372	0.519
	Rostral	7	3.4	2.059	0.778
	Middle	7	2.4	1.564	0.591
	Caudal	7	4.5	2.139	0.808
Adult/SHR/novel	Entire	4	1.0	0.837	0.419
	Rostral	4	0.8	0.806	0.403
	Middle	4	0.6	0.904	0.452
	Caudal	4	1.5	1.241	0.621
Adult/SHR/normal	Entire	6	1.2	0.485	0.198
	Rostral	6	0.2	0.935	0.382
	Middle	6	0.9	0.704	0.287
	Caudal	6	2.5	0.970	0.396
Young/WKY/novel	Entire	5	4.5	1.135	0.508
	Rostral	5	3.5	1.025	0.459
	Middle	5	3.9	1.174	0.525
	Caudal	5	6.0	1.940	0.867
Young/WKY/normal	Entire	5	3.5	0.748	0.335
	Rostral	5	3.2	1.009	0.451
	Middle	5	2.5	1.068	0.477
	Caudal	5	4.7	1.093	0.489
Adult/WKY/novel	Entire	4	0.6	0.682	0.341
	Rostral	4	0.4	0.633	0.316
	Middle	4	1.0	0.853	0.427
	Caudal	4	0.3	1.422	0.711
Adult/WKY/normal	Entire	6	1.4	0.628	0.256
	Rostral	6	0.9	1.114	0.455
	Middle	6	1.3	0.569	0.232
	Caudal	6	2.0	0.850	0.347

There were significant age and strain effects on the average total $^{45}Ca^{2+}$ uptake into the barrel cortex (figure 3.7.4, $p < 0.05$, 2-way MANOVA, Appendix A3.7b). There was no interaction between the two variables namely age and strain in the average total $^{45}Ca^{2+}$ uptake into the barrel cortex or into the different regions. The age effect on total uptake shows that the average total $^{45}Ca^{2+}$ uptake into the entire barrel cortex was significantly lower in adult SHR and WKY than in young SHR and WKY (2-way MANOVA followed by Newman-Keuls test, figure 3.7.4, $p < 0.001$). The strain effect on the other hand, shows that the average total $^{45}Ca^{2+}$ uptake into SHR barrel cortex is significantly lower than WKY (figure 3.7.4, $p < 0.05$).

Separate analysis of the individual regions shows significant strain and age effects on total uptake into the rostral and middle regions of the barrel cortex while the in caudal region only age effect is significant (figure 3.7.5a, 2-way MANOVA, $p < 0.05$). The strain effect shows that total uptake into rostral and middle regions of SHR is significantly lower than uptake into corresponding regions of WKY (figure 3.7.5a, 2-way MANOVA followed by Newman-Keuls test, $p < 0.05$). The age effect shows that total uptake into all regions of adult rats is significantly lower than young rats (figure 3.7.5a, 2-way MANOVA followed by Newman-Keuls test, $p < 0.001$). There was no interaction between age and strain.

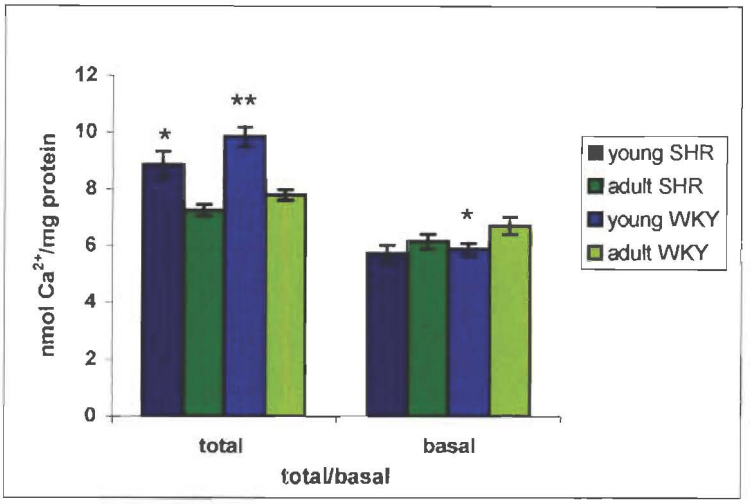

Figure 3.7.4) *Average total, following 2-minute exposure to 100 μM NMDA, and basal $^{45}Ca^{2+}$ uptake into barrel cortex of young and adult SHR and WKY. (n = 10 adult SHR and adult WKY, 10 young WKY and 13 young SHR, 2-way ANOVA *indicates significantly different from corresponding adult value p < 0.001, ** indicates significantly different from corresponding adult value and young SHR value, p < 0.05) Results are mean ± SEM*

Table 3.7.4: Average total uptake, following 2-minute exposure to 100 μM NMDA and basal $^{45}Ca^{2+}$ uptake into barrel cortex of young and adult SHR and WKY. (data depicted in figure 3.7.4)

		Total uptake			**Basal uptake**		
Strain/age	**N**	**Mean**	**SD**	**SEM**	**Mean**	**SEM**	**SD**
Young SHR	13	8.8	1.717	0.476	5.7	1.033	0.287
Adult SHR	10	7.2	0.648	0.205	6.2	0.825	0.261
Young WKY	10	9.8	1.099	0.348	5.9	0.695	0.220
Adult WKY	10	7.8	0.584	0.185	6.7	0.941	0.298

There was a significant age effect on average basal $^{45}Ca^{2+}$ uptake into barrel cortex and further analysis showed that average basal $^{45}Ca^{2+}$ uptake was significantly lower in young SHR and WKY than in adult SHR and WKY (2-way MANOVA followed by Newman-Keuls test, figure 3.7.4, $p < 0.05$). Separate analysis of the regions shows that there was an age effect in basal uptake into the rostral region (2-way MANOVA, $p < 0.001$) but not into the middle and caudal regions of the barrel cortex (2-way MANOVA, $p > 0.1$). Further analysis revealed that basal $^{45}Ca^{2+}$ uptake into the rostral region was significantly lower in adult SHR and WKY than in young SHR and WKY (figure 3.7.5b, 2-way MANOVA followed by Newman-Keuls test, $p < 0.001$). There was no interaction between strain and age in all the regions.

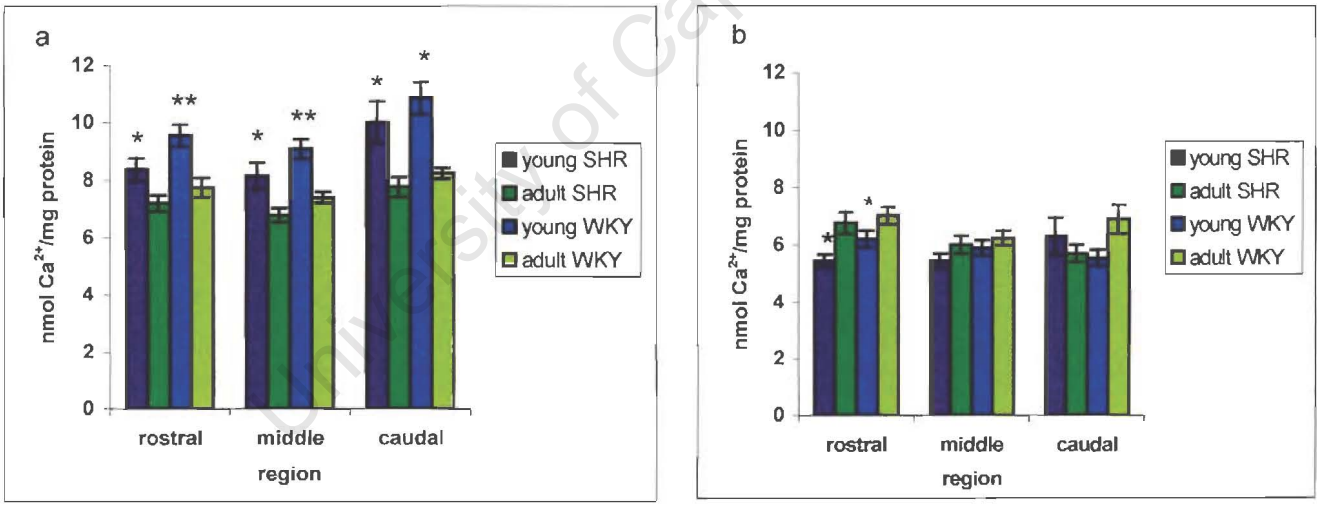

Figure 3.7.5

*a) Total uptake into rostral, middle and caudal regions of the barrel cortex of young and SHR and WKY following 2-minute exposure to 100 μM NMDA (n = 10 adult SHR and 10 adult WKY, 10 young WKY and 13 young SHR, 2-way ANOVA) *indicates significantly different from corresponding adult value p < 0.001, ***

indicates significantly different from corresponding adult value and young SHR value $p < 0.05$.) Results are mean ± SEM

*b) Basal uptake into rostral, middle and caudal regions of the barrel cortex of young and adult SHR and WKY (n = 10 adult SHR & adult WKY, 10 young WKY and 13 young SHR, 2-way ANOVA) *indicates significantly different from corresponding adult value, $p < 0.001$). Results are mean ± SEM*

Table 3.7.5 Total, following 2-minute exposure to 100μM NMDA and basal $^{45}Ca^{2+}$ uptake into rostral, middle and caudal regions of the barrel cortex of young and adult SHR and WKY (data depicted in figure 3.7.5a and b)

			Total uptake			**Basal uptake**		
Strain/Age	**Region**	**N**	**Mean**	**SD**	**SEM**	**Mean**	**SD**	**SEM**
Young/SHR	Rostral	13	8.4	1.470	0.408	5.4	0.792	0.220
	Middle	13	8.2	1.703	0.472	5.4	0.923	0.256
	Caudal	13	10.0	2.669	0.740	6.3	2.325	0.645
Adult/SHR	Rostral	10	7.2	0.863	0.273	6.8	1.227	0.388
	Middle	10	6.8	0.779	0.246	6.0	0.979	0.310
	Caudal	10	7.8	1.089	0.344	5.7	0.955	0.302
Young/WKY	Rostral	10	9.6	1.218	0.385	6.2	0.905	0.286
	Middle	10	9.1	1.057	0.334	5.9	0.879	0.278
	Caudal	10	10.9	1.772	0.560	5.5	0.863	0.273
Adult/WKY	Rostral	10	7.7	1.039	0.328	7.0	0.953	0.301
	Middle	10	7.4	0.626	0.198	6.2	0.807	0.255
	Caudal	10	8.2	0.617	0.195	6.9	1.584	0.501

There was a significant age effect on the average NMDA-stimulated $^{45}Ca^{2+}$ uptake into entire barrel cortex as well as into the rostral, middle and caudal regions of the barrel cortex (figure 3.7.6, $p < 0.001$).

Further analysis (2-way MANOVA followed by Newman-Keuls test) of the results within the age groups shows that NMDA-stimulated $^{45}Ca^{2+}$ uptake into all regions of the barrel cortex was significantly lower in adult WKY and SHR than in young WKY and SHR (figure 3.7.6, $p < 0.05$). There was no interaction between strain and age in NMDA-stimulated $^{45}Ca^{2+}$ uptake into the rostral, middle and caudal regions (figure 3.7.6, $p > 0.1$).

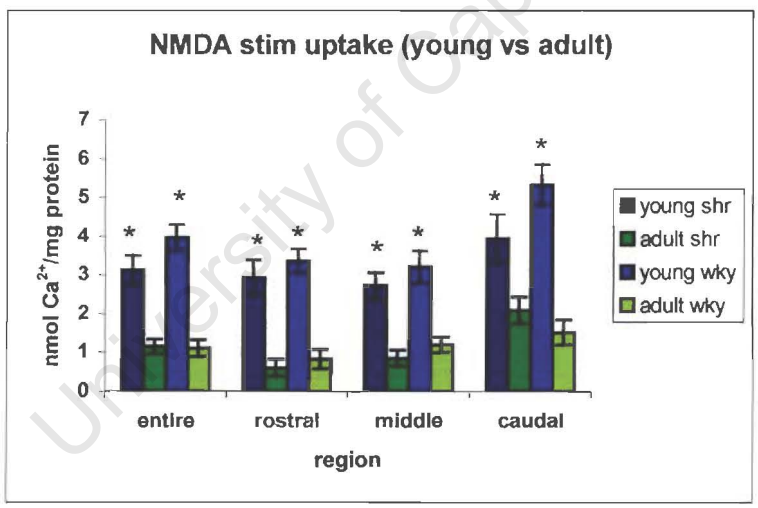

Figure 3.7.6) *Average NMDA-stimulated $^{45}Ca^{2+}$ uptake into barrel cortex and into rostral, middle and caudal regions of young and adult SHR and WKY. (n = 10 adult SHR & WKY, 10 young WKY and 13 young SHR, 2-way ANOVA *indicates significantly different from corresponding adult value, $p < 0.001$). Results are mean ± SEM*

Table 3.7.6: Average NMDA-stimulated $^{45}Ca^{2+}$ uptake into barrel cortex and uptake into rostral, middle and caudal regions of young and adult SHR and WKY (data depicted in figure 3.7.6).

Strain/Age	Region	N	Mean	SD	SEM
Young/SHR	Entire	13	3.1	1.337	0.371
	Rostral	13	2.9	1.631	0.452
	Middle	13	2.7	1.221	0.339
	Caudal	13	3.9	2.238	0.621
Adult/SHR	Entire	10	1.2	0.596	0.189
	Rostral	10	0.6	0.685	0.217
	Middle	10	0.9	0.647	0.205
	Caudal	10	2.1	1.090	0.345
Young/WKY	Entire	10	3.9	1.054	0.333
	Rostral	10	3.4	0.978	0.309
	Middle	10	3.2	1.300	0.411
	Caudal	10	5.3	1.627	0.514
Adult/WKY	Entire	10	1.1	0.677	0.214
	Rostral	10	0.8	0.782	0.247
	Middle	10	1.2	0.619	0.196
	Caudal	10	1.5	0.995	0.315

The average total Ca^{2+} uptake into barrel cortex slices as well as into rostral, middle and caudal regions was significantly higher than basal Ca^{2+} uptake in both young SHR and young WKY (t-test for dependent samples, $p < 0.001$). Total Ca^{2+} uptake into barrel cortex slices of adult SHR and adult WKY was significantly higher than basal Ca^{2+} uptake in all regions of the barrel cortex of adult WKY and into middle and caudal regions of adult SHR (t-test for dependent samples, $p < 0.05$). There was no

difference between basal and total Ca^{2+} uptake into the rostral region of adult SHR (t-test for dependent samples, $p > 0.1$)

3.7.1 SHR vs WKY

The results from the young SHR and WKY (4 to 6 week old) reared in the normal environment were analysed separately and compared with the previous study where SHR was compared to WKY (section 3.6). There was no significant difference (Appendix A 3.7.1) between SHR and WKY in total uptake and basal uptake into the entire barrel cortex (figure 3.7.1.1a ANOVA $p > 0.1$) as well as into the rostral, middle and caudal regions of the barrel cortex (figure 3.7.1.1b ANOVA $p > 0.1$).

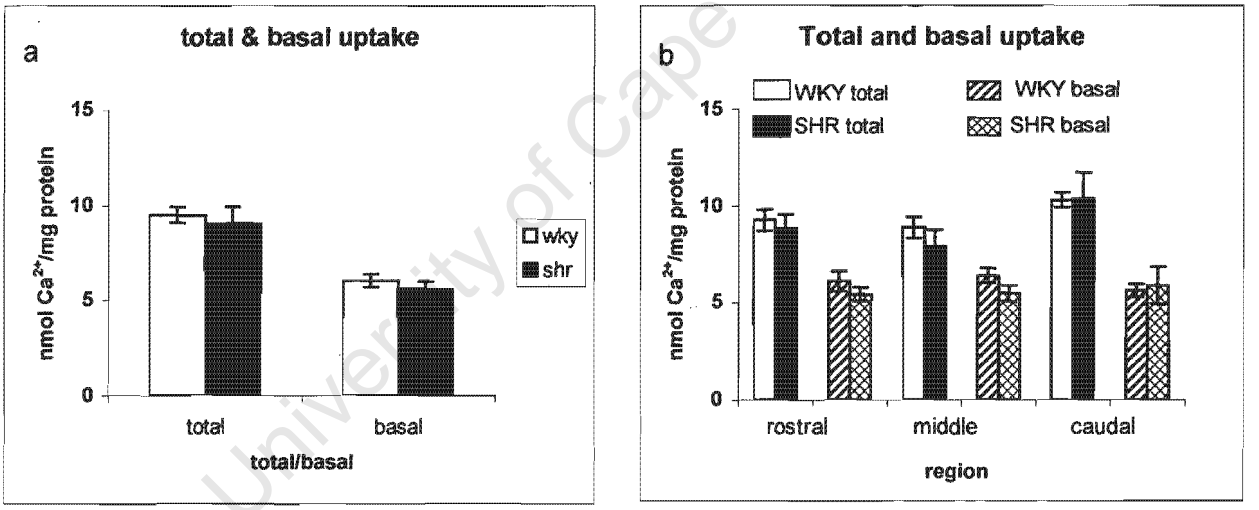

Figure 3.7.1.1

a) Average total uptake, following 2-minute exposure to NMDA, and basal $^{45}Ca^{2+}$ uptake into entire barrel cortex of young WKY and SHR (n = 5 WKY and n = 7 SHR, ANOVA). Results are mean ± SEM

b) Total uptake, following 2-minute exposure to NMDA, and basal $^{45}Ca^{2+}$ uptake into different regions of barrel cortex of young WKY and SHR (n = 5 WKY and n = 7 SHR, ANOVA) Results are mean ± SEM

Table 3.7.1.1a: Average total uptake, following 2-minute exposure to NMDA, and basal $^{45}Ca^{2+}$ uptake into barrel cortex slices of WKY and SHR (data depicted in figure 3.7.1.1a)

		Total uptake			**Basal uptake**		
Strain	**N**	**Mean**	**SD**	**SEM**	**Mean**	**SD**	**SEM**
SHR	7	9.0	2.359	0.892	5.6	1.125	0.425
WKY	5	9.5	0.966	0.432	6.0	0.752	0.336

Table 3.7.1.1b: Total, following 2-minute exposure to NMDA, and basal $^{45}Ca^{2+}$ uptake into rostral, middle and caudal regions of barrel cortex of WKY and SHR (data depicted in figure 3.7.1.1b)

			Total uptake			**Basal uptake**		
Strain	**N**	**Region**	**Mean**	**SD**	**SEM**	**Mean**	**SD**	**SEM**
SHR	7	Rostral	8.8	1.925	0.727	5.4	0.936	0.354
	7	Middle	7.9	2.236	0.835	5.4	1.069	0.404
	7	Caudal	10.4	3.587	1.356	5.9	2.542	0.961
WKY	5	Rostral	9.3	1.224	0.547	6.1	1.146	0.513
	5	Middle	8.9	1.234	0.552	6.4	0.881	0.394
	5	Caudal	10.3	0.817	0.365	5.6	0.766	0.343

There was no significant difference between SHR and WKY in NMDA-stimulated Ca^{2+} uptake into the barrel cortex (figure 3.7.1.2a ANOVA $p > 0.1$). The same result

was obtained when the rostral, middle and caudal regions of the barrel cortex were analysed separately (figure 3.7.1.2b ANOVA $p > 0.1$).

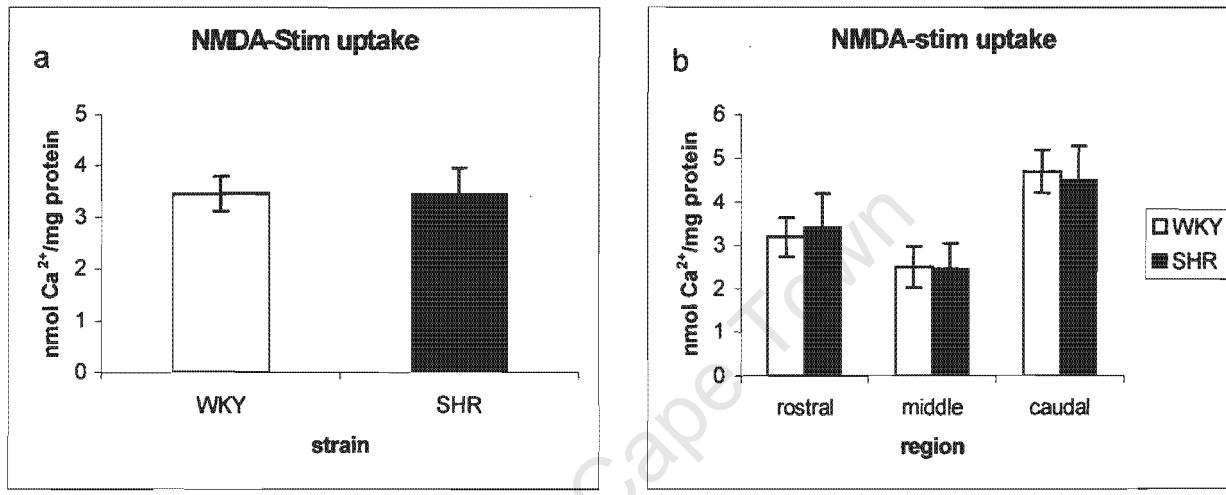

Figure 3.7.1.2

a) Average NMDA-stimulated $^{45}Ca^{2+}$ uptake into barrel cortex of WKY and SHR (n = 5 WKY and n = 7 SHR, ANOVA). Results are mean ± SEM

b) NMDA-stimulated $^{45}Ca^{2+}$ uptake into rostral, middle and caudal regions of barrel cortex of WKY and SHR. (n = 5 WKY and n= 7 SHR, ANOVA). Results are mean ± SEM

Table 3.7.1.2a: Average NMDA-stimulated $^{45}Ca^{2+}$ uptake into barrel cortex slices of WKY and SHR (data depicted in figure 3.7.1.2a)

Strain	N	Mean	SD	SEM
SHR	7	3.4	1.372	0.519
WKY	5	3.5	0.748	0.335

Table 3.7.1.2b) NMDA-stimulated $^{45}Ca^{2+}$ uptake into different regions of barrel cortex of WKY and SHR. (data depicted in figure 3.7.1.2b)

Strain	N	Region	Mean	SD	SEM
SHR	7	Rostral	3.4	2.059	0.778
	7	Middle	2.4	1.564	0.591
	7	Caudal	4.5	2.139	0.808
WKY	5	Rostral	3.2	1.009	0.451
	5	Middle	2.5	1.068	0.477
	5	Caudal	4.7	1.093	0.489

3.8 Pre-frontal cortex

Slices containing the prefrontal cortex and cingulate cortex were dissected from the brains of SHR and WKY. The prefrontal cortex was divided into three regions as described in section 2.2.4 of the methods each region containing two slices and it was subjected to the same assay as the barrel cortex as outlined in section 2.2.5 of the methods. Some animals from both strains were exposed to a maze overnight prior to sacrifice and these were compared to animals that were not exposed to a maze to see if overnight exposure to an enriched environment affected NMDA receptor function differently and whether there was an interaction between strain and environment.

Statistical analysis (2-way MANOVA, Appendix A 3.8) of the results shows no environment effect ($p > 0.1$) while there was a significant strain effect on the average total $^{45}Ca^{2+}$ uptake into prefrontal cortex slices ($p < 0.01$). Further analysis (Newman-Keuls test) showed that the average total $^{45}Ca^{2+}$ uptake into prefrontal cortex slices of SHR was significantly lower than total uptake into prefrontal cortex slices of WKY (figure 3.8.1a, ANOVA, $p < 0.01$). When the rostral, middle and caudal regions were analysed separately, total $^{45}Ca^{2+}$ uptake into the rostral and middle regions of SHR was significantly lower than uptake into the corresponding regions of WKY (figure 3.8.1b, $p < 0.01$) while in the caudal region there was no difference in total $^{45}Ca^{2+}$ uptake between SHR and WKY (figure 3.8.1b, $p > 0.1$). There was no interaction between strain and environment on total uptake ($p > 0.1$).

There was no environment effect on average basal $^{45}Ca^{2+}$ uptake into prefrontal cortex slices (2-way ANOVA, $p > 0.1$) while there was a tendency for a strain effect on average basal $^{45}Ca^{2+}$ uptake into prefrontal cortex (2-way ANOVA, $p = 0.065$).

Separate analysis of the rostral, middle and caudal regions shows that there was neither an environment nor a strain effect in basal uptake into all the regions of the prefrontal cortex (2-way ANOVA, $p > 0.1$). There was no interaction between strain and environment on basal $^{45}Ca^{2+}$ uptake into prefrontal cortex.

Total uptake is significantly higher than basal uptake into barrel cortex slices and into the rostral, middle and caudal regions (t-test for dependent samples, figure 3.8.1b, $p < 0.01$) for both SHR and WKY.

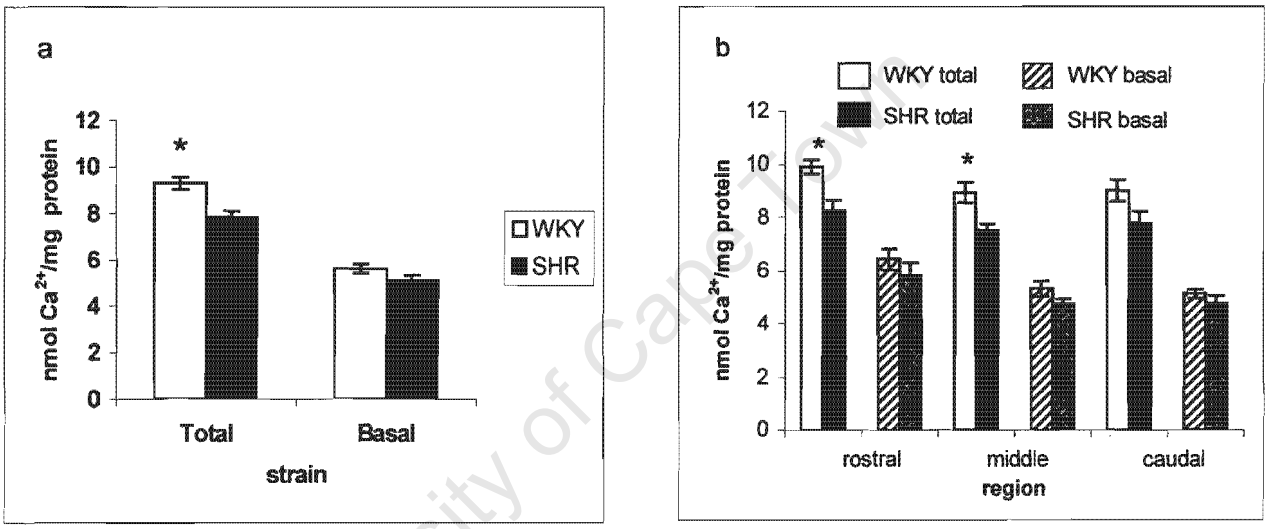

Figure 3.8.1

*a) Average total, following 2-minute exposure to NMDA, and basal $^{45}Ca^{2+}$ uptake into PFC slices of WKY and SHR (n = 10 SHR and 10 WKY, ANOVA, * indicates significantly different from SHR value, $p < 0.01$). Results are mean ± SEM*

*b) Total, following 2-minute exposure to NMDA and basal $^{45}Ca^{2+}$ uptake into different regions of PFC slices of WKY and SHR (n = 10 SHR and 10 WKY, ANOVA, * indicates significantly different from SHR value, $p < 0.01$). Results are mean ± SEM*

Table 3.8.1a: Average total, following 2-minute exposure to NMDA, and basal $^{45}Ca^{2+}$ uptake into PFC slices of WKY and SHR (data depicted in figure 3.8.1a)

		Total uptake			Basal uptake		
Strain	**N**	**Mean**	**SD**	**SEM**	**Mean**	**SD**	**SEM**
SHR	10	7.8	0.840	0.266	5.1	0.597	0.189
WKY	10	9.3	0.853	0.270	5.6	0.602	0.190

Table 3.8.1b Total, following 2-minute exposure to NMDA, and basal $^{45}Ca^{2+}$ uptake into different regions of PFC slices of WKY and SHR (data depicted in figure 3.8.1b).

			Total uptake			Basal uptake		
Strain	**N**	**Region**	**Mean**	**SD**	**SEM**	**Mean**	**SD**	**SEM**
SHR	10	Rostral	8.3	1.184	0.374	5.8	1.469	0.465
	10	Middle	7.5	0.819	0.259	4.7	0.614	0.194
	10	Caudal	7.8	1.443	0.456	4.8	0.915	0.289
WKY	10	Rostral	9.9	0.824	0.261	6.4	1.282	0.405
	10	Middle	8.9	1.175	0.372	5.3	0.932	0.295
	10	Caudal	9.0	1.285	0.406	5.1	0.506	0.160

There was a significant strain effect on average NMDA-stimulated $^{45}Ca^{2+}$ uptake into prefrontal cortex and further analysis (Newman Keuls test) showed that average NMDA-stimulated uptake into SHR prefrontal cortex was significantly lower than uptake into WKY (figure 3.8.2a, $n = 10$ $p < 0.05$). However when rostral, middle and caudal regions of the prefrontal cortex were analysed separately, NMDA-stimulated uptake into rostral and caudal regions of SHR was not significantly different from WKY prefrontal cortex (figure 3.8.2b, $p > 0.1$) while in middle region there was a tendency for NMDA-stimulated uptake to be lower in SHR compared to WKY ($p = 0.067$). There was no environment effect on NMDA-stimulated $^{45}Ca^{2+}$ uptake into the

prefrontal cortex and into the rostral, middle and caudal regions (2-way ANOVA, $p > 0.1$). There was also no interaction between strain and environment on NMDA-stimulated $^{45}Ca^{2+}$ uptake.

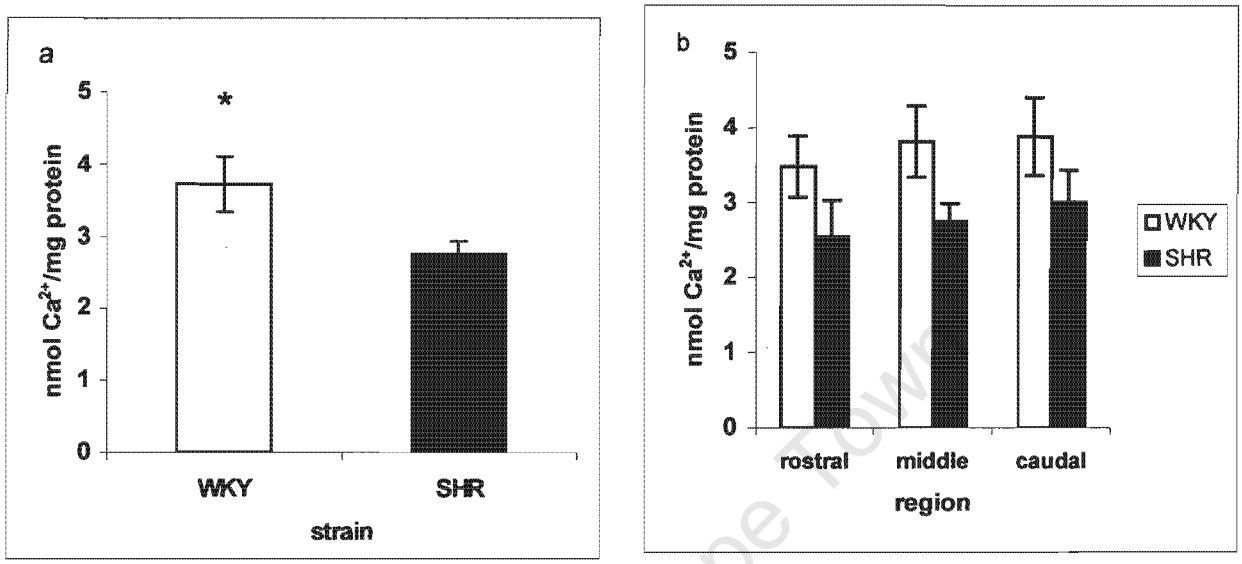

Figure 3.8.2

*a) Average NMDA-stimulated $^{45}Ca^{2+}$ uptake into entire PFC slices for WKY and SHR (n = 10 SHR and n = 10 WKY, ANOVA *indicates significantly different from SHR value, $p < 0.05$). Results are mean ± SEM*

b) NMDA-stimulated $^{45}Ca^{2+}$ uptake into different regions of PFC slices for WKY and SHR. (n = 10 and n = 10 WKY) Results are mean ± SEM

Table 3.8.2a: *Average NMDA-stimulated $^{45}Ca^{2+}$ uptake into entire PFC slices for WKY and SHR (data depicted in figure 3.8.2a)*

Strain	**N**	**Mean** (nmol Ca^{2+}/mg protein)	**SD**	**SEM**
SHR	10	2.8	0.533	0.168
WKY	10	3.7	1.194	0.378

Table 3.8.2b: *NMDA-stimulated $^{45}Ca^{2+}$ uptake into different regions of PFC slices for WKY and SHR (data depicted in figure 3.8.2b)*

Strain	**Region**	**N**	**Mean** (nmol Ca^{2+}/mg protein)	**SD**	**SEM**
SHR	Rostral	10	2.5	1.547	0.489
	Middle	10	2.7	0.766	0.242
	Caudal	10	3.0	1.357	0.429
WKY	Rostral	10	3.4	1.286	0.407
	Middle	10	3.8	1.498	0.474
	Caudal	10	3.9	1.643	0.520

Chapter 4 Discussion

Methods

The slice preparation is a very important tool for studying brain function. The slice preparation retains a considerable degree of functionality whilst providing excellent experimental opportunities for different fields of study for example anatomy, physiology and pharmacology to mention just a few (Collingridge, 1995). Henry McIlwain (Collingridge, 1995) developed the brain slice preparation in the 1950s for biochemical studies of brain tissue (Collingridge, 1995) using both chemical and electrical parameters that could be measured and manipulated by the experimenter (Collingridge, 1995). The slices cut at a thickness of 0.35 mm are the largest that could be adequately supplied with metabolites and oxygen (Collingridge, 1995) and this prompted the use of the same thickness in this study. To validate the preparation McIlwain (Collingridge, 1995) used electrophysiological techniques and found that the slices were not only metabolically viable but also contained neurons with healthy resting membrane potentials (Collingridge, 1995). There are four machines mainly used to prepare brain slices namely the Vibratome, the Vibroslice, the McIlwain/Stoelting tissue chopper and the Farquhar slicer (Lipton *et al.*, 1995). The vibratome is the most difficult to use and requires more time but it is thought to be the most gentle on the tissue (Lipton *et al.*, 1995).

In this study the Vibratome was used and the results obtained show that the slices produced by the vibratome were viable for at least 90 minutes (duration of assay). We were able to measure significant K^+-stimulated uptake of $^{45}Ca^{2+}$ above control

values showing that voltage sensitive Ca^{2+} channels respond to depolarisation by high K^+ concentration. Also the fact that we were able to recover the $^{45}Ca^{2+}$ from the slices at the end of the washing stages of the experiment shows that the cell membranes in the slices were intact. Had the cell membranes in the slices not been intact the $^{45}Ca^{2+}$ would not have been recovered from the tissue at the end of the washing stages of the assay, as the cells would not have retained the $^{45}Ca^{2+}$.

Basal uptake refers to $^{45}Ca^{2+}$ uptake into slices under resting conditions ie without addition of a stimulating agent. The basal uptake probably consists of non-specific binding of Ca^{2+} to the damaged edges of the slices and also uptake into neurons and glial cells, the latter have been shown to participate actively in Ca^{2+} waves as opposed to the past notion that they were just passive participants in brain function (Haydon, 2001). In this study, the term total uptake, refers to the sum of the basal uptake of $^{45}Ca^{2+}$ and $^{45}Ca^{2+}$ uptake in the presence of high K^+ or NMDA through either voltage-sensitive calcium channels (VSCCs) (Melena and Osborne, 2001, Saadoun *et al.*, 1997), NMDA receptor channels (Gosh and Greenberg, 1995) or Ca^{2+} leak pathways (Triggle, 2000). Similarly the K^+-stimulated or NMDA-stimulated uptake refers to the difference between the total and basal $^{45}Ca^{2+}$ uptake by the tissue. Uptake into the entire barrel cortex refers to the average $^{45}Ca^{2+}$ uptake into the three regions of the barrel cortex and this was determined because there is no anatomical basis for the division of the barrel cortex although there was consistency in dividing the slices into the three regions.

It is very important that all the preparations are done at low temperatures and that the brain receives enough oxygen during the tissue preparation in order to keep it alive.

In this study oxygenation was provided using a system of fine tubing made from 1 ml syringes (section 2.2.5) and was maintained for the rest of the experiment. After preparation of the brain block, it was glued to the chuck using Loctite glue in order to hold the brain secure during slicing in the vibratome. It is very important that the amount of glue is carefully controlled as it might interfere with slicing and also it might affect the tissue if it runs up the sides of the cortex. On the other hand there has to be enough glue, evenly spread, so that the brain can be held securely to the chuck and not lift under the pressure of the blade as it is sliced. The process of glueing the brain to the chuck has to be done very quickly since at this point the brain is not immersed in buffer and has no oxygen supply.

Orientation of the brain during slicing (section 2.2.2) is very important as it allows the blade to begin cutting at a small surface and then proceed to cut from the ventral side towards the cortex. The particular orientation used in this study avoids a band of cortical fibres that are not easily cut by the blade and potentially damaging to the slice. A new blade was fitted for every experiment and care was taken not to touch the cutting edge of the blade so that it remained as sharp as possible for the experiment.

Once cut it is important to make as little contact as possible with the slices (especially the area of interest) in order to avoid further damaging the cells and in these experiments a small paint brush was used to pick up slices from beneath and transfer them to the buffer. During dissection of the desired area, it is important to correctly identify the area and make as few cuts as possible on the slice in order to minimise

damage as this may increase the area of non-specific $^{45}Ca^{2+}$ binding to the slices and hence reduce the sensitivity of the method.

The pH of the incubation media was tested randomly after the experiments just to ensure that there was no change which could affect the results. The pH of all buffer solutions was found to be between 7.33 and 7.35 after most experiments which is not significantly different from 7.4, the original pH at which the experiments were supposed to be carried out. This was done at least twice with every batch of new solutions.

K^+ stimulated $^{45}Ca^{2+}$ uptake

Increasing the extracellular concentration of K^+ from 5 mM to 50 mM (or 62.5 mM as used in this study) depolarises the membrane by directly shifting the K^+ equilibrium potential above the threshold potential for voltage dependent Ca^{2+} channel activation (Schlame & Hemmings, 1995). This change leads to opening of voltage-gated calcium channels and entry of Ca^{2+} into cells (Schlame & Hemmings, 1995). The results (section 3.1.1) show a K^+-stimulated uptake of 2.0 nmol, 2.5 nmol, 4.7 nmol Ca^{2+}/mg protein/2-minute incubation for the rostral, middle, caudal regions of the barrel cortex respectively. These results are comparable with results obtained by Feldman *et al.*, (1990) for the visual cortex of kittens where K^+-stimulated uptake of 1.5 nmol Ca^{2+}/mg of protein/2-minute incubation was reported. The small difference might be due to the fact that a different species and brain area was used. Feldman *et al.*, (1990) also used 62.5 mM K^+ to depolarise the cells.

The average basal $^{45}Ca^{2+}$ uptake was 10.6 ± 0.923 nmol Ca^{2+}/mg protein/2-minute incubation while the average total $^{45}Ca^{2+}$ uptake was 13.5 ± 0.415 nmol Ca^{2+}/mg protein/2-minute incubation. When the extracellular Ca^{2+} concentration was reduced from 2.0 mM to 1.2 mM in the HEPES and incubation buffers (section 3.1.2) a slight decrease in both basal and total uptake was observed. Average basal $^{45}Ca^{2+}$ uptake was reduced to 6.3 ± 0.882 nmol Ca^{2+}/mg protein/2minute incubation while the average total $^{45}Ca^{2+}$ uptake was reduced to 8.5 ± 0.428 nmol Ca^{2+}/mg protein/2minute incubation. This decrease was probably due to a smaller electrochemical gradient provided by the lower extracellular Ca^{2+} concentration and also probably by the fact that non-specific binding of calcium to the slices may have been reduced as a result of less calcium being available in the medium. The basal uptake obtained after reduction of the external Ca^{2+} concentration is comparable with basal uptake of 6.0 nmol Ca^{2+}/mg protein into rat cerebral cortex synaptosomes obtained by Simonato *et al.*, (1989) who incubated synaptosomes (1 –1.5 mg protein/ml) in buffer containing 1.3 mM Ca^{2+} in the external medium for 3 minutes. Saadoun *et al.*, (1998) also reported a basal uptake of 5.97 nmol Ca^{2+}/mg protein into rat brain synaptosomes (10 – 20 mg protein/ml) after 1-minute incubation with radioactively labelled Ca^{2+}in buffer containing 1.2 mM Ca^{2+}. However, the total uptake of 14 nmol Ca^{2+}/mg protein /3 minutes obtained by Simonato *et al.*, (1989) after exposing rat cerebral cortex synaptosomes to 50 mM K^+ for 3 minutes was higher than the average total $^{45}Ca^{2+}$ uptake of 8.5 ± 0.428 nmol Ca^{2+}/mg protien/2-minutes incubation obtained in this study. The reduction of external Ca^{2+} concentration from 2 mM to 1.2 mM proved useful, as K^+-stimulated $^{45}Ca^{2+}$uptake into the rostral region became significant. Lowering the K^+ concentration in the incubation buffer (section 3.1.3) on the other

hand had no significant effect on either basal or total $^{45}Ca^{2+}$ uptake and also did not have an effect on K^+-stimulated $^{45}Ca^{2+}$ uptake.

Although there was no significant improvement in K^+-stimulated Ca^{2+} uptake when the buffer conditions were optimised by lowering both extracellular calcium and potassium concentrations to correspond to physiological concentrations of potassium and calcium found in rat cerebrospinal fluid (Davson *et al.,* 1987), the basal uptake was lowered and K^+-stimulated uptake of Ca^{2+} increased by 10 to 20%. K^+-stimulated $^{45}Ca^{2+}$ uptake into the rostral region of the rat barrel cortex was significantly lower than into the middle or caudal region, suggesting a lower concentration of voltage-gated calcium channels in the rostral part of the barrel cortex. These regional differences may have important functional implications in the barrel cortex.

NMDA

In the present study the excitatory amino acid receptor agonist, NMDA, was shown to stimulate calcium uptake into rat barrel cortex slices (section 3.2). $^{45}Ca^{2+}$ uptake through the NMDA receptor channels was chosen as a direct measure of receptor activity in this study as was the case with Oster and Schramm, (1993). The results obtained in this study suggest that buffer containing 3.36 mM K^+ caused sufficient depolarization to overcome the Mg^{2+} blockade of the NMDA receptor channel. Alternatively, depolarization and removal of the magnesium block could have been achieved by glutamate leaking from damaged cells in the slice preparation which in turn could have caused AMPA receptors to be activated, thereby causing depolarization of the cell membrane. At a concentration of 100 μM, NMDA

increased Ca^{2+} uptake by approximately 28% or 2.2 nmol Ca^{2+}/mg protein/2 minutes. This agrees with the level of NMDA-evoked Ca^{2+} uptake into cat visual cortex of 1.7 nmol Ca^{2+}/mg protein/2 minutes (Feldman *et al.,* 1990). 100 μM NMDA was chosen for the present investigation since Feldman *et al.,* (1990) had demonstrated this to be the minimal concentration required to achieve maximal effect. Also at 100 μM, NMDA was not toxic to the cells as it was found not to affect either the viability or the protein content of cultured cerebellar granule cells (Oster and Schramm, 1993). Feldman *et al.,* (1990) observed no effect on Ca^{2+} uptake at 10 μM NMDA. Feldman *et al.,* (1990) reported that NMDA caused a concentration–dependent increase in calcium uptake over a concentration range from 12.5 to 100 μM.

Glycine

NMDA receptor activation requires glycine as a co-agonist, it was considered that glycine might be limiting in the in vitro slice preparation. However, this did not appear to be the case as identical results were obtained with and without glycine in the incubation buffer (section 3.3). NMDA responses are detectable in culture and brain slice preparation because of the presence of endogenous glycine (Ozawa *et al.,* 1998). It could be that there is already enough glycine in the slice preparation because of the damage caused to the cells during slicing. This is doubtful as there are two major steps in the assay i.e the 45-minute equilibration phase and the 5-minute pre-incubation phase in which any excess glycine could be lost before the incubation with $^{45}Ca^{2+}$. Didier *et al.,* (1993) did not observe an increase in $^{45}Ca^{2+}$ uptake into cultured rat cerebellar granule cells after addition of 10 μM glycine. A high concentration of glycine present in the culture medium, which could not be effectively removed during

pre-incubation, was cited as a possible reason (Didier *et al.*, 1993). Aronstam *et al.*, (1994) suggested the presence of endogenous glycine associated with the NMDA receptor in their microvesicle preparation. Aronstam *et al.*, (1994) showed that glycine (100μM) did not affect the level of NMDA-stimulated $^{45}Ca^{2+}$ uptake into rat brain microvesicles but it reduced the inhibition of $^{45}Ca^{2+}$ uptake caused by euflurane and halothane.

On the other hand glycine has some weak Zn^{2+} chelation properties (Paoletti *et al.*, 1997) it might be that it chelates the Zn^{2+} ions early in the preparation hence no matter how many incubation steps, its function can be fulfilled. Zn^{2+} ions are known to be abundant in some nerve terminals and can be released in the synaptic cleft at concentrations of nearly 1 μM (Paoletti *et al.*, 1997). Zn^{2+} ions antagonize native NMDA receptors via either voltage-dependent or independent inhibition (Paoletti *et al.*, 1997).

MK 801

The fact that NMDA-mediated Ca^{2+} uptake into rat barrel cortex slices in this study was completely antagonised by MK-801 which is a selective NMDA receptor antagonist shows that the increase in $^{45}Ca^{2+}$ uptake was due to activation of NMDA receptors. Basal $^{45}Ca^{2+}$ uptake into rostral barrel cortex slices obtained from the right hemisphere (section 3.4) was higher than uptake in the presence of both NMDA and MK-801 (hence a negative value in figure 3.4b). Basal $^{45}Ca^{2+}$ uptake into right hemisphere slices was higher than basal $^{45}Ca^{2+}$ uptake into the left hemisphere slices. Total $^{45}Ca^{2+}$ uptake in the presence of NMDA alone and in the presence of NMDA +

MK801 was similar for both left and right barrel cortex slices. Melena and Osborne, (2001) showed using voltage-sensitive calcium channel blockers that voltage-sensitive calcium channels contribute to NMDA-stimulated Ca^{2+} uptake. Among the voltage-sensitive calcium channels, the L-type channels make a greater contribution to NMDA-stimulated Ca^{2+} uptake than the N- and P/Q types of voltage-sensitive calcium channels in isolated rat retinas (Melena and Osborne, 2001). The contribution however is minimal unless it is a result of NMDA-induced depolarisation of the membrane as the NMDA receptor antagonist MK-801 completely prevented Ca^{2+} uptake into isolated rat retinas thus confirming that uptake into rat retinas was mainly through the NMDA receptors (Melena and Osborne, 2001). Calcium influx into cells can also occur via the calcium permeable AMPA or kainate receptor channels (Gosh and Greenberg, 1995) or calcium leak pathways (Triggle, 1990). The NMDA effect on $^{45}Ca^{2+}$ uptake into barrel cortex slices was also completely antagonised by MK-801 in this study suggesting that uptake was through NMDA receptors thus ruling out the possibility of influx through the calcium permeable AMPA and kainate receptors.

Different K^+ Concentrations

Incubation of barrel cortex slices with different concentrations of potassium and NMDA (section 3.5) was aimed at enhancing the NMDA effect on Ca^{2+} uptake into the slices. This was based on the premise that NMDA receptors require both membrane depolarisation and NMDA binding to open and allow Ca^{2+} influx. It was thought that with elevated external K^+ concentration, the cells would be more

depolarised, the magnesium block could be removed more effectively and there would be more Ca^{2+} influx as a result of NMDA binding.

The results obtained in section 3.5 for the two controls incubated with different K^+ concentrations show that the increase of K^+ concentration to 20 mM from 3.36 mM in the incubation and HEPES buffer did not have a significant effect on basal Ca^{2+} uptake, although the p value of 0.0619 (section 3.5) may be an indication that the effect might be significant had it not been for a small sample size. The Ca^{2+} uptake due to the 2-minute incubation of rostral barrel cortex slices with 20 mM K^+ of 1.4 ± 0.554 nmol Ca^{2+}/mg protein compares well with the 62.5mM K^+-stimulated uptake of 1.8 ± 0.406 nmol Ca^{2+}/mg of protein into the rostral area under the optimised buffer conditions (section 3.1.3). Both controls were from the rostral region.

When brain slices were incubated with 25 μM NMDA in the presence of 3.36 mM K^+, the (25 μM) NMDA-stimulated uptake of 1.6 ± 0.635 nmol Ca^{2+}/mg protein, although not significant, a p value of 0.062 was obtained suggesting that 25 μM could be the subminimal concentration required to induce Ca^{2+} uptake. The effect of 25 μM NMDA on $^{45}Ca^{2+}$ uptake was lower than 100 μM NMDA-stimulated Ca^{2+} uptake into the middle region of 2.6 ± 0.832 nmol Ca^{2+}/mg protein (section 3.2). Feldman *et al.*, (1990) reported a dose-dependent increase in NMDA stimulated uptake with NMDA concentrations ranging from 12.5 μM to 100 μM. Again the small sample size might have contributed to the effect of 25 μM NMDA not being significant.

When brain slices (designated as tests T2, T3 and T4) were incubated with different concentrations of NMDA, T2 (10 μM NMDA), T3 (12.5 μM NMDA) and T4 (25 μM NMDA) in conjunction with elevated extracellular K^+ (20 mM) there was no significant increase in $^{45}Ca^{2+}$ uptake above baseline. These tests (T2, T3 and T4) were compared to control C2 (20 mM K^+) which was apparently higher than T2 and T3 hence negative values in figure 3.5b. $^{45}Ca^{2+}$ uptake in the presence of both elevated K^+ (20 mM) and NMDA (10 μM, 12.5 μM, and 25 μM) is smaller than uptake in the presence of either K^+ or NMDA on their own. These results show that the NMDA effect is not increased in the presence of elevated extracellular K^+.

The observations in this study can be compared to findings of Kierdrowski L., (1999). Kierdrowski L., (1999), using digital fluorescence microscopy showed that elevation of extracellular K^+ concentrations ($[K^+]_E$) from 5.6 mM to 60 mM inhibited 300 μM NMDA-induced Ca^{2+} influx into primary cultures of rat cerebellar granule cells and excitotoxicity due to NMDA receptor activation. Kierdrowski L., (1999) suggested that high $[K^+]_E$ inhibits NMDA-induced Ca^{2+} uptake. Increasing the $[K^+]_E$ depolarises the membrane causing Ca^{2+} influx via voltage-sensitive calcium channels (Schlame and Hemmings, 1995) and because NMDA-stimulated Ca^{2+} uptake is slower compared to Ca^{2+} influx via voltage-sensitive calcium channels, the Ca^{2+} taken up via voltage-sensitive channels reduces the gradient driving Ca^{2+} into the cell via NMDA receptor channels.

NMDA is an essential survival factor when cerebellar granule cells are cultured in medium containing 10 mM KCl but no NMDA is required when the culture medium contains 25 mM KCl (Oster and Schramm, 1993). When NMDA was added to a

cerebellar granule cell culture medium containing 25 mM KCl, it suppressed development of NMDA receptor-mediated $^{45}Ca^{2+}$ uptake with the maximum effect occurring at 100 μM NMDA (Oster and Schramm, 1993). The development program for NMDA receptor activity was resumed after NMDA was removed from the culture medium (Oster and Schramm, 1993). It was suggested that NMDA has the capacity to down-regulate NMDA receptor activity in order to protect cells against toxicity (Oster and Schramm, 1993).

SHR vs WKY

The results (section 3.6) show significant NMDA-stimulated Ca^{2+} uptake above basal levels in all regions of barrel cortex of both SHR and WKY. These results compare well with results obtained for Long Evans rats (section 3.2). There was no difference in NMDA-stimulated $^{45}Ca^{2+}$uptake between SHR and WKY into the entire barrel cortex but when the barrel cortex was divided into different regions, the rostral and caudal regions showed no difference in $^{45}Ca^{2+}$ uptake, whereas NMDA-stimulated Ca^{2+} uptake was significantly lower in the middle region of the SHR barrel cortex compared to WKY. This result may represent an early stage of development of decreased glutamate-stimulated $^{45}Ca^{2+}$ uptake into cerebral cortical neurons. The overall result suggests that NMDA receptor function is not disturbed in SHR.

We previously observed decreased NMDA-stimulated $^{45}Ca^{2+}$ uptake into cerebral cortical synaptosomes of 5- to 7-month-old SHR compared to age-matched WKY, following exposure to different glutamate concentrations (10 nM, 100 nM, 500 nM and 1 mM glutamate) (Russell and Lehohla, 1998; unpublished observations).

Interestingly, depolarization-evoked uptake of $^{45}Ca^{2+}$ via voltage-sensitive calcium channels, into cerebral cortical synaptosomes, achieved by exposure to high external K^+ concentrations, was no different in 5- to 7-month-old SHR and WKY (Russell and Lehohla, 1998; unpublished observations). Basal and total $^{45}Ca^{2+}$ uptake in the presence of 62.5 mM K^+ into cerebral cortical synaptosomes was significantly lower in aged SHR than aged WKY (Russell and Lehohla, 1998 unpublished observations).

Total Ca^{2+} uptake into rostral, middle and caudal regions of SHR and WKY barrel cortex slices detected in the present study compared well with results previously obtained for Long Evans rats (section 3.2). Together the results reflect a similar pattern where the uptake increases from the rostral to the caudal region in all strains. Basal levels of Ca^{2+} uptake into rostral, middle and caudal regions of SHR and WKY barrel cortex were also comparable to previous Long Evans values (section 3.2). Total Ca^{2+} uptake into rostral, middle and caudal regions of SHR barrel cortex slices was significantly lower than uptake into the same WKY regions. Basal uptake of Ca^{2+} into rostral and caudal regions of SHR barrel cortex was significantly lower than uptake into the corresponding WKY regions. There was no significant difference in basal Ca^{2+} uptake between the middle regions of both rat strains. These results, and those observed previously for 5- to 7-month-old rats (Russell and Lehohla, 1998), suggest that calcium metabolism may be disturbed in the cerebral cortex of SHR.

Indeed, there is considerable evidence to suggest that calcium metabolism is disturbed in SHR. Horn *et al.*, (1995) showed that synaptic plasma membranes prepared from SHR cerebrum have significantly diminished Ca^{2+}ATPase activity compared to WKY. This finding implies that Ca^{2+} is removed at a slower rate from SHR

cytoplasm than WKY, hence the concentration gradient that drives $^{45}Ca^{2+}$ into the cell may be smaller in SHR. This may account for the fact that total and basal Ca^{2+} uptake is lower in SHR than WKY in the present study. In addition, the intracellular Ca^{2+} concentration was higher in isolated SHR hearts compared to WKY (Anderson *et al.*, 1999) which could also explain why basal and total uptake are lower in SHR compared to WKY because of the smaller concentration gradient of Ca^{2+}in SHR. The present study extends previous findings where calcium transport across intestinal epithelial brush border membranes of 12- to 15-week-old rats was reduced in SHR compared to WKY, (de Gooyer *et al.*, 1999). These results show that calcium uptake is lower in SHR compared to WKY which agrees with results in the present study. Anderson *et al.*, (1999), also showed that Na^{+}/Ca^{2+} exchange activity is lower in isolated SHR hearts suggesting that Ca^{2+} is removed at a slower rate from the cytoplasm in SHR leading to less Ca^{2+} uptake. These results together with the results of the present study show that calcium uptake is lower in SHR compared to WKY.

The present findings provide evidence that calcium metabolism is disturbed in somatosensory cortex of prehypertensive, 4- to 6-week-old SHR. Previous results have shown alterations of the mechanisms regulating dopamine release from terminals in the nucleus accumbens, caudate-putamen and prefrontal cortex, as well as norepinephrine release from terminals in the prefrontal cortex of SHR (Linthorst *et al.*, 1990; Russell *et al.*, 1995; 1996; 1998; 2000; Russell and Wiggins, 2000). Evidence suggested that vesicle storage of catecholamines might be impaired (Russell *et al.*, 1998). However, since neurotransmitter release is dependent on the influx of calcium ions into presynaptic terminals and varicosities, an underlying disturbance in calcium metabolism may well lead to compensatory mechanisms and alterations in the regulation of neurotransmitter release.

Strain, enriched environment and age effect

Strain (SHR versus WKY)

There was no difference in basal $^{45}Ca^{2+}$ uptake into all regions of SHR and WKY barrel cortex, and this does not agree with the results obtained in section 3.6 where young SHR and WKY were compared. However, the average total $^{45}Ca^{2+}$ uptake into SHR barrel cortex and also total $^{45}Ca^{2+}$ uptake into the rostral and middle regions was significantly lower than average total $^{45}Ca^{2+}$ uptake into WKY and total $^{45}Ca^{2+}$ uptake into the corresponding regions of WKY barrel cortex. The fact that total $^{45}Ca^{2+}$ uptake is lower in SHR agrees with the results in section 3.6 with the exception of the caudal region in which there was no difference in total $^{45}Ca^{2+}$ uptake between SHR and WKY. Similarly, there was no difference in NMDA-stimulated $^{45}Ca^{2+}$ uptake between SHR and WKY and this agrees with results obtained in section 3.6. These findings from section 3.7 do not contradict the fact that NMDA receptor function is not disturbed SHR barrel cortex as seen from the fact that NMDA-stimulated $^{45}Ca^{2+}$ uptake is not different between the two strains. This analysis included both young and adult rats.

When results from the young SHR and WKY (4 to 6 week old, section 3.7) from the normal and enriched environments in the second study were pooled and analysed independently from results of the adults, there was no difference in total $^{45}Ca^{2+}$ uptake between SHR and WKY. The results show a difference in basal $^{45}Ca^{2+}$ uptake into the rostral region but not in average basal $^{45}Ca^{2+}$uptake or basal $^{45}Ca^{2+}$ uptake into the middle and caudal regions. There was no difference in NMDA-stimulated $^{45}Ca^{2+}$ uptake between SHR and WKY and this again agrees with the fact that NMDA

receptor function is not disturbed in SHR seen in the previous study (section 3.6). With the exception of the basal uptake into the rostral region, the results are in agreement with the results obtained when only results from young SHR and WKY rats reared in the normal environment (section 3.7.1) were analysed separately. When the results from the young SHR and WKY reared in the normal environment were analysed separately and compared to the results obtained in section 3.6, the latter results showed no difference between SHR and WKY in basal, total and NMDA-stimulated $^{45}Ca^{2+}$ uptake. However the same pattern of results was observed where basal, total and NMDA-stimulated $^{45}Ca^{2+}$ uptake into the SHR barrel cortex is slightly lower than $^{45}Ca^{2+}$ uptake into WKY barrel cortex except for the rostral region in the second study where NMDA-stimulated $^{45}Ca^{2+}$ uptake was slightly higher in SHR than in WKY. This was probably due to one experiment where SHR values were higher than in the other experiments. Removal of the high SHR value from calculations however did not produce significant results but gave a picture more comparable to that obtained in the first study. The experiment (Table 3.7.2, 3.7.3) with high values was not removed from calculations though.

Comparisons of results of total, basal and NMDA-stimulated $^{45}Ca^{2+}$ uptake in the two studies shows a trend where $^{45}Ca^{2+}$ uptake into SHR barrel cortex is slightly lower than $^{45}Ca^{2+}$ uptake into WKY barrel cortex. Taken together, the results obtained when both adult and young SHR and WKY were compared (section 3.7) and when young SHR and WKY (section 3.7.1.1) are comparable with results in section 3.6. This agrees with the suggestion that calcium metabolism maybe disturbed in SHR and that it is not the NMDA receptor function that is disturbed in SHR.

Enriched versus normal environment

Exposure of young and adult rats to an enriched environment in the present study did not have an effect on NMDA receptor function (section 3.7). The results however showed the same pattern as observed for LE rats (section 3.2) where uptake increases from the rostral to the caudal regions and also the pattern of disturbance of Ca^{2+} metabolism observed for SHR and WKY in section 3.6 is also evident in this study.

Exposure to an enriched environment is an important model of plastic changes in the brain (Filipwoski *et al.*, 2000). The idea was that exposure to an enriched environment might lead to increased NMDA receptor function as it provides the animals with informal learning opportunities (Rosenzweig and Bennett, 1996). An enriched environment is described as a combination of complex inanimate and social stimulation and is enriched in relation to standard laboratory housing conditions (van Praag *et al.*, 2000). The environment is complex and the novel objects as well as their location are changed frequently to provide variation over a period of time (van Praag *et al.*, 2000). The same procedure was adopted in this study where novel objects were changed daily.

It has previously been shown that exposure to an enriched environment for different time periods leads to increases in brain weights and an increase in acetylcholine esterase (AChE) and cholinesterase (ChE) activity (Rosenzweig *et al.*, 1968). Volkmar and Greenough, (1972) used Golgi-staining to show increased higher order branching in layer II, IV and V pyramidal cells and layer IV stellate cells in the rat visual cortex after exposure to an enriched environment for 29 to 31 days. These

results show that the density of dendritic spines and extent of dendritic arborization in the rat cortex are environmentally regulated to a certain extent (Volkmar and Greenough, 1972). It was thought that the increased number and density of dendritic spines and size of receptor areas observed in rats exposed to an enriched environment might reflect a difference in the number of cortical neurotransmitter binding sites (Por *et al.,* 1982). The results obtained by Por *et al.,* (1982) showed that there was no difference in neurotransmitter receptor levels between rats exposed to an enriched environment and controls. Por *et al.,* (1982) exposed rats to an enriched environment for 35 to 55 days and found a 5% increase in cortical weights of animals exposed to an enriched environment compared to their littermates in the normal cage. Using receptor binding assays they however found no evidence that differential rearing environments caused significant differences in dopamine/serotonin, α and β-adrenergic, muscarinic/cholinergic, or GABA receptor levels in the rat cortical membrane preparations (Por *et al.,* 1982). Also Bardo and Hammer, (1991) using autoradiography showed that dopamine D1 and D2 receptor densities in the nucleus accumbens were not different between groups of rats reared in the enriched environment for 30 days and rats reared in the normal environment.

Increased expression of immediate-early genes was suggested to be a consequence of increased intracellular Ca^{2+} concentration (Morgan and Curran, 1989) which in turn is a consequence of neuronal activity (Steiner and Gerfen, 1994). Increased expression of immediate-early genes c-fos and c-jun in the rat barrel cortex as a result of exposure to an enriched environment has been shown by Filipwoski *et al.,* (2000) and Staiger *et al.,* (2000a). It has been argued that changes in the levels of expression of immediate-early genes can reflect changes in neuronal activity (Sagar *et al.,* 1988).

As a result of increased neuronal activity during exploration of the enriched environment one would have expected to measure increased Ca^{2+} uptake in response to stimulation of NMDA receptors but that was not the case in this study. Differences between the two studies include the fact that in this study the animals were exposed to the novel environment for 24 hours over a period of at least two weeks compared to the 20 minute exposure per day used by Filipwoski *et al.,* (2000), where the whiskers were directly stimulated. On the other hand Staiger *et al.*, (2000a) exposed the animals to an enriched environment overnight before experimenting on them and got the same result as Filipwoski *et al.,* (2000). This rules out the possibility that duration of exposure to an enriched environment is critical in this study. This is further supported by the fact that Rosenzweig *et al.*, (1968) did not find any significant difference in brain weights and acetylcholine esterase activity (AChE) between three groups of animals. One group was exposed to an enriched environment for 2.5 hours a day, and spent the rest of the day in the normal cage. Another group was exposed to a novel environment for 4.5 hours per day while another group was exposed to an enriched environment for 24 hours. Thus a few hours of daily exposure to an enriched environment increased brain weights as much as 24 hours exposure (Rosenzweig *et al.,* 1968). In this study most of the young animals were exposed to the enriched environment for a maximum of 2 weeks while the adults were exposed for twelve weeks. The total, basal and NMDA-stimulated $^{45}Ca^{2+}$ uptake was not significantly different between rats exposed to an enriched environment and their corresponding controls for age both groups. This agrees with the fact that the time of exposure to the enriched environment is not critical.

The finding in this study is that Ca^{2+} uptake is not increased by prior exposure to an enriched environment.

Adult versus young

The results obtained in this study (section 3.7) show that NMDA-stimulated Ca^{2+} uptake into barrel cortex slices of adult (12 to 18 weeks old) rats is significantly lower than uptake into young (4 to 6 weeks old) rat barrel cortex slices in both SHR and WKY. The same result was obtained when the rostral, middle and caudal regions were analysed separately. Although not always significant the results show a tendency for basal uptake to be higher in adult rats than in younger rats while in contrast, total uptake seems to be significantly higher in young rats compared to adults. Could it be that the adult brain has a diminished number of NMDA receptors leading to lower NMDA-stimulated uptake of calcium? The ability of the central nervous system (CNS) to respond in a novel way to changing sensory inputs is not constant throughout life (Skibinska *et al.*, 2000). In adult animals plasticity is more restricted than in neonatal and young animals (Skibinska *et al.*, 2000) which is consistent with the suggestion that NMDA receptor function is diminished in adult rats.

The present results suggest that NMDA receptors either become less sensitive with ageing or the number (or density) of receptors diminishes with age. The two could be linked, with less density there may possibly be less sensitivity. However this is not the case as Akaike and Rhee, (1997) have shown that reduced responsiveness of

Meynert neurons to NMDA occurs without affecting the affinity but is due to an abrupt reduction in the number of NMDA receptors.

The first possibility is supported by observations by Kato, (1993) who showed that NMDA receptors from visual cortex of young rats are less sensitive to MK-801 compared to adult visual NMDA receptors. Only 0.3 μM MK 801 was needed to completely block NMDA excitatory postsynaptic potentials in adults while 10 μM MK 801 was needed to block NMDA excitatory postsynaptic potentials in young rats. Tsumoto *et al.,* (1987) showed that NMDA receptors of young kittens are more effective than those of adult cats. This they showed by noting that the minimum intensity of currents required for NMDA to excite visual cortex cells in the kittens was significantly smaller than that needed in the adult cats. Also 2-amino-5-phosphonovaleric acid (APV), a selective NMDA receptor antagonist, significantly suppressed visual responses in only 33% of the cells tested in adult cats while in kittens APV suppressed visual responses in 71% of the cortical cells tested (Tsumoto *et al.,* 1987).

It could be that the density of NMDA receptors decreases with age as this was shown by Tremblay *et al.*, (1988) who measured the density of NMDA receptors in the rat hippocampus using autoradiography. They showed that first there is an increase which peaks in postnatal day 12 and then declines as age progresses. This is further supported by the findings of Wenk and Barnes, (2000) who showed a decrease in NMDA receptor density in the CA1, CA3 and subicular cell regions of the hippocampus, but not in the FD/hilar region, in rats ranging between 3 and 29 months using receptor binding assays. This shows that there is a gradual decrease in the

number of NMDA receptors with increasing age in the hippocampus. Using the specific non-competitive NMDA receptor antagonist MK-801, Serra *et al.,* (1993) showed a significant decrease in the number of NMDA receptors in cerebral cortex, hippocampus and stiratum of 18 and 24 month old male Wistar-Kyoto rats compared to their 3 month old counterparts. Mitchell and Anderson, (1998) also using the NMDA receptor antagonist MK-801, found a significant decrease in [^{3}H]MK-801 binding in the inner frontal cortex, the entorhinal cortex and the lateral straitum of 24 month-old Fischer 344 rats compared to 6-month-old Fischer 344 rats. However there was no significant age-related difference in MK-801 binding in the same areas between 6-month-old and 12-month old rats (Mitchell and Anderson, 1998) and also there was no significant difference in laminar thickness, volume and neuronal density (Mitchell and Anderson, 1998). This shows that the density of NMDA receptors decreases with ageing without any change in the number of neurons or the volume of the brain.

Since the animals used in the present study were much older than postnatal day 12 which is the age at which NMDA receptor density is at its peak (Tremblay *et al.,* 1988) it could be that the density (or number) of NMDA receptors had declined at 4 to 6 weeks of age and continued to decline.

Given the important role that NMDA receptors play in development, it is quite logical to expect them to decrease in density once the brain is fully developed although somehow one imagines that they should still be needed for purposes of learning and memory for which they have been shown to be very useful in the hippocampus (Stecher *et al.,* 1997). Perhaps they are not required to the same extent in adult brain

as during development. Serra *et al.,* (1993) showed that the decrease in the number of NMDA receptors is associated with an increase in sensitivity of [3H]MK-801 binding to the stimulatory actions of glutamate in the hippocampus but not in the cerebral cortex or the striatum. This suggests that in the hippocampus the decline in the number of NMDA receptors is compensated for by the increased sensitivity.

Pre-frontal cortex

The prefrontal cortex is critical for guiding behaviour using working memory which can be conceptualised as a form of short term memory that is distinct from longer-term episodic or semantic memory (Arnsten, 1998). It also plays an essential role in the organisation of mammalian behaviour by adapting internal organs to the external environment via anatomical connections in the brain (Takita *et al.,* 1997). NMDA receptors have been shown to occur in the prefrontal cortex of rats particularly in the medial part (Takita *et al.,* 1997) and increases in intracellular Ca^{2+} have been shown by in vitro calcium macroimaging using fura-2 AM after perfusion with NMDA for 30 seconds (Takita *et al.,* 1997). This increase probably occurred as a result of activation of NMDA receptors as the increase in intracellular calcium was suppressed by an NMDA receptor competitive antagonist D-2-amino-5-phosphopentanoic acid (D-APS) (Takita *et al.,* 1997). It has previously been shown that there were alterations in the mechanism of dopamine as well as norepinephrine release in the prefrontal cortex (Linthorst *et al.,* 1990, Russell and Wiggins, 2000). It was of interest to investigate if there was any disturbance in the glutamatergic system in the prefrontal cortex of SHR.

The results obtained when the prefrontal cortex slices were exposed to NMDA show that there was no significant effect on $^{45}Ca^{2+}$ uptake after exposure to an enriched environment (section 3.8) while a significant strain difference on $^{45}Ca^{2+}$ uptake into the PFC slices was observed. The fact that exposure to an enriched environment did not have an effect on $^{45}Ca^{2+}$ agrees with the results obtained for the barrel cortex (section 3.7). The same reasoning advanced for the barrel cortex results could be applied to these results, although the animals were only exposed to an enriched environment for ± 16 hours as opposed to the many days to which the animals in the barrel cortex studies were exposed to an enriched environment. The protocol used was similar to the one used by Staiger *et al.,* (2000a) who exposed rats to an enriched environment the night prior to experimentation and got a significant increase in the expression of immediate early genes in the barrel cortex.

The significant strain difference on total $^{45}Ca^{2+}$ uptake shows that total $^{45}Ca^{2+}$ uptake into SHR prefrontal cortex slices was significantly lower than total $^{45}Ca^{2+}$uptake into WKY slices. When the regions were analysed separately total $^{45}Ca^{2+}$ uptake was higher in WKY than SHR in the rostral and middle regions but not in the caudal region. On the other hand there was no significant difference in basal $^{45}Ca^{2+}$ uptake between SHR and WKY. The same result was obtained when the regions were analysed separately. The NMDA-stimulated Ca^{2+} uptake was significantly lower in SHR compared to WKY but no significant difference was observed when the rostral, middle and caudal regions were analysed separately. The fact that total $^{45}Ca^{2+}$ uptake is lower in SHR compared to WKY might be an indication of a disturbance in NMDA receptor function in the prefrontal cortex of SHR. However, the value of $p = 0.0658$ obtained when comparing average basal $^{45}Ca^{2+}$ uptake in SHR and WKY shows that

there is a tendency for basal $^{45}Ca^{2+}$ uptake into prefrontal cortex slices of SHR to be lower than WKY which is similar to findings in the barrel cortex. Perhaps the difference in intracellular Ca^{2+} is amplified by exposure to NMDA to give reduced influx which is more apparent when Ca^{2+} channels are open (total uptake) than when they are closed (basal uptake).

Chapter 5 Conclusions

Slices produced by a vibratome in this study were viable since 62.5 mM K^+ caused a significant stimulation of $^{45}Ca^{2+}$ uptake into rat barrel cortex slices above basal levels indicating that voltage-sensitive calcium channels in the cell membranes respond to depolarisation with high external potassium. Decreasing the concentration of calcium in the incubation medium significantly decreased both basal and total uptake but did not have any effect on K^+-stimulated $^{45}Ca^{2+}$ uptake. Reduction of the K^+ concentration in the incubation buffer did not have any effect on basal, total or K^+-stimulated $^{45}Ca^{2+}$ uptake into barrel cortex slices. There were no regional differences in K^+-stimulated uptake into the rostral, middle and caudal regions of the barrel cortex although there appeared to be a trend in which K^+-stimulated $^{45}Ca^{2+}$ uptake increased from the rostral to the caudal region. This might be an indication of a regional difference in the distribution of voltage-sensitive calcium channels in the barrel cortex.

NMDA (100 μM) caused significant $^{45}Ca^{2+}$ uptake into barrel cortex slices. Elevation of external K^+ concentrations in the presence of different concentrations of NMDA did not enhance NMDA-stimulated $^{45}Ca^{2+}$ uptake. Addition of glycine to the medium did not have any effect on NMDA-stimulated $^{45}Ca^{2+}$ uptake, the possible reason being ~~that there was already enough endogenous glycine in the slice preparation. NMDA-~~ stimulated $^{45}Ca^{2+}$ uptake was completely blocked by a non-competitive NMDA receptor channel blocker MK-801. From this data it is concluded that firstly,

functional NMDA receptors are present in the barrel cortex and secondly $^{45}Ca^{2+}$ uptake measured in this study was via the NMDA receptor channels.

The investigation of glutamate receptor function in the SHR rats compared to WKY controls showed that both total and basal $^{45}Ca^{2+}$ uptake into barrel cortex of SHR are lower than total and basal $^{45}Ca^{2+}$uptake into WKY slices. However there was no difference in NMDA-stimulated $^{45}Ca^{2+}$ uptake into barrel cortex of SHR and WKY. Based on these findings and the literature it is concluded that it is not the NMDA receptor function that is disturbed but it is the brain calcium metabolism that is disturbed in SHR rats which are used as a model for attention-deficit hyperactivity disorder.

Exposure to an enriched environment did not have any effect on total, basal or NMDA-stimulated $^{45}Ca^{2+}$ uptake into barrel cortex of both young (4 to 6 weeks old) and adult (12 to 18 weeks old) SHR and WKY rats irrespective of the length of time that they were exposed to the enriched environment. This shows that exposure to an enriched environment does not have an effect on NMDA receptor function in barrel cortex in SHR and WKY. There was no difference in basal $^{45}Ca^{2+}$ uptake between young and adult rats across both strains while total $^{45}Ca^{2+}$ uptake was significantly higher in young rats than in adult rats across both strains. On the other hand NMDA-stimulated $^{45}Ca^{2+}$ uptake into barrel cortex decreased with increased age suggesting that this is due to either a decrease in the number of NMDA receptors or a decrease in the sensitivity of the NMDA receptors with ageing.

NMDA (100 μM) caused significant $^{45}Ca^{2+}$ uptake above basal levels in the prefrontal cortex of both SHR and WKY. Total $^{45}Ca^{2+}$uptake into prefrontal cortex slices of SHR was significantly lower than total $^{45}Ca^{2+}$ uptake into prefrontal cortex slices of WKY while basal $^{45}Ca^{2+}$ uptake into prefrontal cortex of SHR was not significantly different from basal $^{45}Ca^{2+}$ uptake into prefrontal cortex of WKY. NMDA-stimulated $^{45}Ca^{2+}$ uptake into the prefrontal cortex slices of WKY and SHR was not significantly different between the two strains of rat. The results in this study indicate the presence of NMDA receptors in the prefrontal cortex and also indicate a disturbance in calcium metabolism in the prefrontal cortex similar to that seen in the barrel cortex of SHR compared to WKY. Exposure to an enriched environment did not have an effect on NMDA-stimulated $^{45}Ca^{2+}$ uptake into the prefrontal cortex thus agreeing with results obtained for the barrel cortex.

References

Ahissa, E., Sosnik, R., Haidarliu, S. (2000). Transformation from temporal to rate coding in a somatosensory thalamocortical pathway. *Nature* **406**: 302 – 306

Aitken, P.G., Breese, G.R., Dudek, F.F., Edwards, F., Espanol, M.T., Larkman, P.M., Lipton, P., Newman, G.C., Nowak, T.S., Panizzon, K.L., Raley-Susman, K.M., Reid, K.H., Rice, M.E., Sarvey, J.M., Schoepp, D.D., Segal, M., Taylor, C.P., Teyler, T.J., Voulalas, P.J. (1995). Preparative methods for brain slices: a discussion, *J. Neuorsci. Meth.* **59**: 139 – 149.

Akaike, N., Rhee, J.S., (1997) Age related functional changes of the glutamate receptor channels in rat Meynert neurons. *J Physiol.* **504**(3): 665 – 681

Alloway, K.D., Crist, J., Mutic, J.J., Roy, S.A, (1999) Corticostriatal projections from rat barrel cortex have an anisotropic organisation that correlates with vibrissal whisking behaviour. *J Neurosci* **19**(24) 10908 - 10922

Anderson, S.E., Gray, S.D., Atherley, R., Cala, P.M. (1999). Na-dependent changes in intracellular Ca in spontaneously hypertensive rat hearts. *Comp. Biochem. Physiol. A Mol. Integr. Physiol.* **123**: 299 - 309.

Aronstam, R.S., Martin, D.C., Dennison, R.L., (1994) Volatile anesthetics inhibit NMDA-stimulated 45Ca uptake by rat brain microvesicles. *Neurochem. Res* **19**(12): 1515 - 1520

Arnsten, A.F.T. (1998) catecholamine modulation of prefrontal cortical cognitive function. *Trends in cognitive sciences.* **2**(11): 436 -447

Bardo, M.T. and Hammer, R.P. (1991) Autoradiographic localization of dopamine D1 and D2 receptors in rat nucleus accumbens: resistance to differential rearing conditions. *Neurosci.* **45**(2): 281 – 290

Bettler, B. and Mulle, C. (1995) Review: Neurotransmitter Receptors II, AMPA and Kainate receptors. *Neuropharmacology* **34**(2): 123 - 139

Brackett, R.L., Pouw, B., Blyden, J.F., Nour, M., Matsumoto, R.R. (2000) Prevention of cocaine-induced convulsions and lethality in mice: effectiveness of targeting different sites on the NMDA receptor complex. *Neuropharmacol.* **39**: 407 - 418

Buell, S.J. and Coleman, P.D. (1979) Dendritic growth in the aged human brain and failure of growth in senile dementia. *Science* **206**: 854 - 56

Burnasev, N. (1996) calcium permeability of glutamate gated channels in the central nervous system. *Current opinion in neurobiology* **6**:311-3173

Chazot, P.L., Coleman, S.K., Cik, M., Stephenson, F.A. (1994). Molecular characterization of N-Methyl-D-aspartate receptors expressed in mammalian cells yields evidence for the coexistence of three subunit types within a discrete receptor molecule. *J. Biol.Chem.* **269**: 24403-24409.

Chmielowska, J., Steward, M.G., Bourne, R.C, (1988) gamma-Aminobutyric acid (GABA) immunoreactivity in mouse and art somatosensory (SI) cortex: decription and comparison. *Brain Res* **439**(1 - 2): 155 - 168

Choi, D.W. (1988) Calcium-mediated neurotoxicity: relationship to specific channel types and role in ischemic damage. *Trends Neurosci.* **11**(10): 465 - 469

Collingridge, G. L. (1995) The brain slice preparation: a tribute to the pioneer Henry McIlwain. *J. Neurosci. Meth.* **59**: 5 – 9

Davson, H., Welch, K., Segal, M.B., (1987) *Physiology and Pathophysiology of the Cerebrospinal fluid. Churchill Livingstone*

De Gooyer, T.E., Farrugia, W., Wlodek, M.E. (1999). Reduced intestinal epithelial cell brush border membrane calcium transport in spontaneously hypertensive rats. *J. Hypertens.* **17**: 777-84.

Didier, M., Heaulme, M., Gonalons, N., Soubrie, P., Bockaert, J., Pin, J.P., (1993) 35mM K(+)-stimulated Ca2+ uptake in cerebellar granule cell cultures mainly results from NMDA receptor activation. *Eur. J Pharmacol* **244**(1): 57 – 65

Egger, V., Feldmeyer, D., Sakmann, B., (1999) Coincidence detection and changes of synaptic efficacy in spiny stellate neurons in rat barrel cortex. *Nature Neuroscience* **2** 1098-1105

Feldman, D., Sherin, J.E., Press, W.A., Bear, M.F., (1990). N-methyl-D-aspartate evoked calcium uptake by kitten visual cortex maintained in vitro. *Exp. Brain Res.* **80**: 252-259

Feldmeyer, D., Egger, V., Lubke, J., Sakmann, B., (1999). Reliable synaptic connections between pairs of excitatory layer 4 neurons within a single 'barrel' of a developing rat somatosensory cortex. *J. Physiol.* **521**:169 –190

Feldmeyer, D. and Sakmann, B., (2000) Synaptic efficacy and reliability of excitatory connections between the principal neurons of the input (layer 4) and output layer (layer 5) of the neocortex. *J Physiol* **252**(1): 31 - 39

Filipkowski, R.K., Rydz, M., Berdel, B., Morys, J., Kaczmarek, L., (2000) Tactile experience induces c-fos expression in rat barrel cortex. *Learning and Memory* 7: 116-122

Fleidervish, I.A., Binshtok, A.M., Gutnick, M.J., (1998) Functionally distinct NMDA receptors mediate horizontal connectivity within layer 4 of mouse barrel cortex. *Neuron* **21**: 1055-1065

Fossier, P., Tauc, L., Baux, G., (1999) Calcium transients and neurotransmitter release at an identified synapse. *Trends Neurosci.* **22**(4): 161 - 166

Ganong, W.F. (1999) *Review of Medical Physiology* 19th edition *McGraw Hill*

Gasull, T., DeGregorio-Rocasolano, N., Trullas, R. (2001) Overactivation of alpha-amino-3-hydroxy-5-methylisoxazole-4-propionate and N-methyl-D-aspartate but not kainate receptors inhibits phosphatidylcholine synthesis before excitotoxic death. *J. Neurochem* **77**(1): 13 – 22

Gosh, A. and Greenberg, M.E., (1995) Calcium signalling in neurons: molecular mechanisms and consequences. *Science* **268**: 239 -247

Govender, A., (1999) Glutamate-stimulated calcium uptake into rat barrel cortex slices Honours thesis

Hayama, T., and Ogawa, H., (1997) Regional differences of callosal connections in the granular zones of the primary somatosensory cortex in rats. *Brain Res Bull* **43**(3): 341 - 347

Haydon, P.G. (2001) Glia: Listening and talking to the synapse. *Nat. Neurosci. reviews* **2**: 185-193.

Hendley, E.D. (2000) WKHA rats with genetic hyperactivity and hyperreactivity to stress: a review. *Neurosci. and Biobehav. Revs* **24**: 41 - 44

Herrera-Marschitz, M., You, Z.B., Goiny, M., Meana J.L., Silveira, R., Godukhin, O.V., Chen, Y., Espinoza, S., Petterson, E., Loidl, C.F., Lubec, G., Anderson, K., Nylander, I., Terenius, L., Ungerstedt, U. (1996) On the origin of extracellular

glutamate levels monitored in the basal ganglia of the rat by in-vivo microdialysis. *J. Neurochem* **66**; 1726-1735

Himelstein, J., Newcorn, J.H., Halperin, J.M., (2000). The neurobiology of attention-defict hyperactivity disorder. *Front. Biosci.* **5**: D461-478.

Hollmann, M., Heinemann, S. (1994) Cloned glutamate receptors. *Annu. Rev. Neurosci.* **17**: 31 – 108

Honda, H., Shibuya, T., Salafsky, B., (1990) Brain synaptosomal Ca^{2+} uptake: comparison of Sprague-Dawley, Wistar-Kyoto and sponataneously hypertensive rats. *Comp. Biochem. Physiol*, **95B**(3): 555 – 558

Horn, J.L., Janicki, P.K., Franks, J.J., (1995). Diminished brain synaptic plasma membrane Ca^{2+}-ATPase activity in spontaneously hypertensive rats: association with reduced anesthetic requirements. *Life Sci.* **56**: PL427-432.

Jaarsma, D., Sebens, J.B., Korf, J., (1991). Localiztion of NMDA and AMPA receptors in rat barrel field. *Neurosci. Lett.* **133**: 233 - 236

Jabslonka, B., Gierdalski, M., Siucinska, E., Skangiel-Kramska, J., Kossut M. (1995) Partial blocking of NMDA receptors restricts plastic changes in adult mouse barrel cortex. *Behav. Brain Res.* **66**: 207 - 216

Janssens, N. and Lesage, A.S., (2001) Glutamate receptor subunit expression in primary neuronol and secondary glial cell cultures. *J Neurochem* 77(6): 1457 -1474

Kandel, E.R., Schwartz, J.H., Jessell, T.M., (1999) *Principles of Neural Science, McGraw Hill*

Kannurpatti, S.S., Joshi, P.G., Joshi, N.B., (2000) Calcium sequestering ability of mitochondria modulates influx of calcium through glutamate receptor channel. *Neurochem. Res.* **25** (12): 1527 – 1536

Kato, N., (1993) Synaptic N-methyl-D-aspartate receptors in the neonatal rat visual cortex are less sensitive to MK 801 than in adult. *Brain Res.* **608**(1): 166 - 168

Keller, A., (1995). Synaptic organisation of the barrel cortex. *Cerebral Cortex* **11**: 221 - 262.

Kennedy, M.B., (1989). Regulation of neuronal function by calcium. *Trends Neurosci.* **12**(11) 417 – 420

Kidd, F.L., and Isaac, J.T.R., (2000) Glutamate transport blockade has a differential effect on AMPA and NMDA receptor-mediated synaptic transmission in the developing barrel cortex. *Neuropharmacol.* **39**: 725 – 732

Kiedrowski, L., (1999). Elevated extracellular K^+ concentrations inhibit N-Methyl-D-Aspartate-induced Ca^{2+} influx and excitotoxicity. *Mol. Pharmacol* **56**: 737 - 743

Kolb, B. and Whishaw, I.Q., (1998) Brain plasticity and behavior. *Annu. Rev. Psychol.* **49**: 43 – 64

Laaris, N., Carlson, G.C., Keller, A., (2000) Thalamic-evoked synaptic interactions in barrel cortex revealed by optical imaging. *J. Neurosci.* **20**(4): 1529 - 1537

Land, P.W., Buffer, S.A. Jr, Yaskosky, J.D. (1995) Barreloids in Adult Rat Thalamus: Three-Dimensional Architecture and Relationship to Somatosensory Cortical Barrels. *J. Comp. Neurol.* **355**: 573 – 588

Linthorst, A.C.E., Van Den Buuse, M., De Jong, W., Versteeg, D.H.G., (1990). Electrically stimulated [3H]dopamine and [14C]acetylcholine release from nucleus caudatus slices: differences between spontaneously hypertensive rats and Wistar-Kyoto rats. *Brain Res.* **509**:266-72.

Lipton, P., Aitken, P.G., Dudek, F.F.,Eskessen, K., Espanol, M.T., Ferchmin, P.A., Kelly, J.B., Kreisman, N.R., Leybaert, L., Newman, G.C., Panizzon, K.L., Payne, R.S., Phillips, P., Raley-Susman, K.M., Rice, M.E., Santamaria, R., Sarvey, J.M., Schurr, A., Segal, M., Taylor, C.P., Teyler, T.J., Vasilenko, V.Y., Veregge, S., Wu, S.H., Wallis, R.. (1995) Making the best of brain slices: comparing preparative methods, *J. Neurosci. Methods* **59**: 151 –156.

Lipsky, R.H., Xu, K., Zhu, D., Kelly, C., Terhakopian, A., Novelli, A., Marini, A.M. (2001) Nuclear factor kappaB is a critical determinant in N-methyl-D-aspartate receptor-mediated neuroprotection. *J. Neurochem.* **78**(2): 254 – 264

Lu, M.Y., Yin, H.Z., Chiang, J., Weiss, J.H., (1996) Ca^{2+}-permeable AMPA/Kainate and NMDA channels: High rate of Ca^{2+} influx underlies potent induction of injury. *J. Neurosci.* **16**(17): 5457 - 5465

Lubke, J., Egger, V., Sakmann, B., Feldmeyer, D. (2000) Columnar organisation of dendrites and axons of single and synaptically coupled excitatory spiny neurons in layer 4 of the rat barrel cortex. *J. Neurosci.* **14**(20): 5300 - 5311

Mattson, M.P., LaFerla, M.F., Chan, S.L., Leissering, M.A., Shepel, P.N., Geiger, J.D., (2000) Calcium signalling in the ER: its role in neuronal plasticity and neurodegenerative disorders. *Trends Neurosci.* **23**(5): 222 – 229

McDonald, J.W., and Johnston, M.V., (1990) Physiological and pathophysiological roles of excitatory aminoacids during central nevrous system development. *Brain Res. Rev.* **15:** 41 – 70

McGeer, P.L., Eccles, J.C., McGeer, E.G., (1986) *Molecular neurobiology of the brain.* 2nd edition Plenum Press

Melena, J. and Osborne, N., (2001) Voltage-dependent calcium channels in the rat retina: involvement in NMDA-stimulated influx of calcium. *Exp. Eye Res.* **72**: 393-401

Mitchell, J.J., and Anderson, K.J., (1998) Age-related changes in [3H]MK801 binding in the Fischer 344 rat brain. *Neurobiol. Aging* **19**(3): 259 - 265

Miller, G.L., (1959). Protein determination for large number of Samples. *Analytical Chemistry* **31**:964.

Moll, G.H., Heinrich, H., Trott, G.E., Wirth, S., Rothenberger, A. (2000) Deficient intracortical inhibition in drug-naïve children with attention-deficit hyperactivity disorder is enhanced by methylphenidate. *Neurosci. Lett.* **284**: 121 – 125

Morgan, J.I. and Curran, T. (1989) Stimulus-transcription coupling in neurons: role of cellular immediate–early genes. *Trends Neurosci.* **12** (11): 459 -462

Murchison, D. and Griffith, W.H., (1998) Increased calcium buffering in basal forebrain neurons during aging. *J. Neurophysiol.* **80**(1): 350 - 364.

Mori, H. and Mishina, M. (1995) Review: Neurotransmitter Receptors VIII. Structure and function of the NMDA receptor channel. *Neuropharmacol.* **34**(10): 1219 – 1237

Nakanishi, S. (1992) Molecular diversity of glutamate receptors and implications for brain function. *Science* **258**(5082): 597 - 603

Nakanishi, S. (1994) Metabotropic glutamate receptors: Synaptic transmisssion, modulation and plasticity. *Neuron* **13**(5): 1031 - 1037

Oosterlaan, J. and Sergeant, J.A. (1998) Response inhibition and response re-engagement in attention-deficit/hyperactivity disorder, disruptive, anxious and normal children. *Behav. Brain Res.* **94**: 33 –43.

Ossowska, K., Wolfarth, S., Schulze, G., Wardas, J., Pietraszek, M., Lorenc-Koci, E., Smialowska, M., Coper, H., (2001) Decline in motor functions in ageing is related to the loss of NMDA receptors. *Brain Res.* **907**: 71 – 83

Oster, Y. and Schramm, M. (1993) Down-regulation of NMDA activity by NMDA. *Neurosci. Lett.* **163**: 85 - 88

Ozawa, S., Kamiya, H., Tsuzuki, K., (1998) Glutamate receptors in the mammmalian central nervous system. *Progress in neurobiol.* **54**: 581 – 619

Packard Liquid Scintillation Analyzer Operation Manual (1986) Packard instrument company USA

Paoletti, P., Ascher, P., Neyton, J. (1997) High-affinity Zinc inhibition of NMDA NR1-NR2A receptors. *J. Neurosci.* **17**(15): 5711 - 5725

Paxinos, G. and Watson, C. (1986). *The rat brain in stereotaxic coordinates*, Academic Press, New York.

Peng, T. and Greenamyre, T.J., (1998) Privileged access to mitochondria of calcium influx through N-Methyl-D-Aspartate receptors. *Mol Pharmacol.* **53**: 974 - 980

Peterson, B.E., Goldreich, D., Merzenich, M.M., (1998) Optical imaging and electrophysiology of rat barrel cortex. I. Responses to small single-vibrissa deflections. *Cereb. Cortex* **8**: 173 - 183

Peterson, C.C.H. and Sakmann, B., (2000) The excitatory neuronal network of rat layer 4 barrel cortex. *J. Neurosci.* **20**(20): 7579 - 7586

Por, S.B., Bennett, E.L., Bondy, S.C., (1982) Environmental enrichment and Neurotransmitter receptors. *Behav. and neural biology* **34**: 132 - 140

Ramakers, G.J.A., Avci, B., van Hulten, P., van Ooyen, A., van Pelt, J., Pool, C.W., Lequin, M.B. (2001) The role of calcium signalling in early axonal and dendritic morphogenesis of rat cerebral cortex neurons under non-stimulated growth conditions. *Dev. Brain Res.* **126**: 163-172

Ripellino, J.A., Neve, R.L., Howe, J.R. (1998) Expression of heteromeric interactions of non-N-methyl-D-aspartate glutamate receptor subunits in the developing and adult cerebellum. *Neuroscience* **82**(2): 485 - 497

Rosenzweig, M.R, Love, W., Bennett, E.L (1968) Effects of a few hours a day of Enriched experience on Brain chemistry and Brain weights. *Physiol. Behav* **3**(6): 819 - 825

Rosenzweig, M.R, Bennett, E.L, (1996) Psychobiology of plasticity: effects of training and experience on brain and behavior. *Behav. Brain Res.* **78**: 57 – 65

Rosenzweig, M.R. (1996) Aspects of the search for neural mechanisms of memory. *Annu. Rev Psychol* **47**: 1 - 32

Rothman, S.M. and Olney, J.W. (1987) Excitotoxicity and the NMDA receptor. *Trends Neurosci.* **10**(7): 299 -302

Russell, V.A., Allie, S., Wiggins, T. (2000) Increased noradrenergic activity in prefrontal cortex slices of an animal model for attention-deficit hyperactivity disorder – the spontaneously hypertensive rat. *Behav. Brain Res.* **117**: 69-74

Russell, V.A., de Villiers, A., Sagvolden, T., Lamm, M., Taljaard, J. (1995). Altered dopaminergic function in the prefrontal cortex, nucleus accumbens and caudate-putamen of an animal model of Attention-Deficit Hyperactivity Disorder - the spontaneously hypertensive rat. *Brain Res.* **676**:343-51.

Russell, V.A., de Villiers, A.S., Sagvolden, T., Lamm, M.C.L., Taljaard, J.J.F. (1996). Impaired vesicular storage of dopamine in an animal model for Attention-deficit

Hyperactivity disorder – the spontaneously hypertensive rat. *Soc. Neurosci. Abstr.* **22**:2082.

Russell, V.A., de Villiers, A., Sagvolden, T., Lamm, M., Taljaard, J. (1998). Differences between electrically-, ritalin- and d-amphetamine-stimulated release of [^{3}H]dopamine from brain slices suggest impaired vesicular storage of dopamine in an animal model for Attention-Deficit Hyperactivity Disorder. *Behav. Brain Res.* **94**:163-71.

Russell, V.A., Lehohla, M. (1998). Neurotransmitter disturbances in an animal model for attention-deficit hyperactivity disorder. *SAMJ* **88**:1161 Abstract.

Russell, V.A., Wiggins, T. (2000) Increased glutamate-stimulated norepinephrine release from prefrontal cortex slices of spontaneously hypertensive rats. *Metab Brain Dis* **15**(4): 297 - 304

Saadoun, S., Lluch, M., Rodriguez-Alvarez, J, Blanco, I., Rodriguez, R. (1998) Extracellular acidification modifies Ca^{2+} fluxes in rat brain synaptosomes. *Biochem and Biophysical Res. Com* **242**: 123 - 128

Sagar, S.M., Sharp, F.R., Curran, T. (1988) Expression of c-fos protein in brain: metabolic Mapping at the cellular level. *Science* **240**: 1328 - 1331

Sagvolden, T., Hendley, E.D., Knardahl, S. (1992a). Behavior of hypertensive and hyperactive rat strains: Hyperactivity is not unitarily determined. *Physiol. Behav.* **52**:49-57.

Sagvolden, T., Metzger, M.A., Sagvolden, G. (1993a). Frequent reward eliminates differences in activity between hyperkinetic rats and controls. *Behav. Neural Biol.* **59**:225-9.

Sagvolden, T., Metzger, M.A., Schiørbeck, H.K., Rugland, A-L, Spinnangr, I., Sagvolden, G. (1992b). The spontaneously hypertensive rat (SHR) as an animal model of childhood hyperactivity (ADHD): Changed reactivity to reinforcers and to psychomotor stimulants. *Behav. Neural Biol.* **58**:103-12.

Sagvolden, T., Pettersen, M.B., Larsen, M.C. (1993b). Spontaneously hypertensive rats (SHR) as a putative animal model of childhood hyperkinesis: SHR behaviour compared to four other rat strains. *Physiol. and Behav.* **54**:1047-55.

Sagvolden, T., Sergeant, J.A. (1998). Attention deficit/hyperactivity disorder – from brain dysfunctions to behaviour. *Behav. Brain Res.* **94**:1-10.

Sagvolden, T., Wultz, B., Moser, E.I., Moser, M. B., Mørkrid, L. (1989). Results from a comparative neuropsychological research program indicate altered reinforcement mechanisms in children with ADD. In: Sagvolden T, Archer T, editors. *Attention deficit disorder: Clinical and basic research*, Lawrence Erlbaum Associates, Hillsdale, New Jersey, pp261-86.

Schlame, M. and Hemmings, Jr M.D. (1995) Inhibition by volatile Anaesthetics of endogenous glutamate release from synaptosomes by a presynaptic mechanism. *Anesthesiology* **82**: 1406 –1416

Schubert, D., Staiger, J.F., Cho, N., Kotter, R., Zilles, K., Luhmann, H.J., (2001) Layer-specific intracolumnar and transcolumnar functional connectivity of layer V pyramidal cells in rat barrel cortex. *J Neurosci* **21**(10) 3580 – 3592

Seeburg, H. P. (1993) The TINS/TIPS lecture. The molecular biology of mammalian glutamate receptor channels. *Trends Neurosci* **16**(9): 359 – 365

Simonato, M., Jope, R.S., Bianchi, C. and Beani, L. (1989) Lack of excitatory amino acid-induced effects on calcium fluxes measured with $^{45}Ca^{2+}$ in rat cerebral cortex synaptosomes. *Neurochem. Res* **14**: 677 –682

Skibinska, A., Glazewski, S., Fox, K., Kossut, M. (1999) Age-dependent response of the mouse barrel cortex to sensory deprivation: a 2-deoxyglucose study. *Exp. Brain Res.* **132**: 134 – 138

Solanto, M. V. (1998). Neuropsychopharmacological mechanisms of stimulant drug action in attention deficit hyperactivity disorder: a review and integration. *Behav. Brain Res.* **94**: 127 – 152

Staiger, J.F., Bisler, S., Schleicher, A., Gass, P., Stehle, J.H., Zilles, K. (2000a). Exploration of a novel environment leads to the expression of inducible transcription factors in barrel related columns. *Neuroscience* **99**: 7 - 16

Staiger, J.F., Kotter, R., Zilles, K., Luhmann, H.J. (2000b) Lamina characteristics of functional connectivity in rat barrel cortex revealed by stimulation with caged-glutamate. *Neurosci Res.* **37**: 49 - 58

Stecher, J. Muller, W.E. Hoyer, S. (1997) Learning abilities depend on NMDA-receptor density in hippocampus in adult rats. *J. Neural Transm.* **104**: 281 – 289

Steiner, H., Gerfen, C.R. (1994) Tactile sensory input regulates basal and apomorphine-induced immediate-early gene expression in rat barrel cortex. *J Comp Neurol* **344**: 297 – 304

Takita, M., Yokoi, H., Mizuno, T. (1997) NMDA receptor clustering in rat prefrontal cortex revealed by in vitro calcium macroimaging. *Neuroreport* **8**: 551 – 553

Taylor, E. (1998) Clinical foundations of hyperactivity research. *Behav Brain Res* **94**: 11 - 24

Tremblay, E., Roisin, M.P., Represa, A., Charriant-Marlangue, C., Ben-Ari, Y. (1988) Transient increased density of NMDA binding sites in the developing rat hippocampus. *Brain Res.* **461**: 393 –396

Triggle, D.J. (1990) Calcium, calcium channels, and calcium channel antagonists. *Can. J. Physiol. Pharmacol* **68**: 1474 - 1481

Tsumoto, T., Hagihara, K., Sato, H., Hata, Y. (1987) NMDA receptors in the visual cortex of young kittens are more effective than those of adult cats. *Nature* **327**(6122): 513 – 514

Udenfriend, S., Spector, S. (1972) Spontaneously Hypertensive Rat. *Science* **176**: 1155 – 1156

Varju, P., Schlett, K., Eisel, U., Madarasz, E. (2001) Schedule of NMDA receptor subunit expression and functional channel formation in the course of invitro-induced neurogenesis . *J. Neurochem.* 77(6): 1444 - 1456

Volkmar, F.R. and Greenough, W.T. (1972) Rearing complexity affects branching of dendrites in the visual cortex of the rat. *Science* **176**: 1445 - 1447

Wenk, G.L., Barnes, C.A. (2000) Regional changes in the hippocampal density of AMPA and NMDA receptors across the lifespan of the rat. *Brain Res.* **885**: 1 - 5

White, E.L. and DeAmicis, R.A. (1977) Afferent and efferent projections of the region in mouse SmL cortex contains the posteromedial barrel subfield. *J. Comp. Neurol.* **175**(4): 455 - 482

Wilson, M.A., Stephen, K.L., Johnston, M.V., (1998). Expression of NMDA receptor subunit mRNA after MK-801 treatment in neonatal rats. *Dev. Brain Res.* **109**: 211 – 220

Wollmuth, L.P., and Sakmann, B. (1998) Different mechanisms of Ca^{2+} transport in NMDA and Ca^{2+} permeable AMPA glutamate receptor channels. *J. Gen Physiol* **112:** 623 – 636

Woolsey, T.A. and Van der Loos, H. (1970). The structural organisation of layer IV in the somatosensory region (SI) of mouse cerebral cortex. *Brain Research* **17**:205 – 242

Wright, A.K., Norrie, L., Arbuthnott, G.W. (2000) Corticofugal axons from adjacent 'barrel' columns of rat somatosensory cortex: cortical and thalamic terminal patterns. *J. Anat.* **196**: 379 – 390

Zanelli, S.A., Numagami, Y., McGowan, J.E., Mishra, O.P., Delivoria-Papadopoulus, M. (1999). NMDA receptor-mediated calcium influx in cerebral cortical synaptosomes of the hypoxic guinea pig fetus. *Neurochem Res* **24**(3): 437 – 446

Zhang, Y. and Lipton, P. (1999) Cytosolic Ca^{2+} Changes during *In Vitro* Ischemia in rat hippocampal slices: Major roles for Glutamate and Na^{+}-dependent Ca^{2+} Release from Mitochondria. *J. Neurosci* **19**(9): 3307 - 3315

Zigmond, J.M., Bloom, F.E., Landis, S.C., Roberts, J.L., Squire, L.R. (1999) *Fundamental Neuroscience, Academic Press*

Appendices

Appendix 1

An example of a spreadsheet used to capture data from the scintillation counter and calculate nmol Ca^{2+}/mg protein including protein determination

results from 19/03/01 (136 days from 03/11/00) EXPT 10 (normal cage) WKY male

no NMDA (control) 0.006727 3.3638

H2O	CPM	Tsie	% EFF	DPM
0	12321	470.96	82.50	14934.4
50ul	12204	436.3	81.72	14934.4
250ul	12234	395.8	81.92	14934.4
600ul	12548	365.66		14934.4
1ml	12777	338.66		14934.4
1.5ml	11882	302.81	78.09	14934.4
2 ml	11598	243.9	77.66	14934.4

NMDA (test)

H2O	CPM	Tsie	% EFF	DPM
0	12612	464.95	84.45	14934.4
50ul	11989	428.12	80.28	14934.4
250ul	11880	378.82		14934.4
600ul	11753	365.33		14934.4
1ml	12191	326.3	81.63	14934.4
1.5 ml	12185	309.97	81.59	14934.4
2ml	12262	242.92	82.11	14934.4

SAMPLE CALCULATION OF DPM USING EQUATION Y=.0235x + 71.67

NMDA (test)

sample	CPM	tsie	%EFF	DPM	nmol Ca2+>rtn in 600uumol/mg prtn				% uptake
TA	4598	351.98	79.94	5751.70	9.243	1103.3	8.378	2.114	34
TB	3868	347.56	79.64	4591.62	7.379	969.7	7.610	2.285	43
TC	1868	352.58	79.96	2358.61	3.791	402.7	9.413	3.899	77

SAMPLE CALCULATION OF DPM USING EQUATION Y=.0235x + 71.67

no NMDA (control)

sample	CPM	tsie	%EFF	DPM	nmol Ca2+>rtn in 600uumol/mg prtn		
CA	3144	324.49	79.30	3964.92	6.372	1017.3	6.263
CB	2014	337.17	79.59	2530.36	4.066	763.7	5.325
CC	795	353.56	79.98	994.02	1.597	289.7	5.514

STD CALCULATION OF DPM USING EQUATION Y=0.0235x + 71.67

CONTROL

H2O	CPM	Tsie	% EFF	DPM	DPM calc	
0	12321	470.96	82.74		14891.66	avg dpm
50ul	12204	436.3	81.92		14896.91	15315.36
250ul	12234	395.8	80.97		15109.06	
600ul	12548	365.66	80.26		15633.51	
1ml	12777	338.66	79.83		16045.67	
1.5 ml	11882	302.81	78.79		14802.12	
2ml	11598	243.9	77.40		14984.18	

STD CALCULATION OF DPM USING EQUATION Y=0.0235x + 71.67

NMDA

H2O	CPM	Tsie	% EFF	DPM	DPM calc	
0	12612	464.95	82.60		15269.44	avg dpm
50ul	11939	428.12	81.73		14668.89	14940.38
250ul	11880	378.82	80.53		14753.13	
600ul	11753	365.33	80.26		14644.52	
1ml	12191	328.3	79.34		15365.89	
1.5ml	12185	309.97	78.95		15432.98	
2ml	12262	242.92	77.38		15846.75	

PROTEIN DETERMINATION

results from 19/03/01

BSA(ug)	abs 650nm	stim high K	abs 850nm	protein ug	protein in 600ul		
0	0.027	TA 40ul	0.289	75.34	1130.0	mean	stdev
10	0.058	TA 60ul	0.412	111.20	1112.0	1103.3	31.9
20	0.094	TA 80ul	0.519	142.39	1067.9		
40	0.179	TB 40ul	0.255	65.42	981.3		
80	0.316	TB 60ul	0.363	96.91	969.1	969.7	11.4
120	0.445	TB 80ul	0.469	127.81	958.6		
160	0.57	TC 60	0.171	40.93	409.3		
		TC 80ul	0.217	54.34	407.6	402.7	10.0
		TC 120ul	0.299	78.25	391.3		

non stim	abs 650nm	protein ug	prtn in 600ul		
CA 40ul	0.27	69.80	1046.9	mean	stdev
CA 60ul	0.379	101.57	1015.7	1017.3	28.9
CA 80ul	0.483	131.90	989.2		
CB 40ul	0.208	51.72	775.8		
CB 60ul	0.295	77.08	770.8	763.7	16.9
CB 80ul	0.371	99.24	744.3		
CC 60	0.129	28.69	286.9		
CC 80ul	0.188	40.06	300.4	289.7	9.6
CC 120ul	0.224	58.38	281.9		
con 20	0.194	47.64	1429.2		
con 40	0.382	102.45	1536.7		
con 80	0.679	189.04	1417.8		

Appendix 2

An example of a data printout from the Packard liquid scintillation counter

```
Protocol #:10        Name:Vivienne Ca45              06-Oct-01    19:18
Region A: LL-UL= 0.0-256.   Lcr=    0  Bkg= 0.00   %2 Sigma=0.50
Region B: LL-UL= 4.0-256.   Lcr=    0  Bkg= 0.00   %2 Sigma=0.50
Region C: LL-UL=256.-1000   Lcr=    0  Bkg= 0.00   %2 Sigma=0.50
Time = 10.00      QIP = tSIE/AEC      ES Terminator = 15 sec
STANDARD CURVE 21/04/99
Luminescence Correction On
```

TIME	CPMA	A:2S%	CPMB	CPMC	SIS	tSIE	S#	DPM1	FLAG	LUM
10.00	12094	0.58	12000	45.20	134.12	461.37	1			0
10.00	11950	0.58	11860	33.60	126.02	435.12	2			0
10.00	11925	0.58	11849	24.90	110.39	376.60	3			0
10.00	11709	0.58	11644	16.20	100.43	341.74	4			0
10.00	11595	0.59	11531	12.70	93.10	329.84	5			0
10.00	11610	0.59	11552	9.80	82.06	301.59	6			0
10.00	11376	0.59	11332	7.30	68.52	257.89	7			0
10.00	12101	0.58	12008	41.30	135.82	468.14	8			0
10.00	12069	0.58	11979	44.80	130.86	439.29	9			0
10.00	11951	0.58	11870	26.70	117.94	402.05	10			0
10.00	11958	0.58	11889	22.50	104.24	361.07	11			0
10.00	11781	0.58	11716	18.10	94.24	329.40	12			0
10.00	11574	0.59	11516	10.90	83.26	313.37	13			0
10.00	11450	0.59	11404	8.40	69.84	261.72	14			0
10.00	732	2.34	728	4.00	105.66	368.44	15			0
10.00	1092	1.92	1086	5.40	104.14	363.06	16			0
10.00	1277	1.77	1269	5.20	104.29	362.89	17			0
10.00	1176	1.85	1167	4.90	105.10	364.05	18			0
10.00	1749	1.51	1738	5.20	102.87	363.01	19			0
10.00	1556	1.61	1545	4.30	101.35	353.45	20			0

Appendix 3

Statistical analysis of different samples of data from different sets of experiments
T- = total uptake
B-= basal uptake
E- = effect i.e. (total – basal uptake)
entire = average of rostral middle and caudal values

A 3.1 Optimization of Assay conditions

A 3.1.1 (2mM Ca^{2+}/5mMK^{+})

Statistical analysis of data in table 3.1.1a
T-test for Dependent Samples 2mM Ca^{2+}/5mM K^{+}
Marked differences are significant at $p < 0.05$

	Mean	Std.Dv.	N	Diff.	Std.Dv. Diff.	t	df	p
T_entire	13.9	.899						
B_entire	10.6	2.261	6	3.289117	1.493339	5.39506	5	.002954*
T_rostral	12.6	1.549						
B_rostral	10.9	2.470	6	1.686167	3.312881	1.24672	5	.267718
T_middle	12.9	1.401						
B_middle	10.4	2.270	6	2.484333	1.516769	4.01205	5	.010201*
T_caudal	15.1	1.633						
B_caudal	10.4	2.457	6	4.697667	1.594322	7.21742	5	.000796*

Statistical analysis of data in table 3.1.1b
T-test for Dependent Samples 2mM Ca^{2+}/5mMK^{+}
Marked differences are significant at $p < 0.05$

	Mean	Std.Dv.	N	Diff.	Std.Dv. Diff.	t	df	p
E-rostral	2.0	3.049						
E-middle	2.5	1.517	6	-.46467	2.789862	-.40798	5	.700174
E-rostral	2.0	3.049						
E-caudal	4.7	1.594	6	-2.67800	3.342276	-1.96265	5	.106924
E-middle	2.5	1.517						
E-caudal	4.7	1.594	6	-2.21333	1.273184	-4.25825	5	.008028*

A 3.1.2 (1.2mM Ca^{2+}/5mM K^{+})

Statistical analysis of data in table 3.1.2a
T-test for Dependent Samples 1.2mM Ca^{2+}/5mM K^{+}
Marked differences are significant at $p < 0.05$

	Mean	Std.Dv.	N	Diff.	Std.Dv. Diff.	t	df	p
T_entire	8.5	.4282						
B_entire	6.2	.9197	4	2.31425	.499455	9.2671	3	.002659*
T_rostral	8.2	.2972						
B_rostral	6.6	.4994	4	1.63000	.404472	8.0599	3	.003990*
T_middle	8.4	.4045						
B_middle	6.4	1.583	4	2.03225	1.197416	3.3944	3	.042637*
T_caudal	8.9	.6729						
B_caudal	5.7	.8906	4	3.28075	.230503	28.4660	3	.000095*

Statistical analysis of data in table 3.1.2b
T-test for Dependent Samples
Marked differences are significant at $p < 0.05$

	Mean	Std.Dv.	N	Diff.	Std.Dv. Diff.	t	df	p
E-rostral	1.6	.4045						
E-middle	2.0	1.197	4	-.40225	1.242292	-.6476	3	.563389
E-rostral	1.6	.4045						
E-caudal	3.3	.2305	4	-1.65075	.296319	-11.1417	3	.001549*
E-middle	2.0	1.197						
E-caudal	3.3	.2305	4	-1.24850	1.037205	-2.4074	3	.095236

A 3.1.3 (1.2mM Ca^{2+}/3.36mM K^{+})
Statistical analysis of data in table 3.1.3a
T-test for Dependent Samples 1.2mM Ca^{2+}/3.36mM K^{+}
Marked differences are significant at $p < 0.05$

	Mean	Std.Dv.	N	Diff.	Std.Dv. Diff.	t	df	p
T_entire	9.6	.8846						
B_entire	6.8	.6729	4	2.81900	.533420	10.5695	3	.001809*
T_rostral	8.6	.4703						
B_rostral	6.8	.7852	4	1.82650	.812369	4.4967	3	.020531*
T_middle	9.3	.4979						
B_middle	6.6	.8238	4	2.70400	.776989	6.9602	3	.006085*
T_caudal	10.9	1.855						
B_caudal	6.9	.8589	4	3.92650	1.294908	6.0645	3	.008998*

Statistical analysis of data in table 3.1.3b
T-test for Dependent Samples 1.2mM Ca^{2+}/3.36mM K^{+}
Marked differences are significant at $p < 0.05$

	Mean	Std.Dv.	N	Diff.	Std.Dv. Diff.	t	df	p
E-rostral	1.8	.8123						
E-middle	2.7	.7769	4	-.87750	.494816	-3.5468	3	.038179*
E-rostral	1.8	.8123						
E-caudal	3.9	1.294	4	-2.10000	1.835208	-2.2886	3	.106096
E-middle	2.7	.7769						
E-caudal	3.9	1.294	4	-1.22250	1.626048	-1.5036	3	.229711

NB: Although NMDA-stimulated $^{45}Ca^{2+}$ uptake into rostral region (E_rostral) looks different from NMDA-stimulated $^{45}Ca^{2+}$ uptake into caudal region (E_caudal) in figure 3.1.3b, the difference is not statistically significant because of the high standard deviation of the differences between individual pairs of results in the rostral and caudal regions in the different experiments

A 3.1.4 Comparison of Ca^{2+} uptake under different buffer conditions

Statistical analysis of data in tables 3.1.1a and b, 3.1.2a and b, 3.1.3a and b
Analysis of Variance (stats for different conditions.sta)
Marked effects are significant at $p < 0.05$

	SS Effect	df Effect	MS Effect	SS Error	df Error	MS Error	F	p
T_entire	81.5736	2	40.78680	6.94017	11	.630924	64.64610	.000001*
T_rostral	60.2254	2	30.11270	12.91938	11	1.174489	25.63898	.000072*
T_middle	57.7930	2	28.89649	11.06211	11	1.005646	28.73425	.000043*
T_caudal	100.0044	2	50.00221	25.01091	11	2.273719	21.99137	.000143*
B_entire	57.8698	2	28.93491	29.45489	11	2.677717	10.80581	.002536*
B_rostral	61.1987	2	30.59936	33.11443	11	3.010403	10.16454	.003162*
B_middle	53.0387	2	26.51933	35.31943	11	3.210857	8.25927	.006452*
B_caudal	60.9835	2	30.49176	34.76788	11	3.160716	9.64710	.003803*
E_entire	2.2995	2	1.14974	12.75142	11	1.159220	.99183	.401770
E_rostral	.3684	2	.18420	48.97820	11	4.452564	.04137	.959624
E_middle	.9488	2	.47440	17.61550	11	1.601409	.29624	.749360
E_caudal	4.9377	2	2.46887	17.89907	11	1.627188	1.51726	.261862

Newman-Keuls test; Variable: T_entire
Marked differences are significant at $p < 0.05$

	{1} M=13.859	{2} M=8.5103	{3} M=9.5940
2mMCa^{2+} {1}		.000198*	.000173*
1.2mMCa^{2+}/5mM K^+ {2}	.000198*		.065497
1.2mMCa^{2+}/3.36mM K^+ {3}	.000173*	.065497	

Newman-Keuls test; Variable: T_rostral
Marked differences are significant at $p < 0.05$

	{1} M=12.568	{2} M=8.1870	{3} M=8.5892
2mMCa^{2+} {1}		.000396*	.000338*
1.2mMCa^{2+}/5mM K^+ {2}	.000396*		.589001
1.2mMCa^{2+}/3.36mM K^+ {3}	.000338*	.589001	

Newman-Keuls test; Variable: T_middle
Marked differences are significant at $p < 0.05$

	{1} M=12.906	{2} M=8.3995	{3} M=9.3225
2mMCa^{2+} {1}		.000270*	.000381*
1.2mMCa^{2+}/5mM K^+ {2}	.000270*		.194954
1.2mMCa^{2+}/3.36mM K^+ {3}	.000381*	.194954	

Newman-Keuls test; Variable: T_caudal
Marked differences are significant at $p < 0.05$

	{1} M=15.104	{2} M=8.9450	{3} M=10.870
2mMCa^{2+} {1}		.000379*	.001589*
1.2mMCa^{2+}/5mM K^+ {2}	.000379*		.081967
1.2mMCa^{2+}/3.36mM K^+ {3}	.001589*	.081967	

Newman-Keuls test; Variable: B_entire
Marked differences are significant at $p < 0.05$

	{1} M=10.570	{2} M=6.1960	{3} M=6.7750
2mMCa^{2+} {1}		.005484*	.005316*
1.2mMCa^{2+}/5mM K^+ {2}	.005484*		.606309
1.2mMCa^{2+}/3.36mM K^+ {3}	.005316*	.606309	

Newman-Keuls test; Variable: B_rostral
Marked differences are significant at $p < 0.05$

	{1} M=10.882	{2} M=6.5570	{3} M=6.7628
2mMCa^{2+} {1}		.008571*	.004618*
1.2mMCa^{2+}/5mM K^+ {2}	.008571*		.862176
1.2mMCa^{2+}/3.36mM K^+ {3}	.004618*	.862176	

Newman-Keuls test; Variable: B_middle
Marked differences are significant at $p < 0.05$

	{1} M=10.421	{2} M=6.3672	{3} M=6.6185
2mMCa^{2+} {1}		.015348*	.008871*
1.2mMCa^{2+}/5mM K^+ {2}	.015348*		.837385
1.2mMCa^{2+}/3.36mM K^+ {3}	.008871*	.837385	

Newman-Keuls test; Variable: B_caudal
Marked differences are significant at $p < 0.05$

	{1} M=10.407	{2} M=5.6642	{3} M=6.9437
2mMCa^{2+} {1}		.005558*	.014056*
1.2mMCa^{2+}/5mM K^+ {2}	.005558*		.303574
1.2mMCa^{2+}/3.36mM K^+ {3}	.014056*	.303574	

A 3.2 NMDA-stimulated $^{45}Ca^{2+}$ uptake

Statistical analysis of data in table 3.2a
T-test for Dependent Samples (nmda3.sta) NMDA
Marked differences are significant at $p < 0.05$

	Mean	Std.Dv.	N	Diff.	Std.Dv. Diff.	t	df	p
T_entire	8.7	1.172						
B_entire	6.0	.2412	5	2.72660	1.270763	4.79780	4	.008662*
T_rostral	8.0	1.467						
B_rostral	6.0	.4682	5	2.00820	1.542884	2.91044	4	.043659*
T_middle	8.8	1.374						
B_middle	6.2	.7101	5	2.59940	1.859480	3.12584	4	.035327*
T_caudal	9.4	1.493						
B_caudal	5.8	.7499	5	3.57220	2.103983	3.79646	4	.019162*

Statistical analysis of data in table 3.2b
T-test for Dependent Samples (nmda3.sta) NMDA
Marked differences are significant at $p < 0.05$

	Mean	Std.Dv.	N	Diff.	Std.Dv. Diff.	t	df	p
E-rostral	2.0	1.536						
E-middle	2.6	1.859	5	-.58680	2.089901	-.62784	4	.564170
E-rostral	2.0	1.536						
E-caudal	3.6	2.104	5	-1.55960	2.738186	-1.27361	4	.271778
E-middle	2.6	1.859						
E-caudal	3.6	2.104	5	-.97280	2.076550	-1.04753	4	.353977

A 3.3 Effect of Glycine on NMDA stimulated $^{45}Ca^{2+}$ uptake

Statistical analysis of data in table 3.3a
T-test for Dependent Samples (statsg.sta) GLYCINE
Marked differences are significant at $p < 0.05$

	Mean	Std.Dv.	N	Diff.	Std.Dv. Diff.	t	df	p
B_left	7.6	.542447						
B_right	7.8	.765924	5	-.16460	.562793	-.6540	4	.548815
B_left	7.6	.542447						
T_NMDA left	9.9	.285069	5	-2.33460	.342701	-15.2329	4	.000108*
B_left	7.6	.542447						
T_NMDA + Gly left	9.7	.726511	5	-2.15060	.908152	-5.2952	4	.006107*
B_right	7.8	.765924						
T_NMDA right	9.9	.582865	5	-2.18200	1.168154	-4.1768	4	.013955*
B_right	7.6	.765924						
T_NMDA + Gly right	9.9	1.281654	5	-2.16000	1.591689	-3.0345	4	.038612*
T_NMDA left	9.9	.285069						
T_NMDA + Gly left	9.7	.726511	5	.18400	.651745	.6313	4	.562131
T_NMDA right	9.9	.582865						
T_NMDA + Gly right	9.9	1.281654	5	.02200	.969683	.0507	4	.961972

Statistical analysis of data in table 3.3b
T-test for Dependent Samples (statsg.sta)
Marked differences are significant at $p < 0.05$

	Mean	Std.Dv.	N	Diff.	Std.Dv. Diff.	t	df	p
E_NMDA left	2.3	.342701						
E_NMDA right	2.2	1.168154	5	.152600	.914748	.373025	4	.728056
E_NMDA left	2.3	.342701						
E_NMDA + Gly left	2.2	.908152	5	.184000	.651745	.631284	4	.562131
E_NMDA right	2.2	1.168154						
E_NMDA + Gly right	2.2	1.591689	5	.022000	.969683	.050731	4	.961972
E_NMDA + Gly left	2.2	.908152						
E_NMDA + Gly right	2.2	1.591689	5	-.009400	1.215855	-.017287	4	.987035

A 3.4 Antagonising NMDA effect with MK-801

Statistical analysis for data in table 3.4a
T-test for Dependent Samples (mk801.sta)
Marked differences are significant at $p < 0.05$

	Mean	Std.Dv.	N	Diff.	Std.Dv. Diff.	t	df	p
B-left B-right	5.7 6.6	.4930 1.057	3	-.91600	.566858	-2.79886	2	.107466
B-left T-NMDA left	5.7* 8.6*	.4930* .5632*	3*	-2.88600*	.649448*	-7.69684*	2*	.016464*
B-left T-MK801 left	5.7 5.6	.4930 .9267	3	.05400	.499325	.18731	2	.868695
B-right T-NMDA right	6.6 8.1	1.057 .9269	3	-1.55267	1.490361	-1.80446	2	.212924
B-right T-MK801 right	6.6 5.4	1.057 .9784	3	1.17067	.696603	2.91077	2	.100542
T-NMDA left T-MK801 left	8.6* 5.6*	.5633* .9267*	3*	2.94000*	.754336*	6.75061*	2*	.021247*
T-NMDA right T-MK801 right	8.1* 5.4*	.9269* .9784*	3*	2.72333*	.915500*	5.15232*	2*	.035667*

Statistical analysis of data in table 3.4b
T-test for Dependent Samples (mk-801final.sta)
Marked differences are significant at $p < .05000$

	Mean	Std.Dv.	N	Diff.	Std.Dv. Diff.	t	df	p
E-NMDA left E-NMDA right	2.9 1.6	.649448 1.490361	3	1.33333	.929041	2.486	2	.130819
E-NMDA left E-MK801 left	2.9 -.1	.649448 .499325	3	2.94000	.754336	6.751	2	.021247*
E-NMDA right E-MK801 right	1.6 -1.2	1.490361 .696603	3	2.72333	.915500	5.152	2	.035667*

A 3.5 Effect of different K^+ concentrations on NMDA stimulated $^{45}Ca^{2+}$ uptake

Statistical analysis for data in table 3.5a
T-test for Dependent Samples (k+ dose response final.sta)
Marked differences are significant at $p < 0.05$

	Mean	Std.Dv.	N	Diff.	Std.Dv. Diff.	t	df	p
T2 T3	6.9 6.6	1.693643 1.047002	5	.35100	1.126043	.69701	4	.524184
T2 T4	6.9 8.0	1.693643 1.045084	5	-1.00720	.980664	-2.29658	4	.083252
T3 T4	6.6 8.0	1.047002 1.045084	5	-1.35820	.432811	-7.01699	4	.002172*
C1 T1	6.3 8.0	1.172642 2.438459	5	-1.62180	1.418963	-2.55571	4	.062923
C1 C2	6.3 7.8	1.172642 1.866640	5	-1.42520	1.239781	-2.57049	4	.061947
C2 T2	7.8 6.9	1.866640 1.693643	5	.82200	1.237486	1.48531	4	.211643
C2 T3	7.8 6.6	1.866640 1.047002	5	1.17300	1.438378	1.82352	4	.142294
C2 T4	7.8 8.0	1.866640 1.045084	5	-.18520	1.193338	-.34703	4	.746060

A 3.6 Comparison between SHR and WKY

Statistical analysis for data in table 3.6.1, 3.6.2, 3.6.3 a and b
Analysis of Variance (shrwky final stats.sta)
Marked effects are significant at $p < 0.05$

	SS Effect	Df Effect	MS Effect	SS Error	df Error	MS Error	F	p
T_entire	12.39812	1	12.39812	16.86734	17	.992197	12.49563	.002544*
T_rostral	9.89928	1	9.89928	14.20911	17	.835830	11.84365	.003115*
T_middle	12.95184	1	12.95184	33.81099	17	1.988882	6.51212	.020630*
T_caudal	14.57799	1	14.57799	40.37178	17	2.374811	6.13859	.024022*
B_entire	4.66297	1	4.66297	8.30544	17	.488555	9.54439	.006654*
B_rostral	5.94586	1	5.94586	16.67287	17	.980757	6.06253	.024789*
B_middle	.17789	1	.17789	23.39914	17	1.376420	.12924	.723650
B_caudal	13.08986	1	13.08986	15.39914	17	.905832	14.45065	.001427*
E-entire	1.95832	1	1.95832	15.46638	17	.909787	2.15251	.160594
E-rostral	.67401	1	.67401	24.67206	17	1.451297	.46442	.504745
E-middle	10.09398	1	10.09398	34.94144	17	2.055379	4.91101	.040618*
E-caudal	.04005	1	.04005	39.21025	17	2.306485	.01736	.896713

Newman-Keuls test; Variable:(shrwky final stats.sta) Average Total uptake
Marked differences are significant at $p < 0.05$

	{1} M=10.484	{2} M=8.8483
WKY {1}		.002680*
SHR {2}	.002680*	

Newman-Keuls test; Variable: (shrwky final stats.sta) Total uptake rostral region
Marked differences are significant at $p < 0.05$

	{1} M=9.8631	{2} M=8.4011
WKY {1}		.003261*
SHR {2}	.003261*	

Newman-Keuls test; Variable:(shrwky final stats.sta) Total uptake middle region
Marked differences are significant at $p < 0.05$

	{1} M=10.309	{2} M=8.6368
WKY {1}		.020774*
SHR {2}	.020774*	

Newman-Keuls test; Variable:(shrwky final stats.sta) Total uptake caudal region
Marked differences are significant at $p < 0.05$

	{1} M=11.281	{2} M=9.5069
WKY {1}		.024162*
SHR {2}	.024162*	

Newman-Keuls test;(shrwky final stats.sta) Average basal uptake
Marked differences are significant at $p < 0.05$

	{1} M=7.0934	{2} M=6.0900
WKY {1}		.006817*
SHR {2}	.006817*	

Newman-Keuls test; Variable:(shrwky final stats.sta) Basal uptake rostral region
Marked differences are significant at $p < 0.05$

	{1} M=7.4399	{2} M=6.3069
WKY {1}		.024927*
SHR {2}	.024927*	

Newman-Keuls test;:(shrwky final stats.sta) Basal uptake caudal region
Marked differences are significant at $p < 0.05$

	{1} M=7.6856	{2} M=6.0045
WKY {1}		.001572*
SHR {2}	.001572*	

Newman-Keuls test;:(shrwky final stats.sta) NMDA-stim uptake middle region
Marked differences are significant at $p < 0.05$

	{1} M=4.1543	{2} M=2.6780
WKY {1}		.040740*
SHR {2}	.040740*	

T-test for Dependent Samples (shrwky final stats.sta)SHR
Marked differences are significant at $p < 0.05$

	Mean	Std.Dv.	N	Diff.	Std.Dv. Diff.	t	df	p
T_entire	8.8	1.032						
B_entire	6.1	.7559	8	2.758208	1.109089	7.03406	7	.000205*
T_rostral	8.4	.9608						
B_rostral	6.3	.8054	8	2.094250	1.319111	4.49047	7	.002830*
T_middle	8.6	1.444						
B_middle	6.0	1.210	8	2.678000	1.462089	5.18062	7	.001280*
T_caudal	9.5	1.296						
B_caudal	6.0	1.031	8	3.502375	1.506042	6.57765	7	.000311*

T-test for Dependent Samples (shrwky final stats.sta) SHR
Marked differences are significant at $p < 0.05$

	Mean	Std.Dv.	N	Diff.	Std.Dv. Diff.	t	df	p
B-rostral	6.306875	.805419						
B-middle	5.958750	1.209634	8	.348125	1.288521	.76417	7	.469737
B-rostral	6.306875	.805419						
B-caudal	6.004500	1.030858	8	.302375	.514171	1.66335	7	.140192
B-middle	5.958750	1.209634						
B-caudal	6.004500	1.030858	8	-.045750	1.567570	-.08255	7	.936521

T-test for Dependent Samples (shrwky final stats.sta) WKY
Marked differences are significant at $p < 0.05$

	Mean	Std.Dv.	N	Diff.	Std.Dv. Diff.	t	df	p
T_entire	10.5	.9701						
B_entire	7.1	.6562	11	3.390939	.837656	13.42613	10	.000000*
T_rostral	9.9	.8802						
B_rostral	7.4	1.101	11	2.423182	1.237871	6.49243	10	.000070*
T_middle	10.3	1.386						
B_middle	6.2	1.147	11	4.154273	1.413418	9.74812	10	.000002*
T_caudal	11.3	1.691						
B_caudal	7.7	.8922	11	3.595364	1.527518	7.80644	10	.000015*

T-test for Dependent Samples (shrwky final stats.sta)WKY
Marked differences are significant at $p < 0.05$

	Mean	Std.Dv.	N	Diff.	Std.Dv. Diff.	t	df	p
B-rostral	7.439909	1.101453						
B-middle	6.154727	1.147024	11	1.28518	1.420624	3.00042	10	.013334*
B-rostral	7.439909	1.101453						
B-caudal	7.685636	.892215	11	-.24573	1.329776	-.61287	10	.553641
B-middle	6.154727	1.147024						
B-caudal	7.685636	.892215	11	-1.53091	1.520729	-3.33883	10	.007505*

T-test for Dependent Samples (shrwky final stats.sta)SHR
Marked differences are significant at $p < .05000$

	Mean	Std.Dv.	N	Diff.	Std.Dv. Diff.	t	df	p
T-rostral	8.401125	.960766						
T-middle	8.636750	1.444189	8	-.23563	1.057600	-.63015	7	.548606
T-rostral	8.401125	.960766						
T-caudal	9.506875	1.296436	8	-1.10575	.856738	-3.65051	7	.008172*
T-middle	8.636750	1.444189						
T-caudal	9.506875	1.296436	8	-.87012	1.621399	-1.51788	7	.172836

T-test for Dependent Samples (shrwky final stats.sta)WKY
Marked differences are significant at $p < .05000$

	Mean	Std.Dv.	N	Diff.	Std.Dv. Diff.	t	df	p
T-rostral	9.86309	.880205						
T-middle	10.30900	1.386046	11	-.44591	1.148972	-1.28716	10	.227032
T-rostral	9.86309	.880205						
T-caudal	11.28100	1.691347	11	-1.41791	1.904774	-2.46889	10	.033168*
T-middle	10.30900	1.386046						
T-caudal	11.28100	1.691347	11	-.97200	1.803230	-1.78777	10	.104104

A 3.7a Effect of strain, novel environment and age on NMDA-stimulated $^{45}Ca^{2+}$ uptake

Statistical analysis for data in table 3.7.1a and 3.7.2b
Summary of all Effects; design: Average Basal uptake (summary 3.sta)
1-STRAIN, 2-AGE, 3-ENVR

	df Effect	MS Effect	Df Error	MS Error	F	p-level
1	1	1.446687	35	.782237	1.849422	.182547
2	1*	5.146045*	35*	.782237*	6.578624*	.014767*
3	1	1.628473	35	.782237	2.081815	.157953
12	1	.578406	35	.782237	.739425	.395697
13	1	.011251	35	.782237	.014383	.905224
23	1	1.668078	35	.782237	2.132444	.153130
123	1	.789621	35	.782237	1.009439	.321933

Newman-Keuls test; Average Basal uptake (summary 3.sta)
Probabilities for Post Hoc Tests
MAIN EFFECT: AGE

	{1} 5.806901	{2} 6.511333
.... young .... {1}		.013510*
.... adult .... {2}	.013510*	

Summary of all Effects; design: Basal uptake rostral region (summary 3.sta)
1-STRAIN, 2-AGE, 3-ENVR

	df Effect	MS Effect	Df Error	MS Error	F	p-level
1	1	3.23076	35	.975212	3.31288	.077300
2	1*	12.88319*	35*	.975212*	13.21067*	.000885*
3	1	.95727	35	.975212	.98160	.328605
12	1	.36438	35	.975212	.37364	.544977
13	1	.87990	35	.975212	.90227	.348688
23	1	.27571	35	.975212	.28272	.598284
123	1	.55940	35	.975212	.57362	.453892

Newman-Keuls test; Basal uptake rostral region (summary 3.sta)
Probabilities for Post Hoc Tests
MAIN EFFECT: AGE

	{1} 5.824099	{2} 6.938687
.... young .... {1}		.000867*
.... adult .... {2}	.000867*	

Summary of all Effects; design: Basal uptake middle region (summary 3.sta)
1-STRAIN, 2-AGE, 3-ENVR

	df Effect	MS Effect	df Error	MS Error	F	p-level
1	1	1.052863	35	.807433	1.303963	.261243
2	1	2.508405	35	.807433	3.106641	.086705
3	1	.061276	35	.807433	.075890	.784566
12	1	.199665	35	.807433	.247283	.622104
13	1	1.262686	35	.807433	1.563828	.219402
23	1	2.114743	35	.807433	2.619093	.114563
123	1	.151368	35	.807433	.187469	.667688

Summary of all Effects; Basal uptake caudal region;(summary 3.sta)
1-STRAIN, 2-AGE, 3-ENVR

	df Effect	MS Effect	Df Error	MS Error	F	p-level
1	1	.61560	35	2.495145	.246721	.622499
2	1	2.66369	35	2.495145	1.067550	.308586
3	1	9.59473	35	2.495145	3.845359	.057879
12	1*	11.10057*	35*	2.495145*	4.448868*	.042149*
13	1	.01743	35	2.495145	.006984	.933873
23	1	3.59209	35	2.495145	1.439631	.238258
123	1	2.33728	35	2.495145	.936732	.339760

Newman-Keuls test; Basal uptake caudal region (summary 3.sta)
Probabilities for Post Hoc Tests
INTERACTION: 1 x 2

	{1} 6.332964	{2} 5.805167	{3} 5.542000	{4} 7.083416
SHR young .... {1}		.446796	.488500	.281397
SHR adult .... {2}	.446796		.703601	.164348
WKY young .... {3}	.488500	.703601		.130444
WKY adult .... {4}	.281397	.164348	.130444	

Summary of all Effects; design: Total uptake rostral region (summary 3.sta)
1-STRAIN, 2-AGE, 3-ENVR

	df Effect	MS Effect	Df Error	MS Error	F	p-level
1	1*	8.05961*	35*	1.446471*	5.57191*	.023953*
2	1*	20.93533*	35*	1.446471*	14.47338*	.000548*
3	1	.27491	35	1.446471	.19006	.665545
12	1	1.18237	35	1.446471	.81741	.372118
13	1	1.50003	35	1.446471	1.03703	.315501
23	1	1.35659	35	1.446471	.93786	.339473
123	1	1.48757	35	1.446471	1.02841	.317491

Summary of all Effects; design: Average Total uptake (summary 3.sta)
1-STRAIN, 2-AGE, 3-ENVR

	df Effect	MS Effect	Df Error	MS Error	F	p-level
1	1*	6.15636*	35*	1.456189*	4.22772*	.047286*
2	1*	33.14555*	35*	1.456189*	22.76185*	.000032*
3	1	.51459	35	1.456189	.35338	.556028
12	1	.57176	35	1.456189	.39264	.534981
13	1	.68593	35	1.456189	.47104	.497029
23	1	.03912	35	1.456189	.02687	.870743
123	1	.85785	35	1.456189	.58911	.447911

Newman-Keuls test; Average Total uptake (summary 3.sta)
Probabilities for Post Hoc Tests
MAIN EFFECT: STRAIN

	{1} 8.057018	{2} 8.827504
SHR .... {1}		.044207*
WKY .... {2}	.044207*	

Newman-Keuls test; Average Total uptake (summary 3.sta)
Probabilities for Post Hoc Tests
MAIN EFFECT: AGE

	{1} 9.336154	{2} 7.548368
.... young .... {1}		.000144*
.... adult .... {2}	.000144*	

Newman-Keuls test; Total uptake rostral region (summary 3.sta)
Probabilities for Post Hoc Tests
MAIN EFFECT: STRAIN

	{1} 7.794878	{2} 8.676455
SHR .... {1}		.022095*
WKY .... {2}	.022095*	

Newman-Keuls test; Total uptake rostral region (summary 3.sta)
Probabilities for Post Hoc Tests
MAIN EFFECT: AGE

	{1} 8.946082	{2} 7.525250
.... young .... {1}		.000569*
.... adult .... {2}	.000569*	

Summary of all Effects; design: Total uptake middle region (summary 3.sta)
1-STRAIN, 2-AGE, 3-ENVR

	df Effect	MS Effect	Df Error	MS Error	F	p-level
1	1	5.79208	35	1.492308	3.88129	.056780
2	1*	24.34607*	35*	1.492308*	16.31438*	.000279*
3	1	.90132	35	1.492308	.60398	.442286
12	1	.31116	35	1.492308	.20851	.650760
13	1	.13963	35	1.492308	.09357	.761505
23	1	.39306	35	1.492308	.26339	.611024
123	1	.04161	35	1.492308	.02788	.868353

Newman-Keuls test; Total uptake middle region (summary 3.sta)
Probabilities for Post Hoc Tests
MAIN EFFECT: AGE

	{1} 8.635519	{2} 7.103312
.... young .... {1}		.000343*
.... adult .... {2}	.000343*	

Summary of all Effects; design: Total uptake caudal region (summary 3.sta)
1-STRAIN, 2-AGE, 3-ENVR

	df Effect	MS Effect	Df Error	MS Error	F	p-level
1	1	4.83067	35	3.504239	1.37852	.248281
2	1*	60.25060*	35*	3.504239*	17.19363*	.000204*
3	1	.46038	35	3.504239	.13138	.719188
12	1	.38898	35	3.504239	.11100	.740992
13	1	2.66984	35	3.504239	.76189	.388687
23	1	.00307	35	3.504239	.00088	.976537
123	1	1.83568	35	3.504239	.52384	.474017

Newman-Keuls test; Total uptake caudal region (summary 3.sta)
Probabilities for Post Hoc Tests
MAIN EFFECT: AGE

	{1} 10.42691	{2} 8.016541
.... young .... {1}		.000281*
.... adult .... {2}	.000281*	

Summary of all Effects; design: Average NMDA-stimulated uptake (summary 3.sta)
1-STRAIN, 2-AGE, 3-ENVR

	df Effect	MS Effect	Df Error	MS Error	F	p-level
1	1	1.46367	35	.820929	1.78294	.190408
2	1*	61.44902*	35*	.820929*	74.85303*	.000000*
3	1	.10670	35	.820929	.12997	.720626
12	1	1.78357	35	.820929	2.17262	.149425
13	1	.89955	35	.820929	1.09577	.302372
23	1	1.23520	35	.820929	1.50464	.228147
123	1	2.40588	35	.820929	2.93068	.095760

Newman-Keuls test; Average NMDA-stimulated uptake (summary 3.sta)
Probabilities for Post Hoc Tests
MAIN EFFECT: AGE

	{1} 3.568001	{2} 1.133778
.... young .... {1}		.000122*
.... adult .... {2}	.000122*	

Summary of all Effects; design: NMDA-stimulated uptake rostral region: (summary 3.sta)
1-STRAIN, 2-AGE, 3-ENVR

	df Effect	MS Effect	Df Error	MS Error	F	p-level
1	1	1.01565	35	1.305706	.77786	.383815
2	1*	60.35884*	35*	1.305706*	46.22699*	.000000*
3	1	.44981	35	1.305706	.34450	.561011
12	1	.26809	35	1.305706	.20532	.653257
13	1	.25070	35	1.305706	.19201	.663944
23	1	.17869	35	1.305706	.13685	.713658
123	1	3.07630	35	1.305706	2.35605	.133789

Newman-Keuls test; NMDA-stimulated uptake rostral region: (summary 3.sta)
Probabilities for Post Hoc Tests
MAIN EFFECT: AGE

	{1} 3.122033	{2} .7095000
.... young .... {1}		.000122*
.... adult .... {2}	.000122*	

Summary of all Effects; design: NMDA-stimulated uptake middle region (summary 3.sta)
1-STRAIN, 2-AGE, 3-ENVR

	df Effect	MS Effect	Df Error	MS Error	F	p-level
1	1	1.67037	35	.967319	1.72680	.197367
2	1*	40.38015*	35*	.967319*	41.74441*	.000000*
3	1	1.85055	35	.967319	1.91307	.175383
12	1	.03965	35	.967319	.04099	.840722
13	1	.43807	35	.967319	.45287	.505394
23	1	3.67769	35	.967319	3.80194	.059240
123	1	.46402	35	.967319	.47970	.493129

Newman-Keuls test; NMDA-stimulated uptake middle region (summary 3.sta)
Probabilities for Post Hoc Tests
MAIN EFFECT: AGE

	{1} 2.976313	{2} 1.003042
.... young .... {1}		.000123*
.... adult .... {2}	.000123*	

Summary of all Effects; design: NMDA-stimulated uptake caudal region (summary 3.sta)
1-STRAIN, 2-AGE, 3-ENVR

	df Effect	MS Effect	Df Error	MS Error	F	p-level
1	1	1.76648	35	2.553946	.69167	.411237
2	1*	88.22491*	35*	2.553946*	34.54455*	.000001*
3	1	2.78812	35	2.553946	1.09169	.303260
12	1*	10.82402*	35*	2.553946*	4.23815*	.047029*
13	1	2.83221	35	2.553946	1.10895	.299526
23	1	3.38399	35	2.553946	1.32500	.257499
123	1	4.91844	35	2.553946	1.92582	.173989

Newman-Keuls test; NMDA-stimulated uptake caudal region (summary 3.sta)
Probabilities for Post Hoc Tests
MAIN EFFECT: AGE

	{1} 4.605620	{2} 1.688875
.... young .... {1}		.000123*
.... adult .... {2}	.000123*	

Newman-Keuls test; NMDA-stimulated uptake caudal region (summary 3.sta)
Probabilities for Post Hoc Tests
INTERACTION: 1 x 2

	{1} 3.888440	{2} 1.993333	{3} 5.322800	{4} 1.384417
SHR young .... {1}		.009930*	.046242*	.002760*
SHR adult .... {2}	.009930*		.000198*	.386258
WKY young .... {3}	.046242*	.000198*		.000168*
WKY adult .... {4}	.002760*	.386258	.000168*	

T-test for Dependent Samples (summary 3.sta) YOUNG SHR
Marked differences are significant at $p < 0.05$

	Mean	Std.Dv.	N	Diff.	Std.Dv. Diff.	t	df	p
B_entire T_entire	5.7 8.86	1.033 1.717	13	-3.12172	1.336637	-8.4208	12	.000002*
B_rostral T_rostral	5.4 8.4	.7919 1.470	13	-2.92515	1.631295	-6.4653	12	.000031*
T_middle B_middle	8.2 5.4	1.703 .9234	13	-2.72162	1.220737	-8.0385	12	.000004*
T_caudal B_caudal	10.0 6.3	2.669 2.325	13	-3.71831	2.727476	-4.9154	12	.000357*

T-test for Dependent Samples (summary 3.sta) ADULT SHR
Marked differences are significant at $p < 0.05$

	Mean	Std.Dv.	N	Diff.	Std.Dv. Diff.	t	df	p
B_entire	6.2	.8249						
T_entire	7.2	.6478	10	-1.09800	.616136	-5.63541	9	.000319*
B_rostral	6.8	1.227						
T_rostral	7.2	.8628	10	-.44200	.889861	-1.57073	9	.150694
B_middle	6.0	.9794						
T_middle	6.8	.7788	10	-.78750	.758556	-3.28294	9	.009485*
B_caudal	5.7	.9551						
T_caudal	7.8	1.089	10	-2.06450	1.135679	-5.74857	9	.000277*

T-test for Dependent Samples (summary 3.sta) WKY YOUNG
Marked differences are significant at $p < 0.05$

	Mean	Std.Dv.	N	Diff.	Std.Dv. Diff.	t	df	p
B_entire	5.9*	.6949*						
T_entire	9.8*	1.099*	10*	-3.96323*	1.053671*	-11.8945*	9*	.000001*
B_rostral	6.2*	.9046*						
T_rostral	9.6*	1.218*	10*	-3.35880*	.977707*	-10.8636*	9*	.000002*
B_middle	5.9*	.8790						
T_middle	9.1*	1.057*	10*	-3.20790*	1.300485*	-7.8004*	9*	.000027*
B_caudal	5.5*	.8632*						
T_caudal	10.9*	1.772*	10*	-5.32300*	1.626761*	10.3474*	9*	.000003*

T-test for Dependent Samples (summary 3.sta) WKY ADULT
Marked differences are significant at $p < 0.05$

	Mean	Std.Dv.	N	Diff.	Std.Dv. Diff.	t	df	p
B_entire	6.7*	.9412						
T_entire	7.8*	.5838	10*	-1.07870*	.734141*	-4.64645*	9*	.001208*
B_rostral	7.0*	.9534						
T_rostral	7.7*	1.039	10*	-.71960*	.938169*	-2.42555*	9*	.038261*
B_middle	6.2*	.8074						
T_middle	7.4*	.6263	10*	-1.17200*	.660230*	-5.61348*	9*	.000329*
B_caudal	6.9*	1.584						
T_caudal	8.2*	.6169	10*	-1.34450*	1.348484*	-3.15293*	9*	.011682*

A 3.7b Effect of strain and age on NMDA-stimulated $^{45}Ca^{2+}$ uptake 2 way MANOVA

Statistical analysis of data in **table3.7.3**
Summary of all Effects; design: T_entire (summary 3.sta)
1-STRAIN, 2-AGE

	df Effect	MS Effect	df Error	MS Error	F	p-level
1	1	6.22932	39	1.361034	4.57690	.038721*
2	1	35.29036	39	1.361034	25.92908	.000009*
12	1	.53433	39	1.361034	.39259	.534592

Newman-Keuls test; T_entire (summary 3.sta)
Probabilities for Post Hoc Tests
MAIN EFFECT: STRAIN

	{1} 8.048661	{2} 8.814816
SHR .... {1}		.038089*
WKY .... {2}	.038089*	

Newman-Keuls test; T_entire (summary 3.sta)
Probabilities for Post Hoc Tests
MAIN EFFECT: AGE

	{1} 9.343528	{2} 7.519950
.... young {1}		.000124*
.... adult {2}	.000124*	

Summary of all Effects; design:T-rostral region (summary 3.sta)
1-STRAIN, 2-AGE

	df Effect	MS Effect	df Error	MS Error	F	p-level
1	1	7.90360	39	1.428107	5.53432	.023788*
2	1	23.61416	39	1.428107	16.53529	.000224*
12	1	1.08260	39	1.428107	.75806	.389263

Newman-Keuls test; T_rostral region (summary 3.sta)
Probabilities for Post Hoc Tests
MAIN EFFECT: STRAIN

	{1} 7.787154	{2} 8.650150
SHR .... {1}		.023378*
WKY .... {2}	.023378*	

Newman-Keuls test; T_rostral region (summary 3.sta)
Probabilities for Post Hoc Tests
MAIN EFFECT: AGE

	{1} 8.964504	{2} 7.472800
.... young {1}		.000320*
.... adult {2}	.000320*	

Summary of all Effects; design:T_middle region (summary 3.sta)
1-STRAIN, 2-AGE

	df Effect	MS Effect	Df Error	MS Error	F	p-level
1	1	6.38563	39	1.381027	4.62382	.037789*
2	1	24.90044	39	1.381027	18.03037	.000130*
12	1	.29140	39	1.381027	.21100	.648532

Newman-Keuls test; T_middle region (summary 3.sta)
Probabilities for Post Hoc Tests
MAIN EFFECT: STRAIN

	{1} 7.471342	{2} 8.247050
SHR .... {1}		.037170*
WKY .... {2}	.037170*	

Newman-Keuls test; T_middle region (summary 3.sta)
Probabilities for Post Hoc Tests
MAIN EFFECT: AGE

	{1} 8.625093	{2} 7.093300
.... young {1}		.000233*
.... adult {2}	.000233*	

Summary of all Effects; design:T-caudal region (summary 3.sta)
1-STRAIN, 2-AGE

	df Effect	MS Effect	df Error	MS Error	F	p-level
1	1	4.61865	39	3.277497	1.40920	.242369
2	1	63.55908	39	3.277497	19.39257	.000080*
12	1	.37592	39	3.277497	.11470	.736674

Newman-Keuls test; T_caudal region (summary 3.sta)
Probabilities for Post Hoc Tests
MAIN EFFECT: AGE

	{1} 10.44104	{2} 7.993750
.... young {1}		.000187*
.... adult {2}	.000187*	

Statistical analysis of data in **table 3.7.4**
Summary of all Effects; design: B-entire (summary 3.sta)
1-STRAIN, 2-AGE

	df Effect	MS Effect	df Error	MS Error	F	p-level
1	1	1.337766	39	.801487	1.669104	.203982
2	1	4.219323	39	.801487	5.264366	.027234*
12	1	.450425	39	.801487	.561987	.457959

Newman-Keuls test; B_entire (summary 3.sta)
Probabilities for Post Hoc Tests
MAIN EFFECT: AGE

	{1} 5.801053	{2} 6.431600
.... young {1}		.026772*
.... adult {2}	.026772*	

Summary of all Effects; design: B-rostral region (summary 3.sta)
1-STRAIN, 2-AGE

	df Effect	MS Effect	Df Error	MS Error	F	p-level
1	1	2.73188	39	.938864	2.90977	.095998
2	1	12.13800	39	.938864	12.92838	.000898*
12	1	.61828	39	.938864	.65854	.422001

Newman-Keuls test; B_rostral region (summary 3.sta)
Probabilities for Post Hoc Tests
MAIN EFFECT: AGE

	{1} 5.822527	{2} 6.892000
.... young {1}		.000989*
.... adult {2}	.000989*	

Summary of all Effects; design: B-middle region (summary 3.sta)
1-STRAIN, 2-AGE

	df Effect	MS Effect	Df Error	MS Error	F	p-level
1	1	1.229053	39	.812463	1.512750	.226088
2	1	2.179800	39	.812463	2.682954	.109472
12	1	.139897	39	.812463	.172188	.680448

Summary of all Effects; design: B-caudal region (summary 3.sta)
1-STRAIN, 2-AGE

	df Effect	MS Effect	Df Error	MS Error	F	p-level
1	1	.50140	39	2.625020	.191010	.664488
2	1	1.44392	39	2.625020	.550061	.462736
12	1	10.07036	39	2.625020	3.836300	.057333

Statistical analysis of data in **table 3.7.5**
Summary of all Effects; design:E_entire (summary 3.sta)
1-STRAIN, 2-AGE

	df Effect	MS Effect	df Error	MS Error	F	p-level
1	1	1.56614	39	.855748	1.83013	.183903
2	1	61.11673	39	.855748	71.41904	.000000*
12	1	1.57921	39	.855748	1.84541	.182124

Newman-Keuls test; E_entire (summary 3.sta)
Probabilities for Post Hoc Tests
MAIN EFFECT: AGE

	{1} 3.578241	{2} 1.178433
.... young {1}		.000117*
.... adult {2}	.000117*	

Summary of all Effects; design:E_rostral(summary 3.sta)
1-STRAIN, 2-AGE

	df Effect	MS Effect	df Error	MS Error	F	p-level
1	1	1.16883	39	1.289035	.90675	.346843
2	1	62.39772	39	1.289035	48.40654	.000000*
12	1	.11014	39	1.289035	.08544	.771606

Newman-Keuls test; E_rostral (summary 3.sta)
Probabilities for Post Hoc Tests
MAIN EFFECT: AGE

	{1} 3.142027	{2} .7172000
.... young {1}		.000117*
.... adult {2}	.000117*	

Summary of all Effects; design: E_middle (summary 3.sta)
1-STRAIN, 2-AGE

	df Effect	MS Effect	df Error	MS Error	F	p-level
1	1	1.81444	39	1.033710	1.75527	.192927
2	1	40.12194	39	1.033710	38.81354	.000000*
12	1	.05623	39	1.033710	.05440	.816800

Newman-Keuls test; E_middle (summary 3.sta)
Probabilities for Post Hoc Tests
MAIN EFFECT: AGE

	{1} 2.964758	{2} 1.020350
.... young {1}		.000117*
.... adult {2}	.000117*	

Summary of all Effects; design: E_ caudal (summary 3.sta)
1-STRAIN, 2-AGE

	df Effect	MS Effect	df Error	MS Error	F	p-level
1	1	1.75834	39	2.655166	.66223	.420713
2	1	84.99541	39	2.655166	32.01134	.000002*
12	1	10.24928	39	2.655166	3.86013	.056600

Newman-Keuls test; E_caudal (summary 3.sta)
Probabilities for Post Hoc Tests
MAIN EFFECT: AGE

	{1} 4.627900	{2} 1.797850
.... young {1}		.000118*
.... adult {2}	.000118*	

Comparison between young wky and young shr from both novel and normal environment
Analysis of Variance (summary 3.sta)
Marked effects are significant at p < .05000

	SS Effect	df Effect	MS Effect	SS Error	df Error	MS Error	F	p
T_entire	5.54578	1	5.54578	46.2357	21	2.201702	2.518861	.127436
T_rostral	7.90203	1	7.90203	39.2897	21	1.870937	4.223568	.052516
T_middle	5.00931	1	5.00931	44.8701	21	2.136672	2.344446	.140656
T_caudal	4.06376	1	4.06376	113.7293	21	5.415681	.750370	.396149
B_entire	.12553	1	.12553	17.1619	21	.817234	.153605	.699063
B_rostral	3.16873	1	3.16873	14.8921	21	.709148	4.468355	.046664*
B_middle	1.17081	1	1.17081	17.1863	21	.818394	1.430624	.244993
B_caudal	3.23700	1	3.23700	71.5957	21	3.409317	.949457	.340949
E_entire	3.35046	1	3.35046	27.2968	21	1.299845	2.577583	.123321
E_rostral	1.06338	1	1.06338	40.5347	21	1.930225	.550908	.466168
E_middle	1.33658	1	1.33658	33.1037	21	1.576369	.847889	.367608
E_caudal	10.91742	1	10.91742	83.9475	21	3.997500	2.731063	.113288

Newman-Keuls test; Variable: B_rostral (summary 3.sta)
Marked differences are significant at p < 0.05

	{1} M=5.4482	{2} M=6.1969
SHR {1}		.046802*
WKY {2}	.046802*	

A 3.7.1 Comparison between young SHR and WKY reared in the normal environment

Analysis of Variance (summary 3.sta)
Marked effects are significant at p < .05000

	SS Effect	df Effect	MS Effect	SS Error	df Error	MS Error	F	p
T_entire	.618496	1	.618496	37.12948	10	3.712948	.166578	.691773
T_rostral	.617627	1	.617627	28.21771	10	2.821771	.218879	.649925
T_middle	2.762753	1	2.762753	36.09587	10	3.609587	.765393	.402170
T_caudal	.007869	1	.007869	79.88076	10	7.988076	.000985	.975579
B_entire	.580717	1	.580717	9.85374	10	.985374	.589336	.460418
B_rostral	1.374859	1	1.374859	10.50799	10	1.050799	1.308394	.279328
B_middle	2.507149	1	2.507149	9.95696	10	.995696	2.517986	.143638
B_caudal	.220940	1	.220940	41.12291	10	4.112291	.053727	.821375
E_entire	.000590	1	.000590	13.54198	10	1.354198	.000435	.983762
E_rostral	.149499	1	.149499	29.51267	10	2.951267	.050656	.826458
E_middle	.006202	1	.006202	19.23587	10	1.923587	.003224	.955836
E_caudal	.145154	1	.145154	32.22561	10	3.222561	.045043	.836188

A 3.8 NMDA-stimulated $^{45}Ca^{2+}$ uptake into PFC of SHR and WKY

Summary of all Effects; design: (pfc stats3.sta) T_entire
1-STRAIN, 2-ENVR3

	df Effect	MS Effect	Df Error	MS Error	F	p-level
1	1*	10.33826*	16*	.782908*	13.20494*	.002234*
2	1	.36163	16	.782908	.46190	.506452
12	1	.00009	16	.782908	.00011	.991795

Newman-Keuls test; T_entire (pfc stats3.sta)
Probabilities for Post Hoc Tests
MAIN EFFECT: STRAIN

	{1} 7.837533	{2} 9.275467
SHR .... {1}		.002376*
WKY .... {2}	.002376*	

Summary of all Effects; design: (pfc stats3.sta) T_ rostral region
1-STRAIN, 2-ENVR3

	df Effect	MS Effect	Df Error	MS Error	F	p-level
1	1*	13.44800*	16*	1.091033*	12.32594*	.002897*
2	1	1.25902	16	1.091033	1.15397	.298654
12	1	.00098	16	1.091033	.00090	.976461

Newman-Keuls test; T_rostral region (pfc stats3.sta)
Probabilities for Post Hoc Tests
MAIN EFFECT: STRAIN

	{1} 8.257500	{2} 9.897500
SHR .... {1}		.003034*
WKY .... {2}	.003034*	

Summary of all Effects; design: (pfc stats3.sta) T_middle region
1-STRAIN, 2-ENVR3

	Df Effect	MS Effect	Df Error	MS Error	F	p-level
1	1*	10.38385*	16*	1.093384*	9.496978*	.007148*
2	1	.84831	16	1.093384	.775855	.391451
12	1	.12215	16	1.093384	.111716	.742540

Newman-Keuls test; (pfc stats3.sta) T_middle region
Probabilities for Post Hoc Tests
MAIN EFFECT: STRAIN

	{1} 7.493300	{2} 8.934400
SHR .... {1}		.007314*
WKY .... {2}	.007314*	

Summary of all Effects; design: (pfc stats3.sta) T_caudal region
1-STRAIN, 2-ENVR3

	df Effect	MS Effect	Df Error	MS Error	F	p-level
1	1	7.597746	16	1.934377	3.927748	.064944
2	1	2.569728	16	1.934377	1.328452	.266011
12	1	.084370	16	1.934377	.043616	.837205

Summary of all Effects; design: (pfc stats3.sta) B_entire
1-STRAIN, 2-ENVR3

	df Effect	MS Effect	Df Error	MS Error	F	p-level
1	1	1.339721	16	.343709	3.897837	.065869
2	1	.439957	16	.343709	1.280027	.274567
12	1	.528017	16	.343709	1.536232	.233053

Summary of all Effects; design: (pfc stats3.sta) B_rostral region
1-STRAIN, 2-ENVR3

	df Effect	MS Effect	Df Error	MS Error	F	p-level
1	1	1.936909	16	2.003130	.966941	.340081
2	1	1.095120	16	2.003130	.546704	.470377
12	1	1.059841	16	2.003130	.529092	.477498

Summary of all Effects; design: (pfc stats3.sta) B_middle region
1-STRAIN, 2-ENVR3

	df Effect	MS Effect	Df Error	MS Error	F	p-level
1	1	1.666376	16	.633984	2.628419	.124504
2	1	.794808	16	.633984	1.253672	.279379
12	1	.275890	16	.633984	.435169	.518847

Summary of all Effects; design: (pfc stats3.sta) B_caudal region
1-STRAIN, 2-ENVR3

	df Effect	MS Effect	Df Error	MS Error	F	p-level
1	1	.623398	16	.590252	1.056155	.319380
2	1	.002668	16	.590252	.004520	.947230
12	1	.391160	16	.590252	.662700	.427558

Summary of all Effects; design: (pfc stats3.sta) E_entire
1-STRAIN, 2-ENVR3

	df Effect	MS Effect	Df Error	MS Error	F	p-level
1	1*	4.627220*	16*	.791709*	5.844596*	.027925*
2	1	1.833353	16	.791709	2.315690	.147591
12	1	.884522	16	.791709	1.117231	.306214

Newman-Keuls test; (pfc stats3.sta) E_entire
Probabilities for Post Hoc Tests
MAIN EFFECT: STRAIN

	{1} 2.759533	{2} 3.721533
SHR .... {1}		.028056*
WKY .... {2}	.028056*	

Summary of all Effects; design: (pfc stats3.sta) E_rostral region
1-STRAIN, 2-ENVR3

	df Effect	MS Effect	Df Error	MS Error	F	p-level
1	1	4.442474	16	1.943317	2.286026	.150043
2	1	3.965842	16	1.943317	2.040759	.172364
12	1	1.358247	16	1.943317	.698932	.415454

Summary of all Effects; design: (pfc stats3.sta) E_middle region
1-STRAIN, 2-ENVR3

	df Effect	MS Effect	Df Error	MS Error	F	p-level
1	1	5.662608	16	1.472087	3.846654	.067488
2	1	.174471	16	1.472087	.118520	.735129
12	1	1.746405	16	1.472087	1.186347	.292202

Summary of all Effects; design: (pfc stats3.sta) E_caudal region
1-STRAIN, 2-ENVR3

	df Effect	MS Effect	Df Error	MS Error	F	p-level
1	1	3.870240	16	2.376743	1.628380	.220141
2	1	2.738000	16	2.376743	1.151996	.299053
12	1	.112800	16	2.376743	.047460	.830298

T-test for Dependent Samples (pfc stats3.sta) SHR
Marked differences are significant at $p < 0.05$

	Mean	Std.Dv.	N	Diff.	Std.Dv. Diff.	t	df	p
T_entire	7.8	.8397						
B_entire	5.1	.5969	10	2.734033	.566232	15.26896	9	.000000*
T_rostral	8.3	1.184						
B_rostral	5.8	1.469	10	2.461500	1.695402	4.59121	9	.001307*
T_middle	7.5	.8194						
B_middle	4.7	.6137	10	2.745400	.765636	11.33922	9	.000001*
T_caudal	7.8	1.443						
B_caudal	4.8	.9147	10	2.995100	1.356981	6.97971	9	.000065*

T-test for Dependent Samples (pfc stats3.sta) WKY
Marked differences are significant at $p < 0.05$

	Mean	Std.Dv.	N	Diff.	Std.Dv. Diff.	t	df	p
T_entire	9.3	.8526						
B_entire	5.6	.6019	10	3.654333	1.165255	9.91715	9	.000004*
T_rostral	9.9	.8239						
B_rostral	6.4	1.282	10	3.479100	1.287415	8.54571	9	.000013*
T_middle	8.9	1.175						
B_middle	5.3	.9324	10	3.609200	1.370810	8.32595	9	.000016*
T_caudal	9.0	1.285						
B_caudal	5.1	.5064	10	3.874700	1.643342	7.45607	9	.000039*